Max-Planck-Institut für Meteorologie
Max Planck Institute for Meteorology

The Relative Influences of Volcanic and Anthropogenic Emissions on Air Pollution in Indonesia as Studied With a Regional Atmospheric Chemistry and Climate Model

Melissa Anne Pfeffer

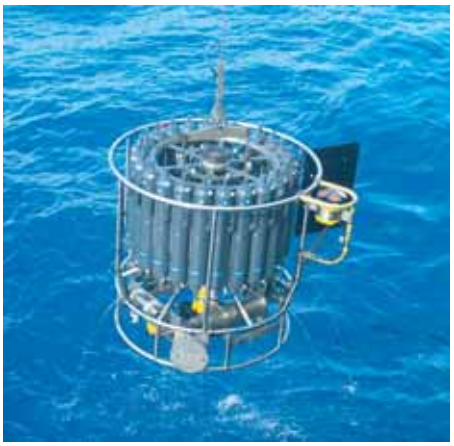

Berichte zur Erdsystemforschung 46/2007

Reports on Earth System Science

Berichte zur Erdsystemforschung 46/2007

The Relative Influences of Volcanic and Anthropogenic Emissions on Air Pollution in Indonesia as Studied With a Regional Atmospheric Chemistry and Climate Model

Dissertation zur Erlangung des Doktorgrades der Naturwissenschaften
im Departement Geowissenschaften der Universität Hamburg
vorgelegt von

Melissa Anne Pfeffer
aus Syracuse, NY USA

Hamburg 2007

Reports on Earth System Science 46/2007

ISSN 1614-1199

Melissa Anne Pfeffer
Max-Planck-Institut für Meteorologie
Bundesstrasse 53
20146 Hamburg
Germany

Als Dissertation angenommen
vom Departement Geowissenschaften der Universität Hamburg

auf Grund der Gutachten von
Prof. Dr. Hartmut Graßl
und
Prof. Dr. Hans Graf

Hamburg, den 14. Juni 2007
Prof. Dr. Kay-Christian Emeis
Leiter des Departements für Geowissenschaften

ISSN 1614-1199

The Relative Influences of Volcanic and Anthropogenic Emissions on Air Pollution in Indonesia as Studied With a Regional Atmospheric Chemistry and Climate Model

Jakarta

Kalimantan

Merapi

Melissa Anne Pfeffer

Hamburg 2007

Table of Contents

Table of Contents — *Continued*

List of Figures

List of Tables

Abstract

The regional atmospheric chemistry and climate model REMOTE has been used to study air pollution in Indonesia. The transport, deposition, and interactions between and relative impacts of emissions from volcanic, anthropogenic, and biomass burning sources have been examined.

The atmospheric loss of volcanic emissions has been shown to be dependent on meteorological conditions and the solubility in water of a given compound. The average annual mean SO_2 loss rate of the Indonesian volcanoes is 1.1 x 10^{-5} s^{-1}, or an e-folding rate of approximately 1 day. This loss rate was found to vary seasonally, be poorly correlated with wind speed, and uncorrelated with temperature or relative humidity. 53 % of the loss of SO_2 is due to conversion to SO_4^{2-}, 42 % due to dry deposition, and 5 % due to lateral transport away from the dominant direction of plume travel. $PbCl_2$ was used as a representative of highly-soluble volcanic compounds and compared with volcanic S to better understand how the solubility of volcanic emissions influences their deposition. High concentrations of $PbCl_2$ are predicted to be deposited near to the volcanoes while volcanic S travels further away until removal from the atmosphere primarily via the wet deposition of SO_4^{2-}. The ratio of the concentration of $PbCl_2$ to SO_2 is found to exponentially decay at increasing distance from the volcanoes. In order to estimate the emission flux of compounds that are not measurable by remote sensing instruments, it is the standard experimental technique to relate remote sensing observations of SO_2 flux from a volcano to the ratio of S to other compounds measured in fumarolic emissions. Assuming that the ratio between the concentrations of highly soluble volcanic compounds and SO_2 within a plume is equal to that observed in fumarolic gases is justified at the distances of < 30 km where such remote sensing observations are typically made.

The interactions of "background" anthropogenic and volcanic pollution with emissions from the catastrophic Indonesian wildfire of 1997 were studied by conducting experiments including and excluding the source of interest. It was found that the atmospheric concentrations of O_3, CO, NO_2, and SO_2 were all increased above the levels generated by the fires by pollution from major cities in the region. The number of days and the distance from the fires where O_3 exceeded the Indonesian hourly air quality standard were increased as a result of this urban pollution. O_3 produced by the urban emissions is shown to enhance the conversion of SO_2 released by the fires to SO_4^{2-}, demonstrating that pollution from different sources are actively altering the atmospheric behavior and lifetime of each other. Volcanic emissions had little influence on surface pollution during the wildfires or on fire emissions.

In order to study the effects of air pollution in Indonesia under more typical conditions than those of the extreme wildfire of 1997, the year 1999 has been examined. In this meteorologically normal year, anthropogenic S has been shown to be deposited above a critical

load value of 0.4 g(S)/m^2-yr in Java, northeastern Sumatra, and peninsular Malaysia. Volcanic S is found to be deposited below this threshold. Anthropogenic SO_4^{2-} is calculated to have an annual mean direct shortwave radiative forcing of -0.063 W/m^2 averaged over the model domain, and volcanic SO_4^{2-} -0.012 W/m^2. The forcing efficiency of anthropogenic SO_4^{2-} is found to be greater than for volcanic when averaged over ocean + land, with annual mean values of -328 W/g(SO_4^{2-}) and -293 W/g(SO_4^{2-}) respectively. Over Java, the anthropogenic SO_4^{2-} forcing efficiency is greater than the volcanic due to the enhancement of negative forcing efficiency over the ocean, as the anthropogenic sulfate is transported over the ocean while the volcanic tends to remain on land. The forcing of the total anthropogenic aerosol was calculated by assuming an external mixture of SO_4^{2-}, organic carbon (OC), and black carbon (BC), indicating an annual mean forcing of -0.13 W/m^2 averaged over the model domain. The total anthropogenic forcing is dominated by OC released by biomass burning. The influence of volcanic emissions relative to anthropogenic emissions on acid deposition and on direct radiative forcing is found to be lower in this study than in previous studies. This is attributed to an increase in anthropogenic emissions due to the simulation of the year 1999, as Indonesian anthropogenic emissions are increasing, the use of modern, realistic emission inventories, including a volcanic inventory with reduced emissions compared to earlier assessments, and the inclusion of biomass burning as an anthropogenic source.

Zusammenfassung

Im Rahmen dieser Doktorarbeit wurde das regionale Rechenmodell für Atmosphärenchemie und Klima REMOTE verwendet, um die Luftverschmutzung in Indonesien zu untersuchen. Die Ausbreitung und Ablagerung von Emissionen aus anthropogenen Quellen, Vulkanen und Biomassenverbrennung sowie deren Wechselwirkungen und relative Einflüsse wurden untersucht.

Die Untersuchungen zeigen, dass der so genannte atmosphärische Verlust vulkanischer Ausstöße von den herrschenden meteorologischen Verhältnissen sowie der Wasserlöslichkeit der jeweiligen chemischen Komponente abhängt. Die durchschnittliche Verlustrate von SO_2 aus indonesischen Vulkanen liegt im Jahresmittel bei 1.1 x 10^{-5} s^{-1}, was einer "e-folding scale", d.h. der zeit, in der die entsprechende Exponentialfunktion um einer Faktor e reduziert wird, von ungefähr einem Tag entspricht. Die Verlustrate obliegt jahreszeitlichen Schwankungen, zeigt eine schwache Korrelation mit der jeweiligen Windgeschwindigkeit und keinerlei Korrelation mit Temperatur und relativer Feuchte. 53 % des Verlustes von SO_2 ist auf Umwandlung in SO_4^{2-} zurückzuführen, 42 % auf trockene Ablagerung und 5 % der Emissionen breiten sich abweichend von der Hauptrichtung der Plumes aus. Das Verhalten von $PbCl_2$ wurde repräsentativ für sehr lösliche vulkanische Komponenten simuliert und mit den Ergebnissen für vulkanischen Schwefel verglichen, um besser zu verstehen, inwieweit die Wasserlöslichkeit vulkanischer Gase deren Ablagerungsverteilung beeinflusst. Die Simulationen ergeben hohe $PbCl_2$-Konzentrationen in der unmittelbaren Nähe der Vulkane, während sich der vulkanische Schwefel weiter ausbreitet, bis er schließlich vornehmlich durch feuchte Ablagerung als SO_4^{2-} der Atmosphäre entzogen wird. Das Verhältnis von $PbCl_2$ zu SO_2 nimmt mit der Entfernung vom Vulkan exponentiell ab. Um den Emissionsfluss der Komponenten abzuschätzen, der mit Fernerkundungsinstrumenten nicht gemessen werden kann, werden gewöhnlich fernerkundlich beobachtete SO_2-Flüsse mit den in vulkanischen Fumarolen gemessenen Verhältnissen von S zu anderen Komponenten in Beziehung gesetzt. Dabei wird angenommen, dass das Verhältnis zwischen stark löslichen vulkanischen Komponenten zu SO_2 innerhalb der Plumes dem in der Fumarole beobachteten entspricht. Nach Erkenntnissen dieser Studie ist dies nur für Distanzen von bis zu 30 Kilometern gerechtfertigt, was der üblichen Entfernung solcher fernerkundlichen Messungen entspricht.

Die Wechselwirkungen vulkanischer und anthropogener "Hintergrundsverschmutzung" mit den Emissionen der katastrophalen indonesischen Waldbrände von 1997 wurden anhand von Experimenten, in denen die jeweiligen Quellen mal eingebunden, mal ausgenommen wurden, analysiert. Die Untersuchungen, dass die aus den Waldbränden stammenden atmosphärischen Konzentrationen von O_3, CO, NO_2 und SO_2 allesamt durch die Luftverschmutzung der Ballungszentren der Region noch weiter verstärkt wurden. Die O_3-Konzentrationen überstiegen als Folge der zusätzlichen städtischen Verschmutzung sowohl an mehr Tagen als auch in weiterer Entfernung von den Bränden den Luftqualitätsgrenzwert für Indonesien. Weiterhin zeigte sich, dass das durch urbane Emmissionen entstandene O_3 die Umwandlung von SO_2 zu SO_4^{2-} verstärkt. Damit wurde dargelegt, dass Verschmutzungen aus unterschiedlichen Quellen sich gegenseitig in ihrem

Verhalten und ihrer Lebensdauer in der Atmosphäre beeinflussen. Vulkanische Emissionen hatten vergleichsweise wenig Einfluss auf die oberflächennahe Verschmutzung oder auf die Waldbrandemissionen.

Um die Auswirkungen der Luftverschmutzung in Indonesien unter gewöhnlicheren Bedingungen als die der extremen Waldbrände von 1997 zu untersuchen, wurde des Weiteren auch das Jahr 1999 simuliert. In diesem meteorologisch betrachtet normalen Jahr zeigte sich, dass anthropogener S auf Java, im Nordosten Sumatras und auf der malaysischen Halbinsel oberhalb der kritischen Belastung von 0.4 g(S)/m^2-yr abgelagert wird. Der vulkanische S hingegen überschreitet diesen Grenzwert innerhalb der Simulationen nicht. Das Jahresmittel des direkten kurzwelligen Strahlungsantriebs des anthropogenen SO_4^{2-} wurde über das Modellgebiet gemittelt mit -0.063 W/m^2 berechnet; für das vulkanische SO_4^{2-} beträgt es -0.012 W/m^2. Die Effizienz des Antriebs durch anthropogenen SO_4^{2-} wurde ebenfalls höher als die durch vulkanischen SO_4^{2-} berechnet, wenn sowohl Land- als auch Meeresgebiete berücksichtigt wurden, er liegt im Jahresmittel bei -328 W/g(SO_4^{2-}) bzw. -293 W/g(SO_4^{2-}). Auf Java ist die Antriebseffizienz von anthropogenen SO_4^{2-} aufgrund der verstärkten negativen Antriebseffizienz über den Ozeanen größer als die von vulkanischem SO_4^{2-}, da das anthropogene SO_4^{2-} auf das Meer hinaus transportiert wird, während das vulkanische SO_4^{2-} hauptsächlich über den Landgebieten verbleibt. Der Antrieb des gesamten anthropogenen Aerosols wurde unter der Annahme einer externen Mischung aus SO_4^{2-}, organischem Kohlenstoff (OC) und schwarzem Kohlenstoff (BC) berechnet und beträgt über das Modellgebiet gemittelt -0.13 W/m^2. Dieser anthropogene Gesamtantrieb wird von OC aus Biomassenverbrennung dominiert. Der Einfluss vulkanischer Emissionen auf saure Ablagerungen und den direkten Strahlungsantrieb im Verhältnis zu den anthropogenen Emissionen fällt im Vergleich zu früheren Studien geringer aus. Dies lässt sich zum einen auf ein Ansteigen der anthropogenen Emissionen in Indonesien, welche durch die Simulationen des Jahres 1999 Berücksichtigung finden, zum anderen auf die Verwendung von modernen, realistischen Emissionsdatenlisten - darunter ein vulkanisches Inventar mit geringeren Emissionen als in früheren Abschätzungen - und die Einbeziehung von Biomassenverbrennung als anthropogene Verschmutzungsquelle zurückführen.

Chapter 1

Introduction

For this dissertation, the atmospheric transport, deposition, and environmental effects of air pollution in Indonesia has been studied with a regional atmospheric chemistry and climate model. Pollution is a significant concern in Indonesia, as over the past two decades, rapid economic and population growth has created vast environmental damage (Resosudarmo, 2002, see Figure 1.1). A significant issue is the quality of air in Indonesia's large cities, with lead (Pb) and fine particulates [1] being the main health concerns (Indonesia Environment Monitor, 2003). Forest fires seasonally contribute to air pollution in Indonesia and neighboring countries. Pollution from volcanoes is also significant in this region with many active volcanoes.

1.1 Sources of air pollution in Indonesia

Anthropogenic emissions in large cities are the main consistent source of air pollution in Indonesia. Sources include energy production, household and industrial use, and transportation (Indonesia Environment Monitor, 2003). In addition to the Pb and fine particulates mentioned above, the primary pollutants of health concern include carbon monoxide (CO), nitrogen oxides (NO_x), hydrocarbons (HC), and sulfur dioxide (SO_2). Tropospheric ozone (O_3) produced by emissions of NO_x is a secondary pollutant of interest. Aerosol particles including black carbon (BC) and organic carbon (OC or primary organic carbon (POC)) are another type of anthropogenic pollution. Secondarily produced aerosol particles include sulfate (SO_4^{2-}) and secondary organic aerosol (SOA). Growth of emissions of the primary pollutants is driven by an increase of motor vehicle transportation and industry and by inefficient energy use (Shah et al., 2000).

[1] e.g. PM_1 or $PM_{2.5}$: any particulate matter with a diameter less than or equal to 1 or 2.5 microns

Land-clearing fires are set every year during the dry season (approximately June-October) and are a periodic source of air pollution in Indonesia. Pollution from these fires is anthropogenic as it is people who set the original fires. In 1997, the normal land-clearing fires grew into an exceptional wildfire that created an international health and economic crisis. Gases and particles released by the fires into the atmosphere are referred to as haze (Heil and Goldammer, 2001). The gaseous compounds include many of the same species released by urban pollution including CO_2, CO, NO_x, and HC. O_3 is also secondarily produced downwind from fires. Particulate fire emissions, the majority of which are carbonaceous (Heil and Goldammer, 2001), are a significant aspect to haze, with the finest particles being the greatest concern for human health. Indonesian fire emissions are strongly influenced by the burning of peat (Langmann and Heil, 2004; Heil et al., 2006). Peat areas are a dense concentration of organic matter, and may release up to 50 times higher emissions for a given area burnt compared with other types of vegetation fires (Levine, 1999).

Indonesia is the region of the world with the largest number of active volcanoes with 76 of the Earth's 539 volcanoes that have been observed erupting (Simkin and Siebert, 1994). Indonesia has continuous volcanic activity, and four-fifths of these 76 volcanoes have erupted within the past century. The Indonesian volcanoes are also remarkably destructive: Indonesia has the highest number of historically recorded eruptions producing fatalaties, damage to agricultural land, mudflows, tsunamis, and pyroclastic flows. Fortunately in recent times, successful evacuations prior to volcanic emergencies have reduced these risks to vulnerable populations in Indonesia (Simkin and Siebert, 1994).

It is important to understand the role of volcanoes in the atmosphere because volcanoes emit high concentrations of environmentally significant compounds. Volcanic emissions are primarily H_2O, followed by CO_2, SO_2, HCl, and other compounds including metals (e.g. Bardintzeff and McBirney, 2000). Volcanoes are the source of most gases in the Earth's atmosphere over geologic timescales (Robock, 2003), and even today, when the concentration of climatically relevant volcanic emissions is an order of magnitude less than that released by human activity, volcanic emissions are responsible for observable climatic effects (Graf et al., 1997). This is because volcanic emissions generally reach higher elevations than most anthropogenic pollutants, which enables volcanic emissions

to remain in the atmosphere longer and travel farther away from source. The most climatically significant gas emitted by volcanoes is SO_2, which is readily converted into SO_4^{2-}. In the troposphere, SO_4^{2-} as well as other acidic volcanic emissions such as HCl and HF can contribute to acid rain. Volcanoes also emit heavy metals that can accumulate to high concentrations in soils and plants.

1.2 Effects of air pollution in Indonesia

The effects of anthropogenic pollution include harm to peoples' health, natural ecosystems, and manmade materials. Lead is a dangerous toxin to people, especially children, impacting many bodily systems, including damaging children's cognitive development and IQ. To address this, leaded gasoline has been phased out in Indonesia (Indonesia Environment Monitor, 2003). Fine particulates irritate the respiratory system promoting asthma and other diseases. SO_2 and NO_x irritate the lungs in their gaseous form and can be removed from the atmosphere as "acid deposition" that damages both natural and manmade surfaces (Shah et al., 2000). Vegetation, including crops, can be harmed if the soil in which they are grown is not able to neutralize the deposited acid. Acidified lakes may become unable to provide fish habitat and buildings can corrode. Acidic aerosol particles harm peoples' health, especially in large urban areas where multiple types of pollution can interact to lower tolerances. CO slows down thinking and reflexes, some hydrocarbons are carcinogenic, and ozone can irritate the eyes, nose, and throat and hamper breathing.

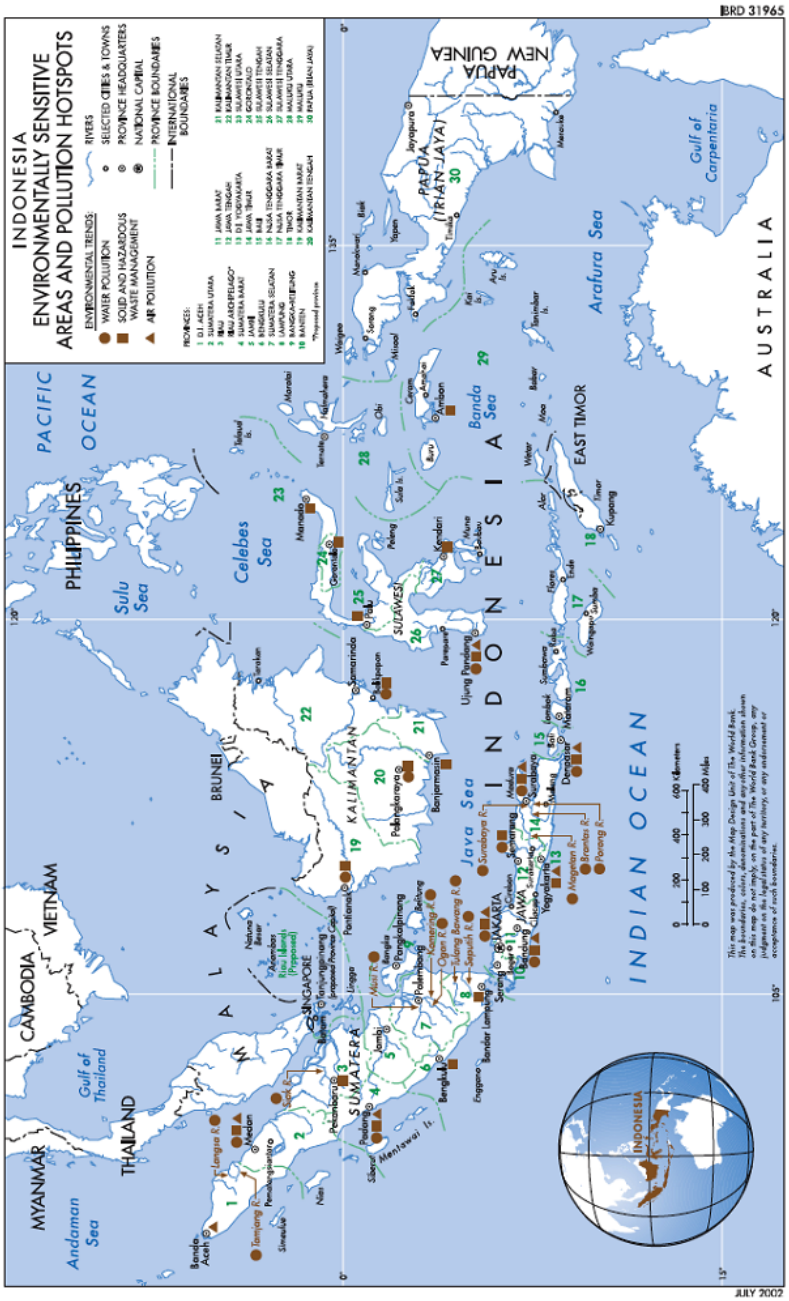

Figure 1.1 Map of Indonesia indicating pollution hotspots. Taken from Indonesia Environment Monitor (2003).

Volcanic emissions can produce local- and regional-scale air pollution that causes illness and increased mortality in people, particularly by SO_2 and SO_4^{2-} (Grattan et al., 2005). The sulfur oxides from volcanic emissions that create both chronic and acute respiratory and eye irritations are generally less than 1 μm in size and acidic. These two qualities possibly interact, increasing their toxicity (Michaud et al., 2005). A very dangerous hazard is the release of CO_2 by volcanoes, which can collect in low topographic areas, displacing air and suffocating people; this phenomenon has killed hundreds of people in Cameroon and in Indonesia (McGee and Gerlach, 1995). Acidic volcanic gases can also kill off vegetation that has long-term exposure to the dry deposition of dilute concentrations of these species (Delmelle et al., 2001). The acidic volcanic gases can also dissolve in water droplets, falling to the earth as acid rain. Trace metals released by volcanoes, such as Pb, can accumulate in plants and lichens in the vicinity of persistently degassing volcanoes (Monna et al., 1999). Acidic crater lakes are formed when heat and volatile species are released by volcanoes into an overlying body of water. The lake cools and condenses soluble and reactive magmatic gases including SO_2, H_2S, HCl, HF, and CO_2 which dissolve and accumulate in the water. Pollution events associated with the release of acidic crater lake waters have occurred at many of the around 40 active volcanoes around the world that contain a lake, including at the Indonesian volcanoes Patuha (Sriwana et al., 1998, 2000) and Ijen (Heikens et al., 2005).

As well as effects at the Earth's surface, air pollution can also have influences in the atmosphere. Atmospheric aerosols affect the radiative budget of the Earth-atmosphere system via direct and indirect forcing. Direct radiative forcing is due to aerosol particles scattering and absorbing solar and thermal infrared radiation, thereby modifying the Earth's albedo. Indirect radiative forcing results from aerosol particles changing clouds' lifetimes and microphysical and radiative properties. SO_4^{2-} is capable of both direct and indirect climatic forcing through the scattering of radiation from the sun and by serving as sites for cloud formation and chemical reactions, such as ozone (O_3) destruction. SO_4^{2-} as well as OC are associated with cooling as they are mainly scattering. BC is absorbing, hence associated with warming, and can influence clouds by evaporating cloud droplets and by acting as ice nuclei.

1.3 Meteorological effects on air pollution in Indonesia

Meteorological conditions have a large impact on Indonesian air pollution. The most significant influence is that people set land-clearing forest fires during the dry season. The severity of the dry season is affected by El Niño Southern Oscillation (ENSO) climate conditions. During ENSO conditions, atmospheric pressure at the surface is above normal in the western Pacific and there is reduced upward motion (Heil and Goldammer, 2001). This produces a reduction in convective activity leading to drought throughout Southeast Asia. The El Niño of 1997-1998 was the strongest in the past 50 years, producing the worst drought conditions in Indonesia in this time period. Under these conditions, manmade fires grew out of control to create a severe international pollution event. This tremendous environmental disaster created health problems and even death for a significant number of people, as well as an estimated economic loss in Indonesia alone of $9 - $10 billion US dollars (Indonesia Environment Monitor, 2003). Other meteorological conditions in addition to drought are also significant. The dominant winds carry pollution, which during the fires of 1997 created a cross-boundary problem as the pollution was carried to Singapore and Malaysia. Strong sunlight promotes the rapid oxidation of species to their secondary products while heavy rainfall washes water soluble species out of the atmosphere quickly. Outside of the dry season, many pollutants do not travel far from their source region.

1.4 Geologic setting of Indonesia

Indonesia is an archipelago of more than 13,000 islands. 76 % of Indonesia's volcanoes are part of the 3,000 km long Sunda Arc, stretching from northwest Sumatra to the Banda Sea (Simkin and Siebert, 1994, Figure 1.2). This portion of the arc is due to the subduction of the Australia plate beneath the Eurasia Plate. Subduction parameters are not consistent along the entire arc. Oblique subduction ($55°$) under Sumatra transitions along a volcanic belt called the Sunda Straits (where Krakatau is located) to the near frontal subduction ($13°$) observed under Java (Mandeville et al., 1996). The Banda Arc to the east of the Sunda Arc is produced by the subduction of the Pacific Plate beneath the Eurasia Plate. To the north of the Banda Arc, the Molucca Sea Plate is being subducted beneath both the

Sangihe Arc to the west and the Halmahera Arc to the east. The convergence of these two arcs is forming a large collisional complex with primarily N-S oriented trenches (Clor et al., 2005).

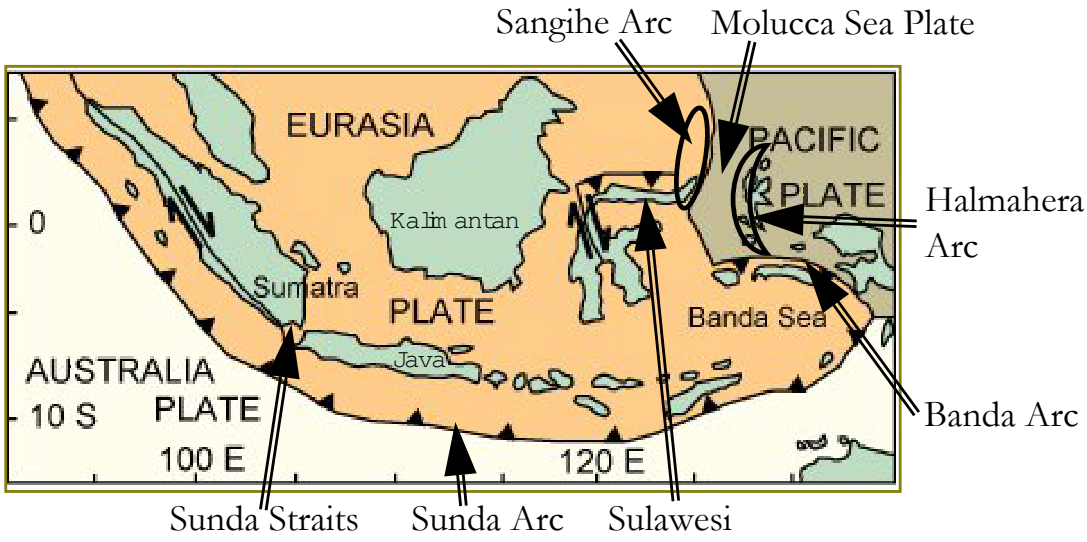

Figure 1.2 Simplified tectonic map of Indonesia. Modified from http://volcano.und.edu which was simplified from Lee and Lawver (1995).

1.5 Model

The atmospheric chemistry and climate model used for this dissertation is the REgional MOdel with Tracer Extension ”REMOTE” (Langmann, 2000). This online model calculates meteorological conditions using the physics of the regional climate model REMO 5.0 (Jacob, 2001) together with the transport and tropospheric chemical reactions of 63 tracer species. Tracers can be transported by horizontal and vertical advection (Smolarkiewitz, 1983), convective up- and down-draft (Tiedtke, 1989), and vertical diffusion (Mellor and Yamada, 1974). Trace species can undergo chemical decay in the atmosphere or can be removed from the atmosphere by wet and dry deposition or transport out of the model boundaries. 158 gasphase reactions from the RADM II photochemical mechanism (Stockwell et al., 1990) are included. 43 longer-lived chemical species are transported between gridboxes and 20 are calculated but too short-lived to be transported. REMOTE was applied with 20 vertical layers of increasing thickness between the Earth’s surface and the 10 hPa pressure level (approximately 23 km). Analysis data of weather observations

from the European Centre for Medium-Range Weather Forecasts (ECMWF) were used as boundary conditions every 6 hours. The physical and chemical state of the atmosphere was calculated every 5 minutes. For the first study (Chapter 3), background concentrations of 39 species (Chang et al., 1987) were specified at the lateral model boundaries. For the latter two studies (Chapters 4 and 5) results from a global chemical transport model (MOZART; Horowitz et al., 2003) simulation (Granier et al., 2003) were used as chemical concentration boundary conditions every 6 hours for 14 chemical species and the other species were specified as for the first study. The simulations were performed at a horizontal resolution of 0.5° (approximately 55 km).

1.6 Objectives and outline of this study

This dissertation is focused on using regional atmospheric chemistry and climate modeling to better understand the atmospheric transport, deposition, and environmental influences of air pollution in Indonesia with an emphasis on volcanic emissions. As one of the largest uncertainties in constraining the impacts of emissions is knowledge of how much is being emitted, the first step in this project was to develop a reasonable volcanic SO_2 emission inventory (Chapter 2). Utilizing this inventory, three complementary modeling studies have been performed for the meteorologically normal years 1985 and 1999 and the extreme ENSO year 1997 described in Section 1.3. The first study examines the influence of meteorological conditions on the loss rate of volcanic SO_2 from the atmosphere as well as the significance of compound solubility in relating remote sensing measurements of SO_2 to other, more soluble, volcanic emissions (Chapter 3). This has been published in the journal Atmospheric Chemistry and Physics (Pfeffer et al., 2006a). The second study examines the role of anthropogenic and volcanic emissions in enhancing the effects of the 1997 Indonesian wildfire pollution event, one of the largest environmental disasters of the last century (Chapter 4). This work has been submitted to the Journal of Geophysical Research- Atmospheres (Pfeffer et al., 2007). The third study examines the relative effects of volcanic and anthropogenic emissions on acid deposition and on direct shortwave radiative forcing by aerosols (Chapter 5). The final chapter of this dissertation provides a summary of the main results of the three studies and an outlook for future research about volcanic air pollution (Chapter 6).

Chapter 2

An inventory of Indonesian volcanic emissions

Despite the significant role of volcanoes within the Earth's climate system, volcanic emissions have been included until now in global and regional climate models in a general, imprecise fashion. One reason it is difficult to realistically incorporate volcanic emissions into climate models is because it is hard to establish reasonable inventories for such emissions. Volcanic emissions are variable in composition and flux rate between different tectonic settings, between different volcanoes in the same tectonic setting, and over short (hours and days) and long (months and years) time scales at each individual volcano. Plume mixing and chemistry is dependent not only on the volcanic emissions but also on meteorological conditions and geographic characteristics. As it is impractical to monitor the emissions of all volcanoes continuously, it is necessary to extrapolate results from the relatively few measurements that are performed.

When one considers volcanic emissions, major eruptions are the first image to come to mind. Most volcanic emissions, however, are released due to continuous, non-eruptive volcanic degassing, with 99 % of volcanic SO_2 released continuously and only 1 % released during sporadic eruptions (Andres and Kasgnoc, 1998). Most research into the climatic impacts of volcanic emissions has focused on violent stratosphere-reaching eruptions. This emphasis has been largely due to the difficulties in observing the less dramatic emissions of passively degassing volcanoes, whereas the large atmospheric perturbations of eruptions can be observed via satellite imagery (Carn and Bluth, 2003). The development of lightweight ground-based remote-sensing techniques has created new opportunities for studying the local and regional influences of degassing volcanoes (McGonigle and Oppenheimer, 2003; Galle et al., 2002).

There are three general methods used to calculate the amount of emissions released by volcanoes: 1) petrologic estimates whereby the difference in concentration of volatiles in

melt inclusions and coexisting matrix glass is assumed to be a minimum estimate of degassing for one eruptive event (e.g. Scaillet et al., 2003) 2) direct measurements whereby SO_2 (and sometimes other species) emission fluxes are measured using remote-sensing instruments (e.g. Stoiber et al., 1983); and 3) satellite observations of relatively large eruptive events providing information on emission concentrations and plume height (e.g. Watson et al., 2004). Such measurements have been performed on relatively few volcanoes and rarely over a significant length of time, but are extrapolated to other, unstudied volcanoes and over time so as to generate estimates of global volcanic emissions. This extrapolation produces a large degree of uncertainty in estimates of global volcanic sulfur emissions, for example: Berresheim and Jaeschke (1983) estimated 7.6 x 10^{12} g SO_2/yr, Andres and Kasgnoc (1998) estimated 10.4 x 10^{12} g SO_2/yr, and Graf et al. (1997) estimated 14.0 x 10^{12} g SO_2/yr released by volcanoes.

Most ground-based remote sensing studies of volcanic emissions thus far have focused on SO_2 because SO_2 within a volcanic plume is typically orders of magnitude greater in concentration than what is found in background ambient air. Until recently, the correlation spectroscopy (COSPEC) instrument (Barringer Research Inc., Canada) was the only inexpensive, portable, and easy to use tool for measuring emissions of SO_2 and NO_2 from industrial and volcanic plumes. In order to calculate the flux rates of other species within a volcanic plume, it has been standard procedure to measure the flux rate of SO_2 using COSPEC, to measure the ratio of sulfur to other compounds in collected fumarolic samples, to assume that these ratios remain constant within the plume from the time the emissions are released until the plume is measured, and to then calculate the corresponding flux rate of the species in question.

In recent years, development of new instruments with the portability and robustness of the COSPEC capable of measuring other species of interest in addition to SO_2 have been developed. Amongst this state of the art arsenal are open-path Fourier-transform infrared spectroscopy (FTIRS) and miniature multi-axis differential-optical-absorption spectroscopy (mini-MAX-DOAS). Mini-MAX-DOAS can provide gas-flux measurements with high time resolution, can be used to estimate plume speed, and performs simultaneous measurements of SO_2, BrO, ClO, and OClO using 2-dimensional plume tomography techniques. Open-path FTIRS is a powerful remote-sensing tool that has been

increasingly used to measure gas emissions in the troposphere from volcanoes including SO_2, HCl, and HF. Improvements in satellite imaging have also made it possible to observe weaker plumes. These technological improvements are providing more information about volcanic-emission fluxes than has been available ever before.

2.1 Flux rates of Indonesian volcanic emissions

The rate at which pollutants are emitted is very important for determining their environmental impacts. The amount of gas produced by a volcano is dependent on the type of magma and the type of activity, varying widely in time and from one volcano to another (Bardintzeff and McBirney, 2000). In the published literature, the SO_2 flux of five mildly erupting and passively degassing Indonesian volcanoes have been measured using COSPEC. Potentially stratosphere-reaching eruptive plumes have been observed with TOMS for four volcanoes and of tropospheric eruptions for two others. The petrologic method has been used to calculate the SO_2 emissions of four large eruptions (Table 2.1). For the few Indonesian volcanoes whose SO_2 flux rates for passive degassing and small eruptions (the source of most volcanic emissions; categories C-E in Table 2.1) have been measured, this ranges from 0.005 - 0.24 Tg SO_2/year, while the relatively rare stratospheric- reaching eruptions (categories A-B) released from 0.2 - 58 Tg SO_2.

2.2 Compositions of Indonesian volcanic emissions

The compositions of emissions being released are also important in determining their potential environmental effects. Emission compositions provide clues about the activity level of the volcano, give information about the original magma composition, and can be used to learn about subduction processes. The compositions of volcanic gases are also important to measure as the ratio of gases collected in fumarolic samples are used to estimate the flux rates of compounds not measured directly. There are very few measurements of

Table 2.1 Measured Indonesian volcano SO_2 emissions

Method	Volcano	Date	Activity level	SO_2 emissions (Tg)	SO_2 flux rate (Tg/yr)
Petrologic	Tambora[1]	10 - 11 Apr. 1815	A	53-58	
	Krakatau[2]	20 May - 21 Oct. 1883	A	5.5	
	Agung[3]	18 Feb. 1963 - 27 Jan. 1964	A	2.5	
	Galunggung[4]	5 Apr. 1982 - 8 Jan. 1983	B	0.2	
TOMS	Colo[8]	23 Jul. 1983	B	0.2	
	Soputan[8]	24 May 1984	B	0.2	
	Banda Api[8]	9 May 1988	B	0.2	
	Makian[8]	17 Jul. 1988	C	0.05	
	Kelut[8]	11 Feb. 1990	C	< 0.05	
	Galunggung[8]	24 Jun. 1982	B	0.4	
	Galunggung[8]	13 Jul. 1982	B	0.4	
	Galunggung[8]	5 Apr. - 19 Sep. 1982	B	1.7	
COSPEC	Galunggung[5]	Aug. 1982 - Jan. 1983	E	0.4	
	Galunggung[7]		B		0.24
	Merapi[6]	1987 - 1993	C		0.04
	Slamet[6]	Jul. 1991	D		0.02
	Merapi[7]		C		0.05
	Tangkubanparahu[7]		C		0.03
	Slamet[7]		C		0.02
	Bromo (Tengger Caldera)[7]		C		0.005

A: Stratosphere-reaching eruption
B: Possible stratosphere-reaching eruption
C: Tropospheric eruption
D: Post-eruptive degassing
E: Between explosions degassing

[1] Self et al. (2004)
[2] Mandeville et al. (1998)
[3] Self and King (1996)
[4] de Hoog et al. (2001)
[5] Bluth et al. (1994)
[6] Nho et al. (1996)
[7] Andres and Kasgnoc (1998)
[8] Bluth et al. (1997)

the compositions of Indonesian volcanic gas emissions. Of 99 volcanoes active within recorded history in the Indonesian region, only 13 have had at least one measurement of fumarolic gas composition performed (Figure 2.1). By subregion, there have been no analyses performed on volcanoes of the Andaman Islands, Sumatra, or on the Halmahera Arc. Some measurements have been performed on volcanoes of Java, the Sunda Arc, the Banda Arc, Sulawesi, the Sangihe Arc, and Krakatau (Table 2.2; see Figure 1.2 in Chapter 1 for a map showing the different regions).

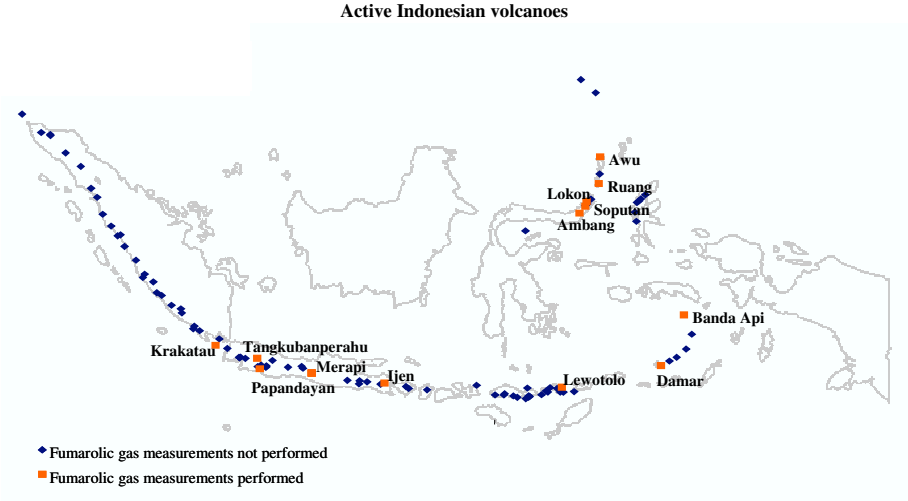

Figure 2.1 Indonesian volcanoes active within recorded history that have not had at least one fumarolic gas composition measurement performed (blue diamonds) and have had (orange squares). Only those volcanoes that have had measurements are labeled by name.

2.3 Inventory of Indonesian volcanic emissions

There are very few measurements of the emission flux rates of the Indonesian volcanoes (Section 2.1). In order to incorporate volcanic emissions into modeling studies in as realistic a manner as possible, two inventories have been developed for this work: a ”maximum” emission estimate and a ”realistic” emission estimate. The inventories were established considering all of the eruptive and passive degassing volcanic activity in Indonesia over the past century so as to remove some of the high natural short-term variability in volcanic eruption frequency. From 1900 to 1993, 63 volcanoes in Indonesia are known to have erupted and 32 additional volcanoes have degassed passively, for a total sum of 95

Table 2.2 Measured Indonesian fumarolic gas compositions*

Region	Volcano	H_2O	CO_2	SO_2	H_2S	HCl	HF	N_2	H_2	CH_4
Krakatau	Krakatau[1]	990	2.5	7	0.01			2	0.2	0
Java	Papandayan[2]	992	7.4		0.2			8.6	4.81	0.03
	Tangkubanperahu[2]	993	4.3	0.19	2.78	1.75		7.6	4.81	0.03
	Merapi[1,3]	929	48.2	5.7	5.6	2.0	0.1	2.5	7.3	0.1
	Ijen (Kawa Ijen)[4]	880	106.4	3.2	8.4	2.3	0.01	0.23	0.01	0
Sunda Arc	Lewotolo[5]	762	126	82.3	9.5	1.13	0.41	16.75	1.83	
Banda Arc	Banda Api[5]	952	44		1.5			2.8	0.45	
	Damar (Wurlali)[5]	869	112	8.7	9.25	3.1	0.005	2.52	0.06	
Sulawesi	Ambang[6]	990	8.83		0.69	0.09	0	0.05	0	0
	Soputan[6]	997	0.65	0.01		0.11	0	1.72	$5x10^{-5}$	$3.4x10^{-4}$
	Lokon-Empung[6]	995	4.3	0.25	0.43	0.04	0	0.04	0.04	0
Sangihe Arc	Ruang[6]	997	2.61	0.14	0.39	0.16	0	0.02	0.06	0
	Awu[6]	998	1.83	0.02	0.01	0.13	0	0.29	0	$1.2x10^{-4}$

*Gas compositions are given in mmol/mol

[1]Allard (1983)

[2]Giggenbach et al. (2001)

[3]Le Guern et al. (1982)

[4]Delmelle et al. (2000)

[5]Poorter et al. (1991)

[6]Clor et al. (2005)

active volcanoes, compared with the 99 volcanoes that have been active in Indonesia in recent history (Simkin and Siebert, 1994). The inventories established for this work contain both continuous and sporadic volcanic emissions. Continuous emissions include passive degassing as well as long-lasting diffusive eruptive emissions while sporadic emissions include short-lived eruptions (typically stronger than continuously erupted emissions).

For both the maximum and realistic emission estimates, the sporadic eruptive volcanic emissions were calculated using the Simkin and Siebert (1994) catalog of volcanic activity. Simkin and Siebert (1994) provide a compilation of the best known estimates of the date and eruption strength for all of the known volcanic activity on Earth. Every recorded eruption has been assigned a volcanic explosivity index (VEI) strength which

is an indicator of the strength of a volcanic event (Newhall and Self, 1982). All of the eruptions recorded in the catalog during the last century (1900–1993) for each active Indonesian volcano were summed. An index estimating the amount of SO_2 released due to each VEI class has been developed by Schnetzler et al. (1997), the volcanic sulfur index "VSI". This index bases the amount of sulfur released by arc volcanos for each VEI class based on 54 eruptions that have been observed with TOMS. This index is best suited for eruptions $\geq$ VEI 4, because TOMS is best at observing large eruptions. Halmer et al. (2002) have proposed a "modified VSI" which is essentially a doubling of the values suggested by Schnetzler et al. (1997), because Halmer et al. (2002) found that Schnetzler et al. (1997)'s values underestimated the amount of SO_2 released by smaller eruptions observed with COSPEC. Halmer et al. (2002), unfortunately, do not provide any of the primary COSPEC measurement data that they used to make this doubling, giving the impression that this doubling is arbitrary. As the VSI proposed by Schnetzler et al. (1997) is based on the quantity of SO_2 observed and reported for eruptions, we find this estimate to be more sound, and have chosen to apply it in favor of the alternative offered by Halmer et al. (2002). The total number of eruptions of each VEI class was multiplied by the maximum amount of SO_2 released by arc volcanoes suggested by the VSI. The SO_2 flux resulting from this multiplication was then divided by the 93 years of the record to generate an annual mean emission estimate. These calculations indicate 290 Gg SO_2/yr released sporadically by the Indonesian volcanoes.

The technique used to estimate the continuous volcanic emissions differed for the maximum and realistic emission estimates. The maximum continuous emissions were taken from Nho et al. (1996) as this work provides the maximum published estimate of SO_2 emissions from the Indonesian volcanoes (Table 2.3: 1600 Gg SO_2/yr released non-eruptively; 1900 Gg SO_2/yr eruptively; for a sum of 3500 Gg SO_2/yr continuous emissions). For the realistic emission estimate, the continuous emissions were calculated by assuming that 60 % of volcanic emissions are eruptive and 40 % are passive, following Halmer et al. (2002) (passive emissions being assumed to contain all of the continuous

Table 2.3 Estimates of Indonesian volcanic emissions

Emission style	SO_2 flux (Gg/yr)	Reference
continuous (non-eruptive)	120	Hilton et al. (2002)
continuous (non-eruptive)	210	Spiro et al. (1992)
continuous (non-eruptive)	1600	Nho et al. (1996)
continuous (eruptive)	1900	Nho et al. (1996)
continuous + sporadic (eruptive + non-eruptive)	2100–2600	Halmer et al. (2002)
continuous (eruptive + non-eruptive)	3500	used in this study*
sporadic (eruptive)	290	calculated for this study
continuous + sporadic (eruptive + non-eruptive)	3790	this study “maximum” estimate
continuous + sporadic (eruptive + non-eruptive)	484	this study “realistic” estimate

*sum from Nho et al. (1996)

emissions). This results in an assessment of 194 Gg SO_2/yr released continuously by the Indonesian volcanoes in the realistic inventory. The continuous emissions were divided evenly amongst the 95 active volcanoes. This is the most reasonable assumption we could make, despite the fact that emission rates of volcanoes are highly variable in time and between different volcanoes, because only a few of the active Indonesian volcanoes have published SO_2 flux measurements. It would have been less reasonable to have scaled the emission flux estimates for individual volcanoes based on the small number of available measurements for the active volcanoes. The division of the continuous emissions between all of the active volcanoes results in a mean continuous SO_2 flux of 37 Gg SO_2/yr for each volcano for the maximum estimate, and 2 Gg SO_2/yr for each volcano for the realistic estimate.

For the maximum estimate, a sum of sporadic and continuous volcanic emissions of about 3800 Gg SO_2/yr is found, and for the realistic estimate, about 480 Gg SO_2/yr (Figure 2.2). The estimated emission fluxes for the individual volcanoes correspond reasonably well with SO_2 flux measurements of Indonesian volcanoes (Table 2.4).

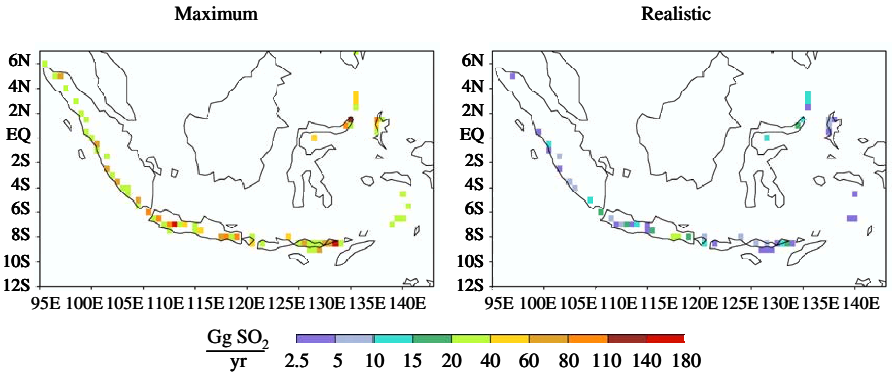

Figure 2.2 Emission inventory of the annual sum of continuous (eruptive + passive) and sporadic (eruptive) volcanic SO_2 emissions for the maximum and realistic emission inventories.

In order for this emission inventory to be included in atmospheric chemistry and climate modeling experiments, the emissions of each individual volcano can be released into the model layer at the actual height of each volcano. The elevations of the volcanoes range from 200 m (Riang Kotang) to 3805 m (Kerinci).

Table 2.4 SO_2 emissions from individual Indonesian volcanoes

Volcano	SO_2 flux from maximum estimate (Gg/yr)	SO_2 flux from realistic estimate (Gg/yr)	SO_2 flux from measurements (Gg/yr)
Bromo (Tengger Caldera)	47.4	12.6	5.1[a]
Galunggung	47.7	12.9	140.5[b]
			240.9[a]
Merapi	55.6	20.8	36.5[c]
			51.1[a]
			73.0[d]
Slamet	45.4	10.6	21.2[e]
Tangkubanparahu	37.5	2.8	27.4[a]

[a] Andres and Kasgnoc (1998)

[b] Bluth et al. (1994)

[c] Dir. Volc. & Geol. Haz. Mit. of Indonesia (2005)

[d] Le Guern (1982)

[e] Nho et al. (1996)

Chapter 3

Atmospheric transport and deposition of Indonesian volcanic emissions

Abstract

A regional climate model has been used to study the transport and deposition of sulfur (SO_2 and SO_4^{2-}) and $PbCl_2$ emissions from Indonesian volcanoes. The sensitivity of the atmospheric loss of these trace species to meteorological conditions and their solubility was examined. Two experiments were conducted: 1) volcanic sulfur released as primarily SO_2 and subject to transport, deposition, and oxidation to SO_4^{2-}; and 2) $PbCl_2$ released as an infinitely soluble passive tracer subject to only transport and deposition. The first experiment was used to calculate SO_2 loss rates from each active Indonesian volcano producing an annual mean loss rate for all volcanoes of 1.1 x 10^{-5} s-1, or an e-folding rate of approximately 1 day. SO_2 loss rate was found to vary seasonally, be poorly correlated with wind speed, and uncorrelated with temperature or relative humidity. The variability of SO_2 loss rates is found to be correlated with the variability of wind speeds, suggesting that it is much more difficult to establish a "typical" SO_2 loss rate for volcanoes that are exposed to changeable winds. Within an average distance of 70 km away from the active Indonesian volcanoes, 53 % of SO_2 loss is due to conversion to SO_4^{2-}, 42 % due to dry deposition, and 5 % due to lateral transport away from the dominant direction of plume travel. The solubility of volcanic emissions in water is shown to influence their atmospheric transport and deposition. High concentrations of $PbCl_2$ are predicted to be deposited near to the volcanoes while volcanic S travels further away until removal from the atmosphere primarily via the wet deposition of H_2SO_4. The ratio of the concentration of $PbCl_2$ to SO_2 is found to exponentially decay at increasing distance from the volcanoes. The more rapid removal of highly soluble species should be considered when observing SO_2 in an aged plume and relating this concentration to other volcanic species. An assumption that the ratio between the concentrations of highly soluble volcanic compounds and SO_2 within a plume is equal to that observed in fumarolic gases is reasonable at small distances from the volcanic vent, but will result in an underestimation of the emission flux of highly soluble species.

3.1 Introduction

Volcanic emissions can have significant environmental effects on local, regional, and global scales depending on how far the emissions are transported away from source prior to deposition. The impacts of volcanic emissions on the environment are defined by several variable characteristics, such as their chemical and physical properties (including solubility and particle size) (Mather et al., 2003), as well as environmental factors, i.e. volcano latitude, the maximum height at which emissions are injected (Halmer and Schmincke, 2003), wind speed, and precipitation.

Volcanic emissions can be released continuously by passive degassing or mild eruptions and can be released sporadically by more violent, and short-lived, eruptions. Violent eruptions can inject volcanic emissions past the tropopause with generally at least one to two stratosphere-reaching eruptions per year (Simkin, 1993; Bluth et al., 1997). Stratosphere-reaching eruption clouds can cause global surface cooling for months up to a few years by sulfate aerosol (SO_4^{2-}) backscattering of incoming shortwave solar radiation (e.g. Textor et al., 2003). It was calculated by Andres and Kasgnoc (1998) that only 1 % of volcanic SO_2 is released sporadically, while 99 % is released continuously. Continuous, tropospheric emissions are rapidly deposited locally and regionally but can have a significant atmospheric impact because they are supplied for long periods of time, and because volcanoes are often at elevations above the planetary boundary layer, allowing those emissions to remain in the troposphere longer than, for example, most anthropogenic S emissions. As an example of the relative significance of non-eruptive volcanic degassing, such sources may be responsible for 24 % of the total annual mean direct radiative top-of-atmosphere forcing (Graf et al., 1997).

Volcanic emissions are primarily H_2O, followed by CO_2, SO_2, HCl, and other compounds (e.g. Bardintzeff and McBirney, 2000). Some volcanic compounds are particularly environmentally important because they are released in extremely small quantities by other sources. For example, volcanoes may be responsible for 11 % of the total global emissions of Cr, and species including Hg, Ni, Cu, and As each contribute more than 5 % (Nriagu, 1989; Mather et al., 2003). Considering the volcanic contribution to natural (non-anthropogenic) emissions, species including Cd, Ni, Hg, and Pb contribute more

than 15 % to the global natural emissions of each. SO_2 has been the most monitored volcanic emission because the concentration of SO_2 within a volcanic plume is typically orders of magnitude greater in concentration than what is found in background ambient air. For the past few decades the majority of volcanic SO_2 observations have been performed with the Correlation Spectrometer (COSPEC), which measures the flux of emitted SO_2 (e.g. Stoiber et al., 1983). The (relatively) large number of published measurements of volcanic SO_2 fluxes is a useful tool for assessing the impact of volcanoes on the atmosphere because SO_2 is an environmentally important gas. SO_2 is readily converted, within days, to SO_4^{2-} aerosol which is climatically significant and is a main component of acid rain.

In addition to ground-based remote sensing (including COSPEC), fumarolic gas sampling and plume particle sampling (e.g. Pfeffer et al., 2006b) have contributed to an improved understanding of the variations in time and between different volcanoes of emission compositions and strengths and, to a lesser extent, about processes occurring within volcanic plumes. There are, however, limitations to what can be accomplished in the field. For example, ground-based remote sensing measurements of volcanic SO_2 fluxes over time at one volcano can be used to observe changes in volcanic activity as an eruption prediction tool in conjunction with other volcano monitoring techniques (for example at Montserrat; Young et al., 2003). Remote sensing instruments can detect changes in SO_2 emissions, but cannot determine unambiguously if the observed variations are due to changes in the volcano itself or to changing meteorological conditions.

Because SO_2 flux rates are the most abundant volcanic emission measurements, such observations have been used to extrapolate to other, unmeasured volcanic compounds: "X". This is done by relating the observed concentration of SO_2 in the plume to the ratio of "X" to total S (SO_2 + H_2S) found in fumarolic gases or condensates. In fumarolic gases, S is found as primarily SO_2 and H_2S, and it is assumed that all S is oxidized immediately upon exposure to air to be found as SO_2. The method of relating "X" to SO_2 assumes that the ratio of the concentrations of "X" to SO_2 remains constant from the time the emissions are released until the plume is measured. This technique has been used, for example, to estimate the annual flux of metals from volcanoes (Hinkley et al., 1999) and to constrain the flux balances of elements at subduction zones (Hilton et al., 2002). The assumption

of a steady ratio of [X]/[SO_2] remains a subject of uncertainty, however. Pyle and Mather (2003), for example, have shown that [Hg]/[SO_2] ratios can vary by an order of magnitude dependent on the type of volcanic activity (passively degassing vs. explosively erupting). The ratio of [X]/[SO_2] can vary not only dependent on the type of volcanic activity, but can also vary in time if the two species are removed at different rates from the plume. As remote sensing measurements of SO_2 flux using COSPEC are performed at distances of up to 30 km away from volcanic craters (for example at Mt. Etna, Weibring et al., 2002), it is important to constrain how reasonable it is to relate observations of SO_2 in an aged volcanic plume to more soluble compounds.

A field study examining the influence of variable meteorological factors on volcanic sulfur was performed by Fujita et al. (2003). They observed that the wet deposition of SO_4^{2-} and the percentage of sulfur deposited as SO_4^{2-} increased with increasing precipitation. McGonigle et al. (2004) attempted to determine what meteorological parameters are the most important for influencing the loss of SO_2 from volcanic plumes by performing repeated scans of SO_2 column concentration using ground-based differential optical absorption spectroscopy (DOAS). They measured the plume of Masaya volcano for several days during the dry season and found that time of day (i.e. insolation strength), relative humidity, and temperature had no significant impact on the measured SO_2 flux rate. We have addressed the question of the influence of meteorological conditions on volcanic plume SO_2 loss using an atmospheric chemistry model. We have exploited this technique to hold the modeled volcanic emissions constant, thus removing the inherent natural variability of volcanic emission rates. This enables us to study what variations in atmospheric transport are due to changing atmospheric conditions rather than due to changes in the volcanic activity. The modeling technique also allows us to study a much longer time period (1 year), consider different seasons, and to perform statistical comparisons between the SO_2 loss rate and the varying meteorological conditions. Modeling also enables us to calculate what portion of SO_2 lost from the volcanic plume is due to the different loss mechanisms: oxidation, deposition, or transport out of the plume, as well as to consider volcanic emissions additional to SO_2. This paper describes a regional atmospheric chemistry modeling study that has been performed to address two questions: 1) How do variable meteorological conditions influence volcanic SO_2 concentration in the atmosphere and SO_2 loss

rates? and 2) How do the transport and deposition patterns of highly soluble volcanic compounds relate to SO_2? This study has been performed over Indonesia because this is the region of the world with the largest number of historically active volcanoes and the region has a relatively continuous emission history with 4/5 of the volcanoes with dated eruptions having erupted here during the past century (Simkin and Siebert, 1994).

3.2 Experimental setup

The regional atmospheric chemistry model REMOTE (Regional Model with Tracer Extension Langmann, 2000) has been used to simulate meteorological conditions for the year 1985, a climatologically "normal" year, i.e. neither "El Niño" nor "La Niña". REMOTE combines the physics of the regional climate model REMO 5.0 with tropospheric chemical equations for 63 chemical species. The physical and dynamical equations in the model (Jacob, 2001) are based on the regional weather model EM/DM of the German Weather Service (Majewski, 1991) and include parameterizations from the global ECHAM 4 model (Roeckner et al., 1996). The chemical tracer transport mechanisms include horizontal and vertical advection (Smolarkiewitz, 1983), convective up- and downdraft (Tiedtke, 1989), and vertical diffusion (Mellor and Yamada, 1974). Trace species can undergo chemical decay in the atmosphere or can be removed from the atmosphere by wet and dry deposition or transport out of the model boundaries. Dry deposition is dependent on friction velocities and ground level atmospheric stability (Wesley, 1989). Wet deposition is dependent on precipitation rate, mean cloud water concentration, and compound solubility (Walcek and Taylor, 1986). 158 gasphase reactions from the RADM II photochemical mechanism (Stockwell et al., 1990) are included. 43 longer-lived chemical species are treated as predicted species and 20 shorter-lived ones as diagnosed species. Within the model, sulfate can be produced by the gas phase oxidation of SO_2 by $OH^{\cdot}$ or the aqueous phase oxidation of SO_2 via five chemical reactions: by H_2O_2, O_3, peroxyacetic acid (PAA), methylhydrogenperoxide (MHP), or via catalysis by Fe^{3+} or Mn^{2+} (see Walcek and Taylor, 1986, and references therein).

The model was applied with 20 vertical layers of increasing thickness between the Earth's surface and the 10 hPa pressure level (approximately 23 km). Analysis data of weather

observations from the European Centre for Medium-Range Weather Forecasts (ECMWF) were used as boundary conditions every 6 hours. The physical and chemical state of the atmosphere was calculated every 5 minutes. Background concentrations of 39 species (Chang et al., 1987), including SO_2, SO_4^{2-}, O_3, and H_2O_2, were specified at the lateral model boundaries. The model domain covers Indonesia and Northern Australia (91° E - 141° E; 19° S - 8° N) with a horizontal resolution of 0.5° (approximately 53 km in longitude and 55 km in latitude) with 101 grid points in longitude and 55 grid points in latitude.

3.2.1 Emission inventory

An annual inventory was established to represent maximum potential volcanic emissions within the modeled region of Indonesia (Figure 3.1). Over the past century, from 1900 to 1993, 63 volcanoes in Indonesia are known to have erupted and 32 additional volcanoes have degassed passively, for a total sum of 95 active volcanoes (Simkin and Siebert, 1994). The inventory established for this work contains both continuous and sporadic volcanic emissions. Continuous emissions include passive degassing as well as long-lasting diffusive eruptive emissions while sporadic emissions include short-lived eruptions (typically stronger than continuously erupted emissions). Continuous emissions were taken from Nho et al. (1996) as this work provides the maximum published estimate of SO_2 emissions from the Indonesian volcanoes (Table 3.1: 1600 Gg SO_2/yr released non-eruptively; 1900 Gg SO_2/yr eruptively; for a sum of 3500 Gg SO_2/yr continuous emissions (which is equivalent to 1750 Gg (S)/yr)). The continuous emissions were divided evenly amongst the 95 active volcanoes. This is the most reasonable assumption we could make, despite the fact that emission rates of volcanoes are highly variable in time and between different volcanoes, because only a few of the active Indonesian volcanoes have published SO_2 flux measurements. It would have been less reasonable to have scaled the emission flux estimates for individual volcanoes based on the small number of available measurements for the active volcanoes. The division of the continuous emissions between all of the active volcanoes results in a mean continuous SO_2 flux of 36.8 Gg SO_2/yr (100 Mg SO_2/day) for each volcano.

Table 3.1 Estimates of Indonesian volcanic emissions

Emission style	SO_2 flux (Gg/yr)	Reference
continuous (non-eruptive)	120	Hilton et al. (2002)
continuous (non-eruptive)	210	Spiro et al. (1992)
continuous (non-eruptive)	1600	Nho et al. (1996)
continuous (eruptive)	1900	Nho et al. (1996)
continuous (eruptive + non-eruptive)	3500	sum from Nho et al. (1996) used in this study
sporadic (eruptive)	290	calculated for this study
continuous + sporadic (eruptive + non-eruptive)	2100–2600	Halmer et al. (2002)
continuous + sporadic (eruptive + non-eruptive)	3790	this study

An estimate of the sporadic eruptive volcanic emissions for the region was established for this work using the Simkin and Siebert (1994) catalog of volcanic activity. Simkin and Siebert (1994) provide a compilation of the best known estimates of the date and eruption strength for all of the known volcanic activity on Earth. Each volcanic eruption is assigned a volcanic explosivity index (VEI) strength which is an indicator of the explosiveness of a volcanic event (Newhall and Self, 1982). All of the eruptions recorded in the catalog during the last century (1900–1993) for each active Indonesian volcano were summed to assemble the sporadic emission inventory. Indexes estimating the amount of SO_2 released due to each VEI class have been developed by Schnetzler et al. (1997), the volcanic sulfur index "VSI", and by Halmer et al. (2002), the "modified VSI". In this study, we have applied the VSI. The total number of eruptions of each VEI class was multiplied by the maximum amount of SO_2 released by arc volcanoes suggested by the VSI. The SO_2 flux resulting from this multiplication was then divided by the 93 years of the record to generate an annual mean emission estimate. Averaging over 93 years removes some of the high natural short-term variability of volcanic activity. These calculations indicate 290 Gg SO_2/yr released sporadically by the Indonesian volcanoes– a sum of sporadic and continuous volcanic emissions of 3800 Gg SO_2/yr (which is equivalent to 1900 Gg (S)/yr). The estimated emission fluxes for the individual volcanoes correspond reasonably well with SO_2 flux measurements of Indonesian volcanoes (Table 3.2).

The emissions of each individual volcano were released into the model layer at the actual

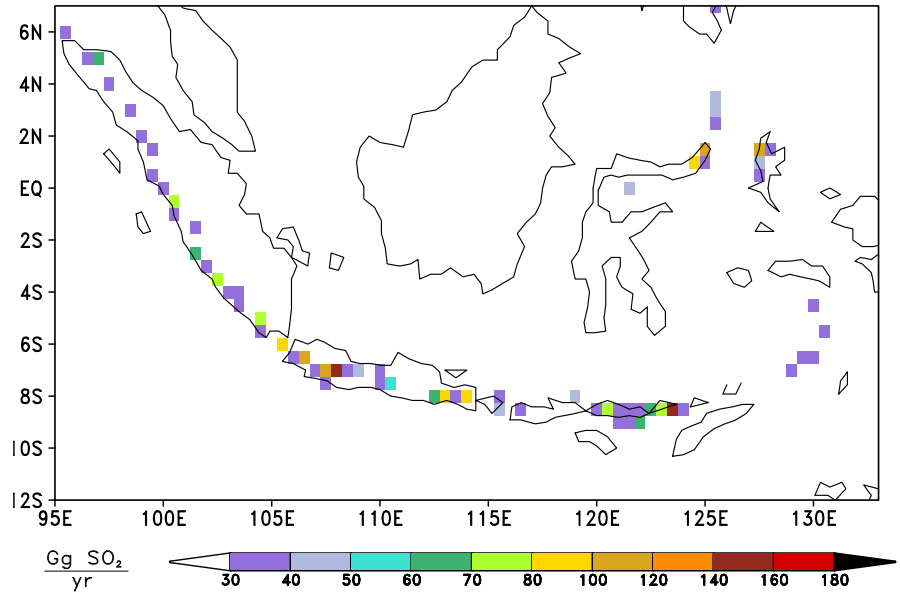

Figure 3.1 Emission inventory of the annual sum of continuous (eruptive + passive) and sporadic (eruptive) volcanic SO_2 emissions.

height of each volcano. The elevations of the volcanoes range from 200 m (Riang Kotang) to 3805 m (Kerinci) corresponding to the first 12 model levels.

3.2.2 Experiments

Two experiments were performed: a) "S Experiment"– volcanic S was released as primarily SO_2 that underwent oxidation to SO_4^{2-} following the major tropospheric chemical reactions and b) "$PbCl_2$ Experiment"– $PbCl_2$ released as an infinitely soluble passive tracer. The "S Experiment" was conducted to observe the transport and deposition patterns of volcanic S: SO_2 + SO_4^{2-}. The volcanic emissions were released into the model as 96 % SO_2 and 4 % SO_4^{2-}. The assumption of an initial presence of some sulfate at the source to account for immediate oxidation processes is common in atmospheric chemistry modeling (e.g. Stier et al., 2005). Calculations have been performed on the results of the "S Experiment" to determine atmospheric SO_2 loss rates from the volcanic plumes. SO_2 loss rate is a function of the concentration of SO_2 at two locations within a volcanic plume, the distance between these two locations, and the time of travel from the first to the second location. The calculations have been performed in order to replicate the analysis of field measurements of tropospheric SO_2 loss rates at individual volcanoes (Oppenheimer

Table 3.2 SO_2 emissions from individual Indonesian volcanoes

Volcano	SO_2 flux from emission inventory (Gg/yr)	SO_2 flux from measurements (Gg/yr)
Bromo (Tengger Caldera)	47.4	5.1[a]
Galunggung	47.7	140.5[b]
		240.9[a]
Merapi	55.6	36.5[c]
		51.1[a]
		73.0[d]
Slamet	45.4	21.2[e]
Tangkubanparahu	37.5	27.4[a]

[a] Andres and Kasgnoc (1998)
[b] Bluth et al. (1994)
[c] Dir. Volc. & Geol. Haz. Mit. of Indonesia (2005)
[d] Le Guern (1982)
[e] Nho et al. (1996)

et al., 1998).

SO_2 loss rate from the model results was calculated as follows: over a given time period (year or season), the mean wind direction of each gridbox containing a volcano ”V” was used to define which of the 8 surrounding gridboxes in the horizontal directions the SO_2 was most likely to be transported to: ”V+1”. This was repeated a second time to define the gridbox “V+2”, a distance of 55 - 200 km (average 120 km) away from the volcano. The mean column burden, or the total mass per area of the given species contained in the entire atmospheric vertical column (up to the top of the model, 10 hPa), of SO_2 at ”V” and ”V+2” were then related following first order kinetics (Equation 3.1).

$$\Phi_{t_1} = \Phi_{t_2} e^{k_1(t_2 - t_1)} \tag{3.1}$$

where:

Φ = Column burden at given time $[kg/m^2]$

$t_2 - t_1$ = time to be transported from location 1 to 2 $[s]$

k_1 = SO_2 loss rate $[s^{-1}]$

The mean wind speed and distance between the two gridboxes were used to calculate the amount of time for transport from ”V” to ”V+2”. The result of the calculation is the yearly or seasonal mean SO_2 loss rate “k_1” for each volcano. Column burden of SO_2 was used in this calculation as opposed to single model level concentrations, as this is a more accurate representation of the data that is obtained by ground-based COSPEC. For some volcanoes, the SO_2 loss rate calculation resulted in a negative or null value. A negative value indicates an increase in the concentration of SO_2 at “V+2” compared with “V”. This can occur when “V+2” contains SO_2 released or transported into the grid box from another volcano. A null value can occur when the wind direction is so variable that the emissions are predicted in the first step to be transported away from the grid box “V” and in the second step returned to it, for a net distance of 0. In both of these situations, the calculated SO_2 loss rates have been excluded from further consideration.

The “$PbCl_2$ Experiment” was conducted to observe the transport and deposition pattern of $PbCl_2$, a highly soluble compound released by volcanoes in relatively large concentrations (e.g. Delmelle, 2003). As $PbCl_2$ is not among the chemicals originally included in REMOTE, we included $PbCl_2$ in the model as an infinitely soluble passive tracer. $PbCl_2$ (solubility $=$ 0.99 g/100 cc ; Lide and Frederikse, 1993) is very soluble, and not infinitely soluble, so the modeling assumption of infinite solubility will lead to a slight over-prediction of the solubility of $PbCl_2$. The $PbCl_2$ is released as a passive tracer, and as such it is transported in the atmosphere and is removed from the atmosphere by wet and dry deposition processes, but it does not react to form other chemical species. The emission inventory was established for volcanic SO_2, so to calculate a corresponding

Table 3.3 Pb/S ratios in Indonesian volcanic gases

Volcano	Pb/S ($\mu g/g$)	Reference
Merapi	420	Nho et al. (1996)
Merapi	35	Symonds et al. (1987)
Papandayan	280	Nho et al. (1996)
Mean	245	the average of the above measurements was applied in this study
Global mean	190	Hinkley et al. (1999)

emission flux of $PbCl_2$ the emissions have been scaled to the ratio of Pb to S in Indonesian fumarolic gases (Table 3.3), which may produce an underestimation of the flux of the volcanic $PbCl_2$, as described earlier.

3.3 Results

The results of the "S Experiment" are presented first, followed by the SO_2 loss rates that have been calculated from these results. The results of the "$PbCl_2$ Experiment" are presented last.

3.3.1 "S Experiment" and calculated SO_2 loss rates

The modeled atmospheric distribution of volcanic S species is shown as annual mean column burden in Figure 3.2 as a) SO_2, b) SO_4^{2-}, and c) total volcanic S (SO_2 + SO_4^{2-}). The atmospheric concentration of SO_2 is much higher than that of SO_4^{2-}, and dominates the sum of the two. The annual mean column burden of SO_2 ranges from 1.5 - 10 kg (S)/km^2 and SO_4^{2-} from 0 - 1.5 kg (S)/km^2. Qualitatively, both SO_2 and SO_4^{2-} show the highest concentrations near to the volcanoes, while away from the volcanoes the concentration decreases, with the dominant transport away from the volcanoes towards the east. Relatively high atmospheric concentrations of the S species are also seen at the northern boundaries of the figures. This is a result of the concentrations of SO_2 and SO_4^{2-} defined at the boundaries of the model domain to represent input from pollution from outside the

modeled region and is not a result of the transport of volcanic S.

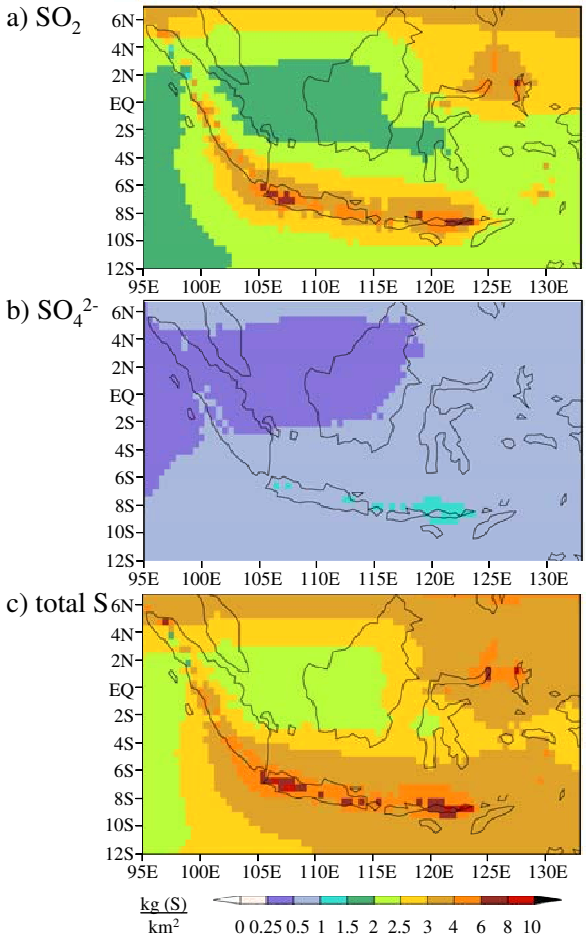

Figure 3.2 Annual mean vertical column burden of **(a)** SO_2, **(b)** SO_4^{2-}, and **(c)** total S: SO_2+SO_4^{2-} for the "S Experiment".

Volcanic S deposition is presented as a) the annual sum of the dry SO_2 deposition, b) dry + wet SO_4^{2-} deposition, and c) the total volcanic S deposition as the sum of the two (Figure 3.3). More than 99 % of SO_4^{2-} is deposited via wet deposition, so only the total SO_4^{2-} deposition is shown. SO_2 is dry deposited in large concentrations close to the volcanoes, up to 3 Mg (S)/km^2, but with almost no deposition away from the volcanoes. SO_4^{2-}, in comparison, has a maximum annual deposition of only up to 1.25 Mg (S)/km^2, with much more significant deposition away from the volcanoes. 83 % of the volcanic S is deposited as SO_4^{2-}. There is an average annual sum of deposition over the entire modeled region of 45.6 kg (S)/km^2 SO_2 and 219.6 kg (S)/km^2 SO_4^{2-}.

The SO_2 loss rates calculated from the model results ($3.2 \times 10^{-7} - 4.1 \times 10^{-5} s^{-1}$)

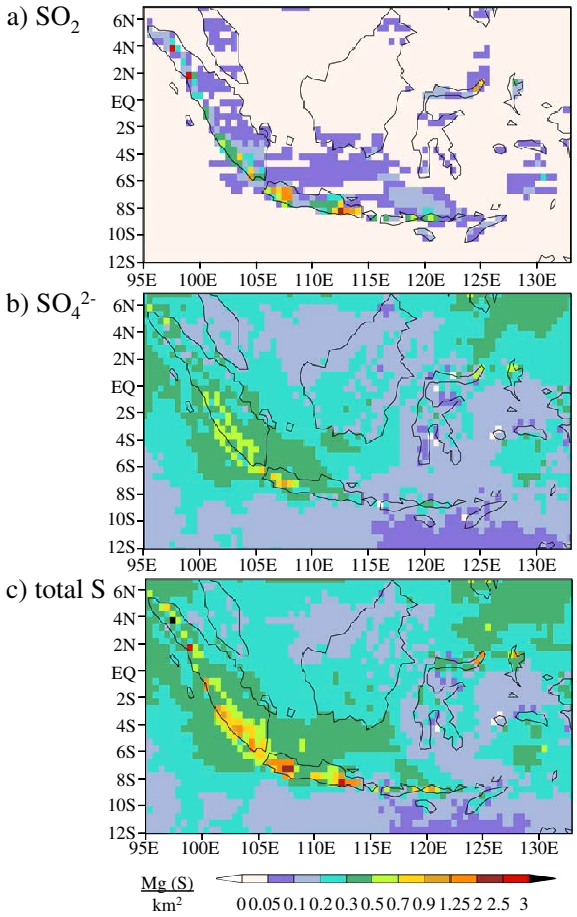

Figure 3.3 Annual sum of the **(a)** dry SO_2 deposition, **(b)** dry + wet SO_4^{2-} deposition, and **(c)** total S: dry SO_2 + dry + wet SO_4^{2-} deposition for the "S Experiment".

agree well in magnitude with SO_2 loss rates measured at individual volcanoes in other parts of the world (1.9 x 10^{-7} - 5.4 x $10^{-3} s^{-1}$) (Figure 3.4) (Oppenheimer et al., 1998). Modeled SO_2 loss rates (yellow squares) are plotted against the actual height of each volcano and measured SO_2 loss rates from Oppenheimer et al. (1998) are plotted against the observed plume height. There is a large variability in SO_2 loss rates measured at different volcanoes, and at Mt. Etna alone, SO_2 loss rates have been observed to vary over 3 orders of magnitude.

Figure 3.5 shows a box plot of the bin wind speed over 1 m/s intervals plotted against SO_2 loss rates. The lower edge of the box represents the 25th percentile value and the upper edge the 75th. The height of each box shows the interquartile range for each bin and is an indicator of the variability of the values. The line across the box indicates the median

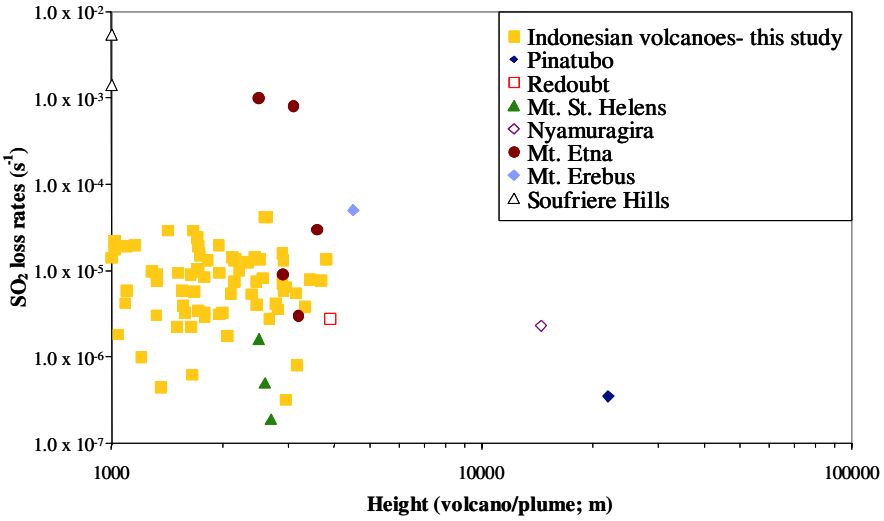

Figure 3.4 Modeled and measured SO_2 loss rates.

(50th percentile). Four outlayer values are shown as open circles and three extreme values as stars. The correlation between windspeed and SO_2 loss rate is weak but statistically significant ($p < 0.01$; $R^2 = 0.2$). There is a general trend of increasing wind speed associated with increased SO_2 loss rates as well as an increase in the variability of the SO_2 loss rates. Temperature and relative humidity, in contrast, demonstrate trivial and non-significant ($R^2 < 0.02$) correlation with SO_2 loss rate. It was relevant to look for a correlation with temperature and relative humidity because these meteorological parameters influence the pathways of SO_2 to SO_4^{2-} formation as well as precipitation, which influences removal processes.

SO_2 loss rates have been calculated for each month and season based on the monsoonal winds: north monsoon (December - March); April/May intermonsoon (April - May); south monsoon (June - September); and October/November intermonsoon (October - November). The north monsoon is distinguished by winds blowing predominantly from China, the south monsoon by winds blowing predominantly from the Indian Ocean and Australia, and the intermonsoon seasons are distinguished by weak and variable direction winds. SO_2 loss rates as a function of season are shown as a box plot in Figure 3.6 with seasonal SO_2 loss rates as green boxes and mean ground-level wind speeds as orange diamonds. Three outlayer values are shown as open circles and one extreme value as a star. The only seasons with outlayers and extreme values are the two monsoon seasons.

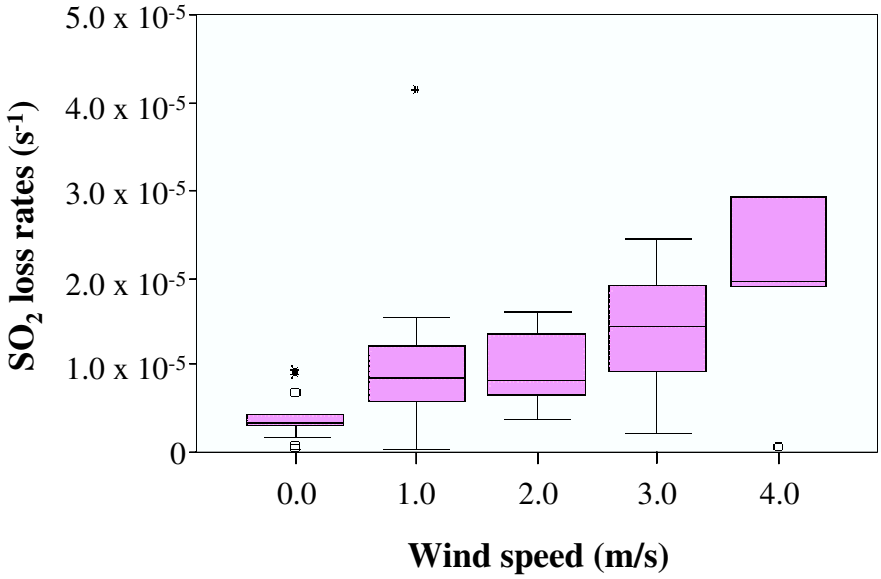

Figure 3.5 Annual mean SO_2 loss rates for each modeled volcano plotted against the annual mean wind speed at the height of each volcano.

Excluding the outlayers and extremes, winter has the lowest variability and spring the highest. The mean seasonal SO_2 loss rates for all volcanoes vary between $9.7 \times 10^{-6} s^{-1}$ (April/May) and $1.3 \times 10^{-5} s^{-1}$ (south monsoon). A greater variability is demonstrated between individual volcanoes than between the seasonal means averaged over all of the volcanoes. The only season with a significantly higher mean SO_2 loss rate is the south monsoon, which is distinguished by the strongest wind speed.

Loss of volcanic SO_2 from the atmosphere can be accomplished via the dry deposition of SO_2 and by oxidation to SO_4^{2-}. There can also be an apparent SO_2 loss due to transport outside of the measured plume (in the field) or outside of the predicted transport route (in the calculations performed on the model results). The percentage of SO_2 lost due to dry deposition was calculated by dividing the annual mean dry deposition of SO_2 for one day by the difference in column burden of SO_2 between locations "V" and "V+1", while the percentage of SO_2 lost due to oxidation was calculated by dividing the annual mean column burden of SO_4^{2-} in grid box "V" by the difference in column burden of SO_2 between locations "V" and "V+1". The remaining lost SO_2 was attributed to lateral transport. The average for all volcanoes within an average of 70 km away from the volcanoes is 53 % of SO_2 loss is due to conversion to SO_4^{2-}, 42 % to dry deposition, and 5 % due to lateral transport. These percentages do not continue at greater distances from the volcanoes.

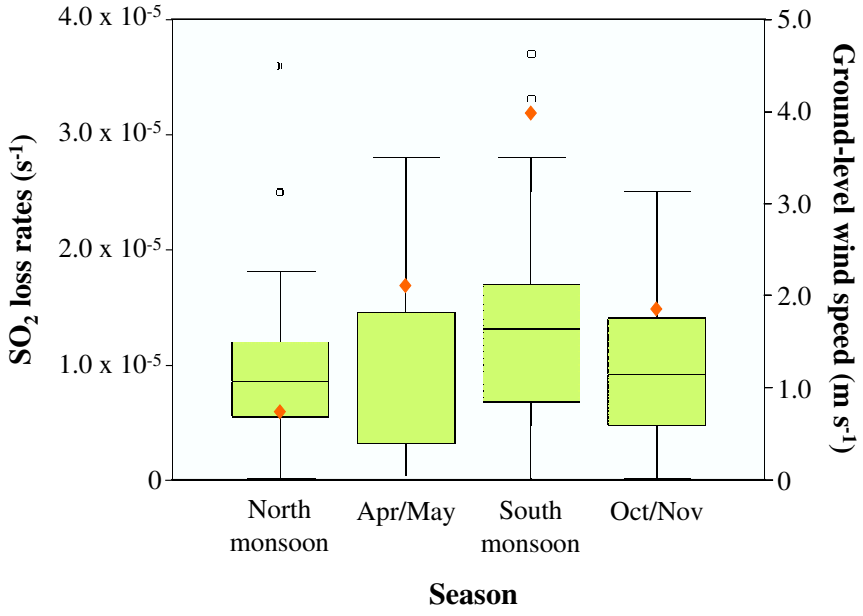

Figure 3.6 Seasonal SO_2 loss rates and ground level wind speeds.

Between locations "V+1" and "V+2" (an average distance of 70-120 km from the volcanoes) the sum of the column burden of SO_4^{2-} and the daily dry deposition of SO_2 is greater than the loss of SO_2. This apparent incongruity can be explained by the transport of SO_2 from other volcanoes into gridbox "V+2". While some sulfate may be transported into box "V+2", the transport of sulfate is much less than that of SO_2 because of sulfate's high solubility and tendency to be washed out of the atmosphere very quickly. Despite the fact that the percentage loss analysis fails between boxes "V+1" and "V+2" due to SO_2 from neighboring volcanoes, we have applied the SO_2 loss rate equation between points "V" and "V+2" rather than between "V" and "V+1". This is because there is only a small difference in the calculated annual mean SO_2 loss rate (e-folding rate of 1.3 day versus 1 day) while there is an increase of 1.5 times as many volcanoes that must be excluded from the loss rate calculation between points "V" and "V+1" compared with between "V" and "V+2".

Temperature, relative humidity, and wind speed have been related to the relative percentage of SO_2 lost due to the dry deposition of SO_2, oxidation to SO_4^{2-}, and transport outside of the predicted plume pathway to see if there is any correlation between variations in the meteorological conditions and the manner in which SO_2 is lost. No such correlation was

found.

3.3.2 ”$PbCl_2$ Experiment”

The modeled atmospheric distribution of volcanic $PbCl_2$ is shown as annual mean column burden in Figure 3.7. The annual mean column burden of $PbCl_2$ ranges from 0 - 3 g (Pb) / km^2. Atmospheric $PbCl_2$ is found in greatest concentrations near to the volcanoes, with only slight easterly transport. The annual sum of the wet and dry $PbCl_2$ deposition is shown in Figure 3.8. More than 99 % of $PbCl_2$ is deposited via wet deposition, so only the sum of the two is presented. The $PbCl_2$ is deposited in concentrations of up to 2 kg (Pb) / km^2 with an average annual sum of 52 g (Pb) / km^2 of $PbCl_2$ deposited in the modeled region.

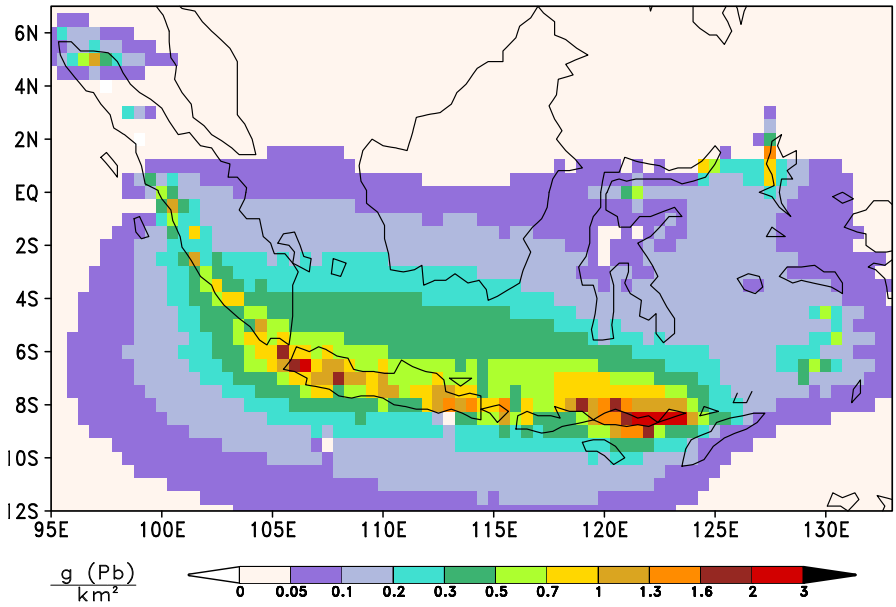

Figure 3.7 Annual mean column burden of $PbCl_2$ for the “$PbCl_2$ Experiment”.

Both the atmospheric burden and deposition of Pb are three orders of magnitude less than that of S. In both experiments, deposition is relatively uniform with relation to distance from any given volcano and not very distinctive for individual volcanoes. We attribute this to the resolution of the model experiments and to the assumption of an even distribution of the continuous volcanic emissions between the active volcanoes. $PbCl_2$ is rapidly deposited very close to the volcanoes, resulting in high local concentrations and a sharp

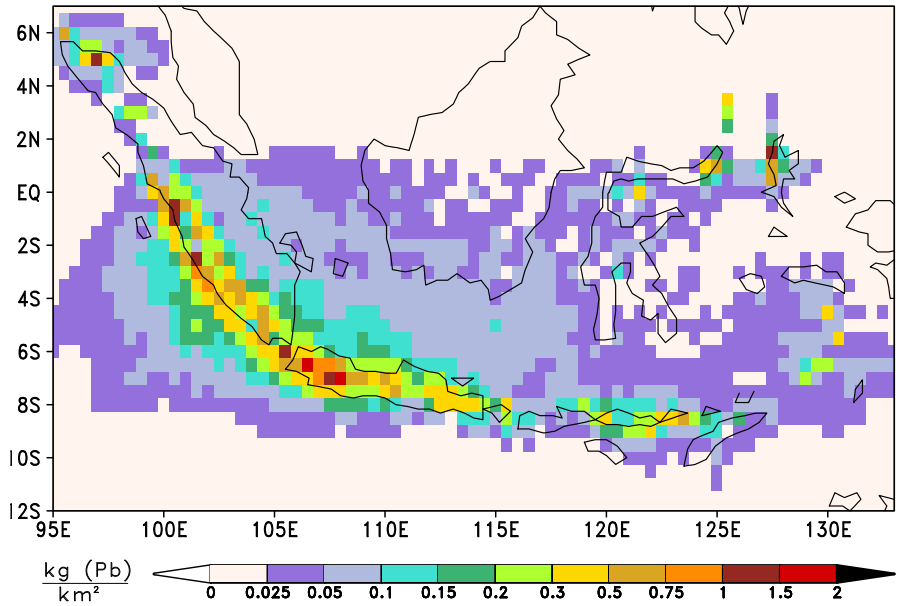

Figure 3.8 Annual sum of dry + wet $PbCl_2$ deposition for the "$PbCl_2$ Experiment".

decline in deposition at greater distances from the volcanoes. While SO_2 is calculated to have an annual mean loss rate of 1.1 x $10^{-5}s^{-1}$, or an e-folding rate of approximately 1 day, $PbCl_2$ is calculated to have a loss rate of 5.3 x $10^{-5}s^{-1}$, or an e-folding rate of approximately 0.2 day. SO_2 is less soluble in rain than $PbCl_2$, and has some dry deposition, but is mostly transported away from the volcanoes prior to conversion to water-soluble SO_4^{2-}. Because most of the SO_2 is transported and then converted to SO_4^{2-} rather than deposited directly as SO_2, there is more S deposition at increasing distances from the volcanoes compared with $PbCl_2$, creating a less steep gradient of S deposition (Figure 3.9), and hence, the larger e-folding rate.

3.4 Discussion

We will interpret the modeling results and discuss how these results can be used to address the two questions described above: 1) How do variable meteorological conditions influence volcanic SO_2 concentration in the atmosphere and SO_2 loss rates? and 2) How do the transport and deposition patterns of highly soluble volcanic compounds relate to SO_2? After addressing these two questions, we will consider how the volcanic emissions may have influenced the peat forests in the region.

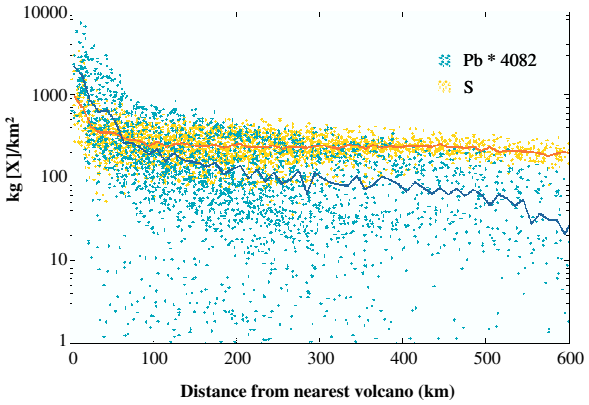

Figure 3.9 Annual sum of total deposition for each modeled grid box as a function of the distance to the nearest volcano ("$PbCl_2$ experiment": blue; "S experiment": yellow). The solid lines (corresponding colors) are the bin mean over 10 km intervals. To show the S and Pb on the same scale, the Pb has been multiplied by 4082, the inverse ratio of Pb / S in Indonesian fumarolic gases.

3.4.1 Meteorological influences on SO_2 loss rate

The large variabilities of SO_2 loss rates measured at individual volcanoes have been attributed to variable atmospheric and plume conditions (Oppenheimer et al., 1998). Our model results suggest, albeit weakly, that the meteorological condition most significantly influencing the variability of SO_2 loss rates is wind speed. The suggested relationship between stronger winds and greater SO_2 loss rates may indicate an increase in dry deposition at higher winds. Within the model, dry deposition is dependent on turbulence, which is enhanced by stronger winds. We did not find, however, a correlation between increased wind speed and an increased percentage of SO_2 lost due to dry deposition. A simpler explanation for the correlation between increased SO_2 loss rate and increased wind speed is that given a constant emission rate, stronger winds transport mass away from an emission source more quickly, reducing the concentration of SO_2 found at a given distance from a volcano. A relationship between stronger winds and greater variability of SO_2 loss rates has been shown. The ramifications of this are that it may be more difficult to obtain a characteristic SO_2 loss rate for a volcano that is exposed to highly variable wind conditions, as opposed to a volcano that is exposed to more constant winds.

The environmental conditions in this study are unique for Indonesia. There are a large number of active volcanoes close to each other, potentially resulting in overlapping

plumes. The transport of SO_2 from other volcanoes into gridboxes under consideration produces a complication for the analysis of the SO_2 loss rates. The strong year-round solar radiation and high rainfall of Indonesia promotes the rapid oxidation of SO_2 to sulfate and the rapid deposition of sulfate. The conclusions drawn in this study about the atmospheric loss of volcanic SO_2 are only applicable to this region and should be extrapolated to other volcanic regions cautiously. Further fieldwork-based research that considers variations in wind speed and apparent SO_2 loss rates may be able to form a more conclusive statement about the possible correlation between wind speed and SO_2 loss rates. If there is indeed such a relationship, it may be important to consider wind speed variations when making interpretations about changes in volcanic activity based on remote SO_2 measurements. Some variations in SO_2 flux observed over time at one volcano may be due to differences in the winds, as opposed to variations in the volcanic emissions.

3.4.2 Differences in transport and deposition patterns due to solubility

The influence of solubility on deposition patterns is illuminated by comparing the results of the two performed experiments (Figure 3.9). The dependency of deposition rate on solubility has implications for the accurate extrapolation of measurements of SO_2 flux in aged volcanic plumes to other compounds. The further away from a volcano such measurements are made, the less accurate it is to assume that the concentration of volcanic SO_2 measured there has the same ratio to more soluble species as the ratio measured in fumarolic gases.

The ratio of $[PbCl_2]/[SO_2]$ in the air decreases with increasing distance from the volcanoes as the $PbCl_2$ is deposited (Figure 3.10). Figure 3.10 is a box plot with the same specifics as for Figures 3.5 and 3.6. Four outlayer values are shown as open circles at location “V”. The interquartile range increases at greater distance from the volcanoes indicating that the variability of the $[PbCl_2]$ / $[SO_2]$ ratio is growing at greater distances from the volcanoes. The median $[PbCl_2]$ / $[SO_2]$ ratio decreases exponentially at greater distances from the volcanoes with the mean exponential rate of decay of the $[PbCl_2]$ / $[SO_2]$ ratio based on these three distances being $y = 106.5e^{-0.002x}$.

where:

y = $[PbCl_2]$ / $[SO_2]$ $(\mu g/g)$

x = distance from volcanoes (km).

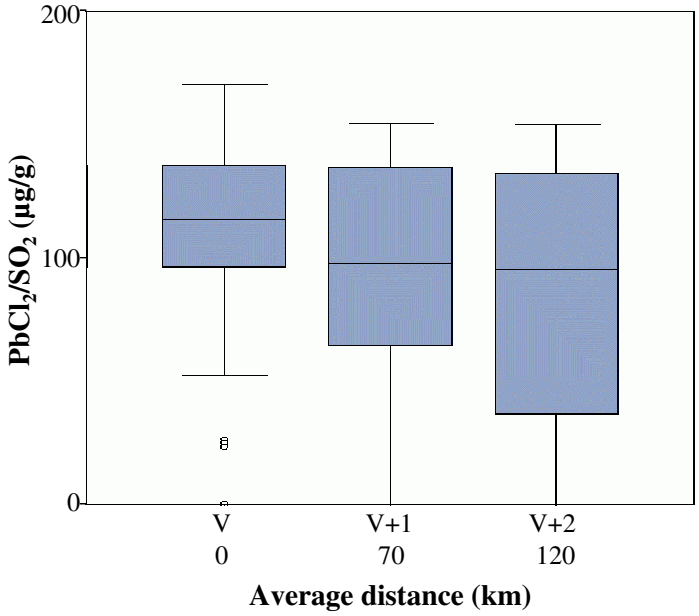

Figure 3.10 Annual mean column burden of $[PbCl_2]/[SO_2]$ for all volcanoes plotted against the mean distance from each volcano (km) for locations "V", "V+1", and "V+2".

The mean $[PbCl_2]$ / $[SO_2]$ ratio at the three distances are: "V" = 107.7; "V+1" = 89.3; and "V+2" = 83.2 $\mu g/g$. The ratio of 107.7 μg $PbCl_2$ / g SO_2 is equivalent to 160.5 μg Pb / g S. This differs from the 245 μg Pb / g S defined as the ratio of Pb / S in the primary volcanic emissions (Table 3.3) because of SO_2 released by other volcanoes and transported into gridbox "V".

Based on this mean rate of decay, we estimate that calculations (e.g. based on COSPEC measurements) which assume a constant [X]/[S] ratio as found in fumarolic gases will result in a 6 % underestimation of the emission flux of highly soluble species at 30 km distance away from a volcanic vent; at 100 km, this would grow to an 18 % underestimation. Our results indicate that the assumption of a constant ratio between SO_2 and other, highly soluble species such as $PbCl_2$ is justified at distances where COSPEC is usually performed.

3.4.3 Comparison between modeled S deposition and peat core samples

We have used the modeling results to examine the hypothesis proposed by Langmann and Graf (2003) that the Indonesian volcanic emissions have had a significant influence on the sulfur content of peat in the area. In order to assess the potential contribution of volcanic emissions to the sulfur content of Indonesian peat, we have compared the modeled S deposition with the concentration of S measured in peat core samples collected in the modeled region. Peat can serve as a historical record of atmospheric deposition for time periods of up to thousands of years. The peat areas of Indonesia may be particularly useful recorders of the deposition of volcanic emissions because of the large number of historical and modern active volcanoes in the vicinity of peat areas (Langmann and Graf, 2003). It has been suggested in several studies that anomalous, high concentrations of S and other chemicals including Pb in peat core samples (collected outside of Indonesia) may be due to volcanic deposition (e.g. Weiss et al., 1997; Roos-Barraclough et al., 2002; Kylander et al., 2005). Within Indonesia, there are two main types of peat: ombrogenous and topogenous (Page et al., 1999). Ombrogenous peat receives nutrients only from atmospheric deposition while topogenous peat also receives nutrients from groundwater. Ombrogenous peat is therefore more useful for interpreting the historical deposition of atmospheric compounds. In this work we have compiled measurement data from the literature of S in four ombrogenous peat areas in Indonesia for comparison with the modeled S deposition (Figure 3.11; Table 3.4).

The average S of each sampled peat core was calculated by multiplying the average percent S in each of the four peat sampling locations with the average peat dry bulk density (0.18 g/cm^3) given by Shimada et al. (2001). This value was multiplied by the minimum (1.7 mm/yr) and maximum (4.3 mm/yr) peat accumulation rates provided by Supardi et al. (1993), resulting in the presented range of values for the S deposition of each peat core. The average % S was calculated from 3-16 samples within each peat core. Peat core samples had both total S and ^{14}C age measured, or had only total S measured and were very close to another peat sample where ^{14}C was measured. S values from portions of the peat cores that were dated to be less than 150 years old were not included in the average as these S values may have been influenced by human activity.

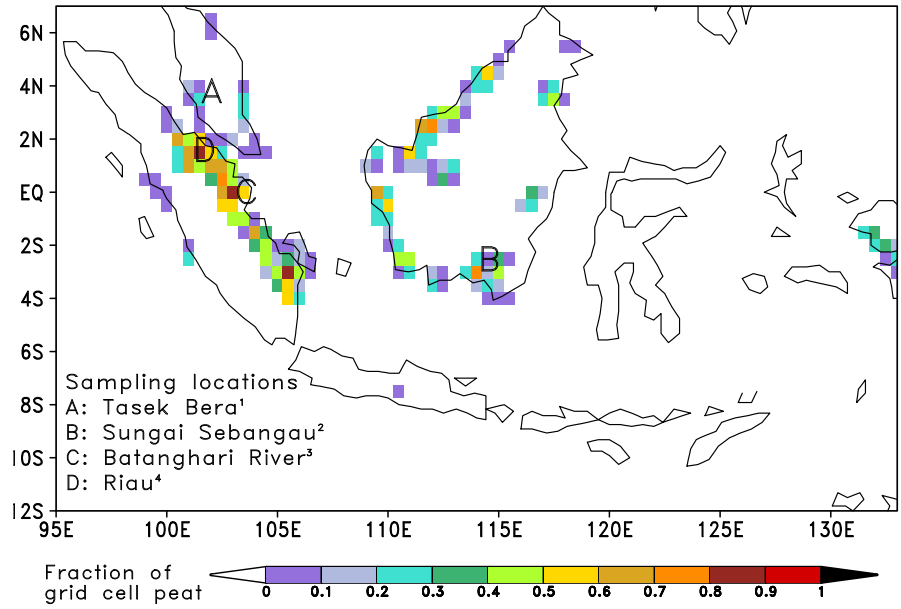

Figure 3.11 Peat sampling locations on a map of the fractional peat coverage of the modeled region (after Heil et al., 2006).
[1] Wüst and Bustin (2001)
[2] Weiss et al. (2002)
[3] Esterle and Ferm (1994)
[4] Supardi et al. (1993)

A comparison between the modeled S deposition and the rate of S deposition measured in the peat core samples reveals values with the same orders of magnitude (Table 3.4). The potential volcanic contribution to the peat S has been calculated on the basis of what percentage of the peat S could be attributed to the deposition of volcanic S. We find that 6 - 72 % of the S measured in the peat samples could have volcanic origin. There is a relatively uniform concentration of volcanic S predicted to be deposited on all four peat areas (215 - 285 kg / km^2-yr). This is because of the distance between the peat areas and the nearest volcanoes (minimum 153 km) and the relatively homogeneous modeled deposition of S at these distances from the volcanoes. It would be helpful to be able to compare the model results with a peat sample collected nearer to the volcanoes, but we have not been able to obtain such a sample. We find the agreement in scale to be a strong indication that the modeled deposition of the volcanic S is reasonable.

Our modeling results indicate that the Indonesian volcanoes have contributed slightly to the quantitative sulfur content of peat in the region. This does not suggest that the volcanic

Table 3.4 Comparison of modeled S deposition and peat core samples

Sampling location	Distance to nearest volcano (km)	Measured S accumulation (kg/km^2-yr)	Modeled S deposition (kg/km^2-yr)	Volcanic S (%)
Riau (A)	153	398–1006[1]	285	28–72
Batanghari River (B)	160	1744–4412[2]	264	6–15
Tasek Bera (C)	258	796–2012[3]	215	11–27
Sungai Sebangau (D)	396	428–1084[4]	253	23–59

[1]Supardi et al. (1993)
[2]Esterle and Ferm (1994)
[3]Wüst and Bustin (2001)
[4]Weiss et al. (2002)

The letters in parenthesis refer to the sampling locations marked in Figure 3.11.

S has little qualitative contribution to the the peat's characteristics. Sulfur cycling within peat is complicated, and peat is not a closed system. Moore et al. (2004) have found that approximately 75 % of anthropogenic S deposited onto peat in eastern Canada is accumulated within the peat. This value may differ depending on the different origins of the S, such as volcanoes, sea spray, and anthropogenic pollution, as this may dictate the state of the deposited S. Thompson and Bottrell (1998) have demonstrated that *Sphagnum*, a common peat plant in Northern latitude peat areas but not in Indonesia, preferentially incorporates partially reduced sulfur species, and it follows that the source of deposited S may influence how it is incorporated into Indonesian peat. Within peat, sulfur can be reduced by bacterial activity, given off as H_2S gas, and transported downwards and laterally out of the peat dependent on the local hydrology (Novák et al., 2005). This study cannot address how the volcanic S may have influenced the properties of the peat, and a field study incorporating other additional tracers for volcanic activity could shed more light on this question.

3.5 Conclusions

This study demonstrates that realistic modeling of volcanic emissions can lead to an improved understanding of the atmospheric processes occurring in the vicinity of active volcanoes. The results of the study show that SO_2 loss rates from the plumes of the Indonesian volcanoes are weakly correlated with wind speed and uncorrelated with relative humidity or temperature and that there is no correlation between these three meteorological phenomena and the relative amount of SO_2 lost due to the dry deposition of SO_2, conversion to SO_4^{2-}, or lateral transport. A relationship is demonstrated between increased wind speed and increased variability of SO_2 loss rates. We recommend that further fieldwork-based research be conducted to explore the possible relationship between wind speed and apparent SO_2 loss rates as variations in wind speed might lead to changes in SO_2 loss rates independent of a change in the state of volcanic activity.

The solubility of the Indonesian volcanic emissions is shown to influence whether they are deposited near to the volcanoes or transported prior to deposition. Highly soluble species such as $PbCl_2$ have high deposition rates near to the volcanoes while the relatively insoluble SO_2 is transported away from the volcanoes until it is oxidized to SO_4^{2-} and then rapidly deposited. The ratio of highly soluble species / [SO_2] decreases exponentially at greater distances from the volcanoes. Our results indicate that an assumption of a constant ratio between highly soluble species and SO_2 from the fumarole to the distances where COSPEC is usually performed is justified at individual volcanoes. Extrapolating from SO_2 measurements to establish global inventories may, however, generate a significant underestimation of the emission rates of highly soluble species, and the solubility effect should be considered.

Acknowledgements

We thank M. Halmer and an anonymous reviewer for their help in focusing the manuscript and making the results clearer. We thank Elina Marmer, Angelika Heil, Patrick Wetzel, and Philipp Weis for their help and discussion and for internally reviewing the manuscript. We also thank the German Climate Computing Center (DKRZ) for computer time to run these experiments. MAP was funded by a stipend from the Ebelin and Gerd Bucerius ZEIT Foundation through the International Max Planck Research School on Earth System Modeling.

Chapter 4

The role of anthropogenic and volcanic emissions during the 1997 Indonesian wildfire pollution event

Abstract

We have used the regional atmospheric chemistry and climate model REMOTE to examine how "background" anthropogenic and volcanic pollution interacted with emissions from the catastrophic Indonesian wildfire of 1997. The model results demonstrate that anthropogenic emissions from major cities in the region increased the atmospheric concentration of O_3, CO, NO_2, and SO_2 above the levels generated by the fires. The anthropogenic emissions increased the number of days and extended the distance from the fires where O_3 exceeded the Indonesian hourly air quality standard. The increased levels of O_3 due to the anthropogenic emissions enhanced the conversion of SO_2 released by the fires to SO_4^{2-}, demonstrating that the urban pollution actively altered the atmospheric behavior and lifetime of the fire emissions. Under the conditions present during the wildfire, volcanic emissions had little influence on surface pollution from the fires.

4.1 Introduction

Air pollution is one of Indonesia's largest environmental problems, having a significant impact on public health and disrupting the Indonesian economy (Aiken, 2004). Elevated concentrations of lead, particulate matter, carbon monoxide, hydrocarbons, sulfur dioxide, and nitrogen dioxide are found in all large cities in the country. Motor vehicles, forest fires, and the industrial sector are considered to be the greatest contributors to the air pollution problem (Energy Information Administration). Land-clearing fires are set every year in Indonesia during the dry season, releasing gases and particles referred to as haze into the atmosphere. These fires are typically extinguished at the onset of the north monsoon rains in October-November. In 1997, however, strong El Niño conditions delayed the onset of the rains and promoted the worst drought conditions in 50 years (Khandekar et al., 2000), allowing the fires to burn uncontrolled for a longer time than usual. Between August and November 1997, land-clearing fires in Kalimantan and Sumatra grew out of control into wildfires producing an environmental disaster. The El Niño conditions also reduced convective activity in the region, preventing the emissions from the fires from mixing upwards in the atmosphere (Heil and Goldammer, 2001). This had the effect of generating high surface concentrations of the pollutants that were transported over a large part of Southeast Asia. While Indonesia experienced the brunt of the pollution effects from the fires (Frankenberg et al., 2004), a multitude of transboundary health and economic problems, significantly in Malaysia (Sastry, 2002; Khandekar et al., 2000) and Singapore (Koe et al., 2001), were also felt. The 1997 fires and their effects have been studied using several different methods, including stationary, balloon, and airplane measurements, satellite observations, illness and mortality surveys, and numerical modelling of atmospheric processes.

The surface and tropospheric concentrations of the fires' emissions including particulate matter (PM), SO_2, CH_4, CO, NO_x, and secondarily produced O_3 were enhanced within the region for all observed pollutants (Davies and Unam, 1999; Fujiwara et al., 1999, 2000; Matsueda et al., 1999; Tsutsumi et al., 1999; Yonemura et al., 2002a,b). Even measurements performed several hundred kilometers from the fires demonstrated significantly elevated concentrations for all of these compounds. Ground-level observations of

the extent of the area burned and of the dispersion of the fires' pollution are relatively sparse, making satellite observations of the region a very important tool. The extent of the fires and associated haze were observed using Advanced Very High Resolution Radiometer (AVHRR) data (Wooster et al., 1998; Fang and Huang, 1998). Nakajima et al. (1999) used AVHRR data to study sulfate and carbonaceous aerosol optical thickness due to the fires, finding that the peak enhancement occurred in October and that the smoke from the fires was dominated by small submicron aerosol particles. The Total Ozone Mapping Spectrometer (TOMS) was used to observe tropospheric column O_3 (TCO) and tropospheric water vapor (Chandra et al., 1998) and total atmospheric O_3 (Kita et al., 2000). TOMS indicated about 10-20 Dobson Units (DU; $1\ \text{DU} = 2.69 \times 10^{16}$ molecules cm^{-2}) of increased tropospheric ozone over the Indonesian region (Chandra et al., 1998) while ground-based measurements indicated an increase of up to 35 DU (Fujiwara et al., 1999). By comparing AVHRR and TOMS data, Nakajima et al. (1999) suggest that sulfate aerosol particles may travel further from the fires than carbonaceous aerosol particles because of the time required for SO_2 released by the fires to convert to sulfate aerosol. Increased tropospheric column concentrations of NO_2, O_3, and H_2CO were observed by the Global Ozone Monitoring Experiment (GOME) during the fires (Burrows et al., 1999).

Several studies into the environmental and radiative effects of the fire emissions have been conducted using climate and aerosol models. A global chemical transport model with a mean climatological state rather than the actual meteorological conditions present during the fire was used by Hauglustaine et al. (1999) to study the increase in tropospheric O_3 due to precursor species released by the fires. A global atmospheric chemistry and transport model was applied by Chandra et al. (2002) who demonstrated a strong enhancement of TCO over Indonesia and most of the western Pacific and a decrease in TCO in the eastern Pacific, concluding that both the fires' emissions and El Niño specific meteorological conditions contributed to the O_3 anomaly. Duncan et al. (2003) expanded on the work of Chandra et al. (2002) using the same model and gaseous emissions while adding the radiative and chemical effects of black carbon (BC) and organic carbon (OC) aerosols from the fires in their study. A major result of this paper was that the dominant transport mechanisms for the CO released by the fires included deep convection off the northwest coast of Sumatra and outflow from Indonesia via easterly winds to the Indian Ocean and

via northwesterly winds to the South Pacific Ocean. They found that the net effect of the fires was to reduce OH and the oxidizing capacity of the troposphere and to reduce radiative forcing at the earth's surface, predominantly by OC and BC. Podgorny et al. (2003) applied an aerosol optical model producing results that agree with those of Duncan et al. (2003): that the aerosol particles released by the fires generated an enhancement in atmospheric solar heating and a corresponding decrease in solar flux reaching the surface over the equatorial region ranging from west of Indonesia to Papua New Guinea. A large uncertainty in these early studies is in the emission inventory applied for the fires, in particular the contribution of peat fires to total fire emissions. Langmann and Heil (2004) and Heil et al. (2006) applied a regional atmospheric chemistry and climate model to study the atmospheric concentration of particulate matter released by the fires. Their simulations were used to resolve uncertainty about different emission scenarios in order to better constrain how much particulate matter was released by the fires, and how much the burning of peat forest contributed to the total pollution.

The present work is able to contribute to a better understanding of this environmental catastrophe because we have conducted the first study of this event that applies a high-resolution regional model including full tropospheric chemistry. We have further included a new improved emission inventory- the RETRO emission database (Schultz et al., submitted, in prep.). In order to model the event as realistically as possible, we have also attempted to include the natural background emissions in the region and this is the first study to include the regionally significant volcanic emissions of SO_2. The fires occurred in an environment of increasing economic development and decreasing environmental quality. This contributed both to the scale of the fires as well as to the levels of air pollution present in the region prior to the burning season from motor vehicles and industry. The goal of this study is to understand if the "background" anthropogenic and volcanic pollution in the region amplified the extent or severity of the air pollution event caused by the 1997 Indonesian wildfires.

4.2 Experimental Setup

In this section we will describe the experiments performed for this study. First, the model will be introduced. Then, the inventories for the anthropogenic, fire, and volcanic emissions will be described. Finally, the three experiments performed for this work will be explained.

4.2.1 Model

The regional atmospheric chemistry model REMOTE (REgional MOdel with Tracer Extension; Langmann, 2000) has been used for this study. REMOTE combines the physics of the regional climate model REMO 5.0 with tropospheric chemical equations for 63 chemical species. The physical and dynamical equations in the model (Jacob, 2001) are based on the regional weather model EM/DM of the German Weather Service (Majewski, 1991) and include parameterizations from the global ECHAM 4 model (Roeckner et al., 1996). The chemical tracer transport mechanisms include horizontal and vertical advection (Smolarkiewitz, 1983), convective up- and down-draft (Tiedtke, 1989), and vertical diffusion (Mellor and Yamada, 1974). Trace species can undergo chemical decay in the atmosphere or can be removed from the atmosphere by wet and dry deposition or transport out of the model boundaries. Dry deposition is dependent on friction velocities and ground level atmospheric stability (Wesley, 1989). Wet deposition is dependent on precipitation rate and mean cloud water concentration (Walcek and Taylor, 1986). 158 gasphase reactions from the RADM II photochemical mechanism (Stockwell et al., 1990) are included. 43 longer-lived chemical species are transported between gridboxes and 20 are calculated but too short-lived to be transported.

The model was applied with 20 vertical layers of increasing thickness between the Earth's surface and the 10 hPa pressure level (approximately 23 km). The model domain covers Indonesia and Northern Australia (91° E - 141° E; 19° S - 8° N) with a horizontal resolution of 0.5° (approximately 55 km). Analysis data of weather observations from the European Centre for Medium-Range Weather Forecasts (ECMWF) were used as meteorological boundary conditions every 6 hours. Results from a global chemical transport

model (MOZART; Horowitz et al., 2003) simulation for the year 1990 (Granier et al., 2003) were used as chemical concentration boundary conditions every 6 hours for 14 chemical species including O_3, CH_2O, and H_2O_2. Background concentrations for 25 other species (Chang et al., 1987) including SO_2 and SO_4^{2-} were specified at the lateral model boundaries. The physical and chemical state of the atmosphere was calculated every 5 minutes.

4.2.2 Emission inventories

The emissions have been divided into three categories: anthropogenic, fire, and volcanic. The Indonesian fires were set by people and are hence an anthropogenic source. For the purposes of this paper, however, the fire emissions are treated as distinct from the other anthropogenic emissions. The anthropogenic and fire emissions include 18 and 19 species, respectively, including SO_2, CO, and NO_2. Some of the anthropogenic species vary monthly while others are an annual mean. The variations of the anthropogenic emissions are small, and so these emissions are shown for only one month, October 1997. All fire species vary monthly, with large variations, so the fire emissions are shown for September, October, and November 1997. The volcanic emissions are a mean value that do not vary monthly and include only SO_2 and SO_4^{2-}.

Anthropogenic emissions

The anthropogenic emission inventory (Table 4.1) was assembled using data available from the Global Emissions Inventory Activity (GEIA, 2006) website. Data was included from the RETRO emission database (Schultz et al., in prep.) and the Edgar V2.0 emission database (Olivier et al., 1996; Bouwman et al., 1997). The RETRO emissions are available as monthly data in 0.5° resolution (the resolution of the model experiments). In the RETRO emissions, a discontinuity occurs at the equator due to the change in the seasons between the northern and southern hemispheres. As the equator is significant in the domain of these model experiments, the RETRO emissions for the southern hemisphere have been applied with the northern hemisphere seasonal cycle to avoid this discontinuity. The data provided from the other sources are available as annual means for the year 1985

or 1990 in 1.0° resolution and have been interpolated to 0.5° for the experiments. The Indonesian anthropogenic emissions range from 1 - 6 % of the global total of anthropogenic emissions.

Fire emissions

The fire emission inventory (Table 4.2) is from the RETRO emission database (Schultz et al., submitted). The emissions (as for the anthropogenic RETRO emissions) are available as monthly data in 0.5° resolution. The species included within the anthropogenic and fire inventories differ in that the fire emissions do not include higher alkanes or butane (which are oxidized in fires very quickly) while the anthropogenic emissions do not include isoprene (which is mainly emitted by vegetation), OC, or total particulate matter (TPM). All of the fire emission species increase dramatically in the dry season (northern hemisphere autumn) compared with the wet season (northern hemisphere spring). In September (the peak month of fire emissions), these emissions range from 62 - 95 % of the global total of fire emissions.

Table 4.1 Indonesian anthropogenic emissions for October 1997

Species	Emissions Gg Oct. 1997
Acetaldehyde[a]	22.3
Alkanes[a;*]	74.0
Aromatics[a;**]	13.0
Black carbon[b]	43.2
Butane + Propane[c]	36.2
CO[c]	2402.0
Ethane[c]	27.7
Ethene[c]	40.5
Formaldehyde[a]	8.2
Ketones[a]	8.4
NH_3[d]	145.8
NO[c]	139.0
NO_2[c]	8.9
Propene[c]	18.7
SO_2[e]	39.8
SO_4^{2-}[e]	2.5
Toluene[c]	22.1
Xylene[c]	15.3

[a] Edgar V2.0; benchmark year 1990

[b] GEIA original inventory; benchmark year 1985; Penner et al. (1993); Dignon et al. (1994)

[c] RETRO

[d] Edgar V2.0; benchmark year 1990; Bouwman et al. (1997)

[e] GEIA original inventory; benchmark year 1985; Benkovitz et al. (1996)

[*] Hexane and higher

[**] Excluding benzene, toluene, xylene, methyl benzene, and trimethyl benzene

Table 4.2 Indonesian fire emissions for September-November 1997

Species	Emissions Gg Sep. 97	Emissions Gg Oct. 97	Emissions Gg Nov. 97
Acetaldehyde	1608.1	1329.3	448.0
Black carbon	355.4	266.2	89.8
Formaldehyde	1151.0	913.6	307.9
CO	134708.3	108791.7	36662.5
Ethane	887.1	689.7	232.0
Ethene	1994.8	1589.8	535.4
Isoprene	544.5	461.1	155.4
Ketones*	940.4	760.6	256.4
NH_3	8408.3	7065.5	2380.7
NO_2	82.6	63.9	21.6
NO	1293.5	999.6	338.1
Organic Carbon	5006.8	3970.4	1338.0
Propane	629.2	479.7	161.1
Propene	2010.3	1634.4	550.2
SO_2	1960.2	1634.0	550.6
SO_4^{2-}	122.5	102.1	34.4
Toluene	730.3	606.4	204.3
TPM	24790.8	20572.5	6935.7
Xylene	69.2	55.6	18.7

*Acetone

Volcanic emissions

The volcanic emission inventory (Table 4.3) was established for this work to represent “realistic” emissions, as contrasted with the ”maximum” emission estimates described in Pfeffer et al. (2006a). This ”realistic” emission estimate takes the 290 Gg (SO_2)/yr calculated to be released eruptively in Indonesia (Pfeffer et al., 2006a), and assumes a ratio of 60 % of emissions released eruptively to 40 % released passively as given by Halmer et al. (2002). This results in an estimate of 194 Gg (SO_2)/yr released passively by the Indonesian volcanoes. The sum over Indonesia of passive and eruptive volcanic emissions is 484 Gg (SO_2)/yr. Estimates of Indonesian volcanic emissions from other authors are presented in Table 4.3. The emissions of each individual volcano were released into the

model layer at the height of each volcano, which lie within the bottom 12 model levels.

Figure 4.1 shows the total emissions from anthropogenic, fire, and volcanic sources for SO_x (SO_2 + SO_4^{2-}) and the total emissions from anthropogenic and fire sources for NO_x (NO_2 + NO) and CO for February and September 1997. For all three species, the fire emissions strongly dominate in September while they are minor in February. Because of the severity of the fires, the total emissions are also greatly increased in September. It can be seen that the fires in September 1997 were strongest in southern Kalimantan and southeastern Sumatra.

Table 4.3 Estimates of Indonesian volcanic emissions

	Emissions (Gg (SO_2)/yr)		
Author	Eruptive	Non-eruptive	Combined
Hilton et al. (2002)	-	120	-
Spiro et al. (1992)	-	210	-
Nho et al. (1996)	1900	1600	3500
Halmer et al. (2002)	-	-	2100-2600
Pfeffer et al. (2006a)	290	3500	3790
this study	290	194	484

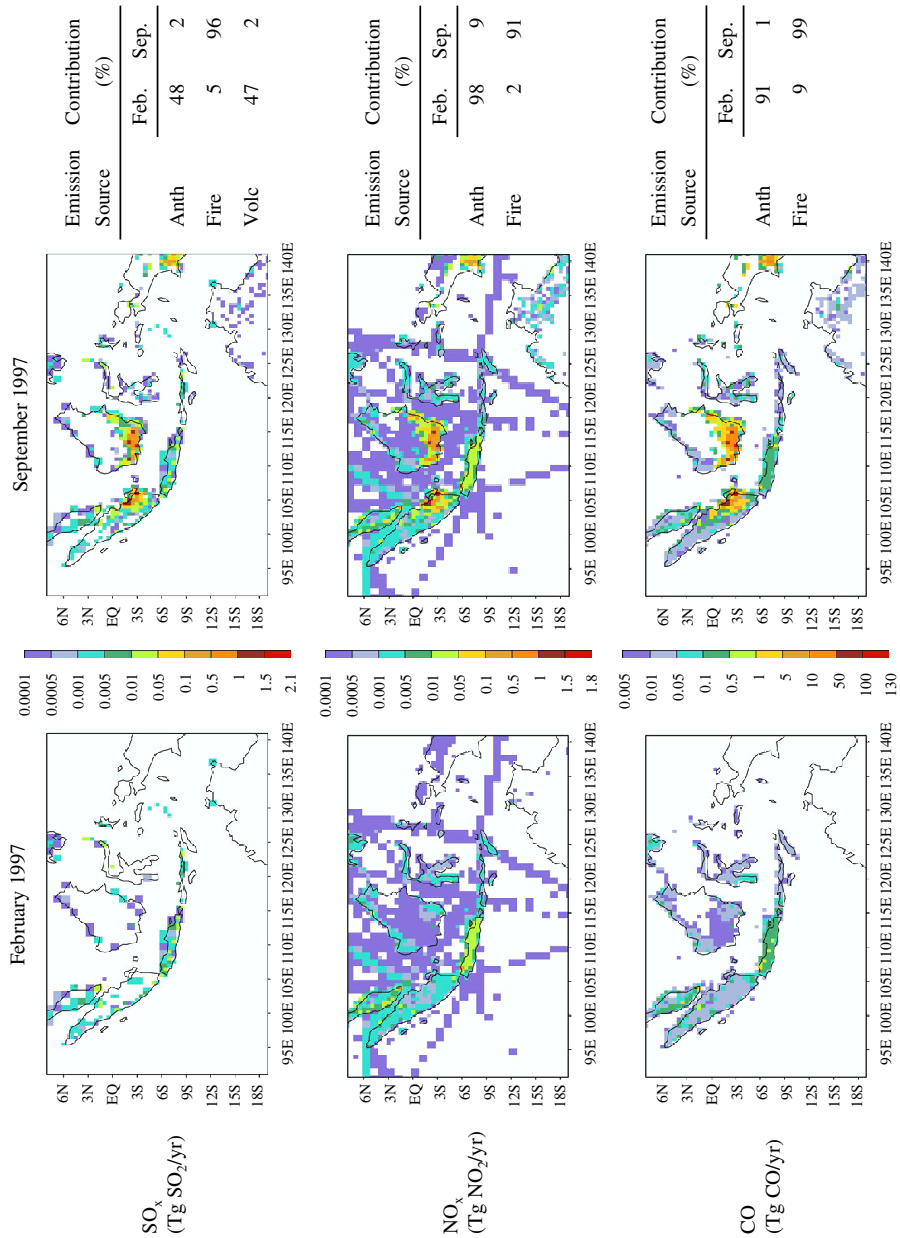

Figure 4.1 Total emissions for the sum of the anthropogenic, fire, and volcanic sources for SO_x, NO_x, and CO for February and September 1997.

4.2.3 Experiments

In order to ascertain the influence of the different emission sources to the air quality in the region, an experiment including all emission sources and two sensitivity experiments excluding an emission source of interest were conducted. 1) Anth-Volc-Fire– emissions from the anthropogenic, volcanic, and fire sources were included in the model experiment: this experiment should be considered the reference experiment as it is the one most closely reflecting real conditions; 2) Volc-Fire– only emissions from the volcanic and fire sources were included while anthropogenic emissions were excluded; and 3) Anth-Fire – only emissions from the anthropogenic and fire sources were included while volcanic sources were excluded. In figures, experiments Anth-Volc-Fire, Volc-Fire, and Anth-Fire will be referred to as AVF, VF, and AF, respectively. All experiments were conducted for the year 1997. The sulfur species, SO_2 and SO_4^{2-}, have been "marked" into four categories: *A, V,* and *F* for the anthropogenic, volcanic, and fire emission sources, respectively, and *B* for the sulfur containing species defined at the boundaries of the simulation area. This marking allows sulfur from each source to be followed individually throughout the experiments as four SO_2 and four SO_4^{2-} tracers.

4.3 Results

The mean ground level concentrations for September-November 1997 are shown for four pollutants: SO_2, NO_2, CO, and O_3 for the experiment Anth-Volc-Fire (Section 4.3.1). These four compounds have been chosen because they are among the pollutants regulated by the Indonesian government and they are active participants in tropospheric chemistry. The subtraction of the results of experiment Volc-Fire from those of Anth-Volc-Fire gives an indication of the relative influence of the anthropogenic pollution, and the subtraction of the results of experiment Anth-Fire from those of Anth-Volc-Fire gives an indication of the relative influence of the volcanic emissions (Section 4.3.2).

4.3.1 Reference Experiment Anth-Volc-Fire

The maximum surface concentrations of SO_2, NO_2, CO, and O_3 in September-November 1997 are found over southeastern Sumatra and southern Kalimantan (Figure 4.2): the locations of the most intense fires. To describe where these pollutants have exceeded the Indonesian air quality standards, these 3-month average values have been compared with the 1-year air quality standards for SO_2 (0.023 ppm; Table 4.4), NO_2 (0.053 ppm), and O_3 (0.025 ppm). This will overestimate the region where the air quality standards were exceeded, because the fires did not last a whole year. The longest standard for CO is the 24-hour standard (8.7 ppm). Comparing the 3-month average values with the 24-hour standard will produce an underestimation of the region with exceedances of CO. Regions with concentrations less than the air quality exceedances are plotted in blue; above in green through red. SO_2, NO_2, and CO have very small regions exceeding the air quality standards. O_3 exceeds the standards in a large portion of the modelling region, with significant exceedances extending from the fires northwestwards over much of western Kalimantan, central Sumatra, and southern Malaysia.

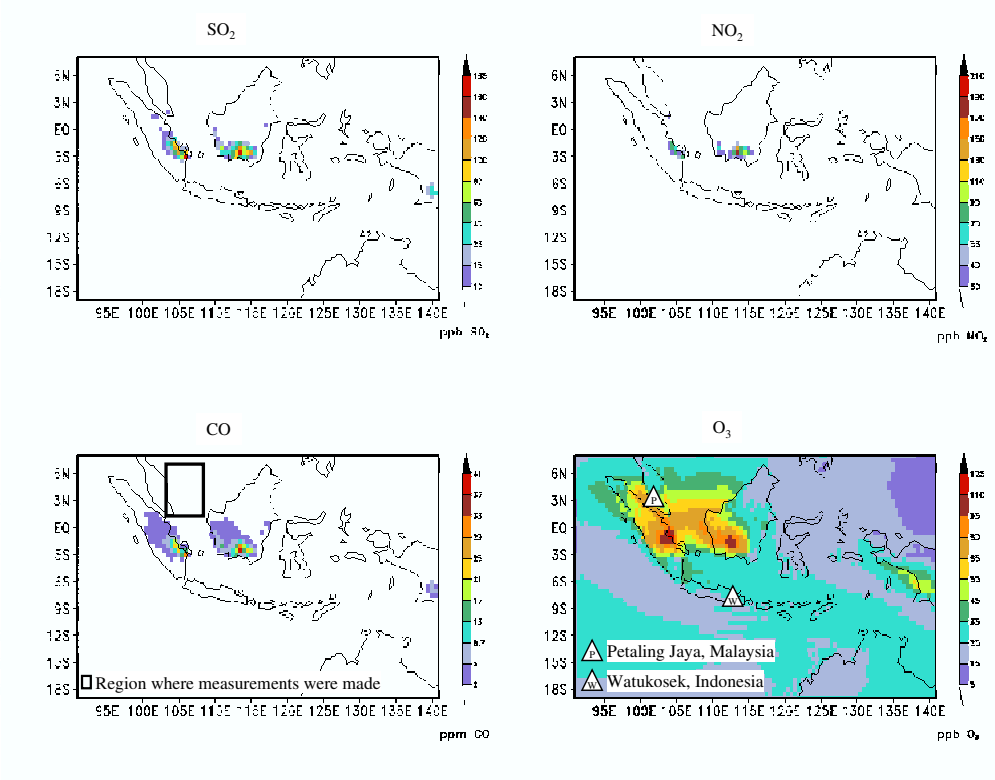

Figure 4.2 Surface concentrations of SO_2, NO_2, CO, and O_3 averaged over September-November 1997 for experiment Anth-Volc-Fire.

The modeled O_3 from September-November 1997 has been compared with ozonesonde measurements performed at two locations: Petaling Jaya, Malaysia and Watukosek, Indonesia (Figure 4.3; for locations of measurements see bottom right panel of Figure 4.2; Fujiwara et al., 2000; Yonemura et al., 2002a). Petaling Jaya is within the region that is modeled to be affected by the fire-related O_3, with surface concentrations greater than the 1-year air quality standard. At Petaling Jaya, the modeled surface O_3 is approximately 3.5 times the measured. The modeled O_3 becomes less than the measured above 3 km. At Watukosek, which is far to the south of the fires and is not modeled to be affected by down-wind transport, the measured O_3 is greater than the O_3 measured at Petaling Jaya. The modeled O_3 at Watukosek is less than the measured over the whole vertical profile, while following the vertical pattern of the measured O_3 quite well. The comparison of the mean value at two locations gives only a crude estimate of the performance of the model simulation. The modeled CO agrees with measurements (Matsueda and Inoue, 1999) better than the O_3 (Figure 4.4). Measurements of CO within the model domain are

Table 4.4 Indonesian air quality standards[a;b]

Pollutant	Averaging time	Standard (μg)/m^3	Standard (ppm)[c]
SO_2	1-hour	900	0.34
	24-hour	365	0.14
	1-year	100	0.023
NO_2	1-hour	400	0.21
	24-hour	150	0.080
	1-year	100	0.053
CO	1-hour	30,000	26.2
	24-hour	10,000	8.7
O_3	1-hour	235	0.12
	1-year	50	0.025

[a] Syahril et al. (2002)

[b] For comparison, the air quality standards of the US EPA (ppm) are: SO_2 24-hour: 0.14; NO_2 1-year: 0.053; CO 1-hour: 35; O_3 8-hour: 0.08

[c] Calculated assuming 25° C and 1 ATM

only available for October 20, 1997 between 1 - 7° N and 103 - 109.5° E (for locations of measurements see bottom left panel of Figure 4.2). The modeled CO is consistently higher than the measured.

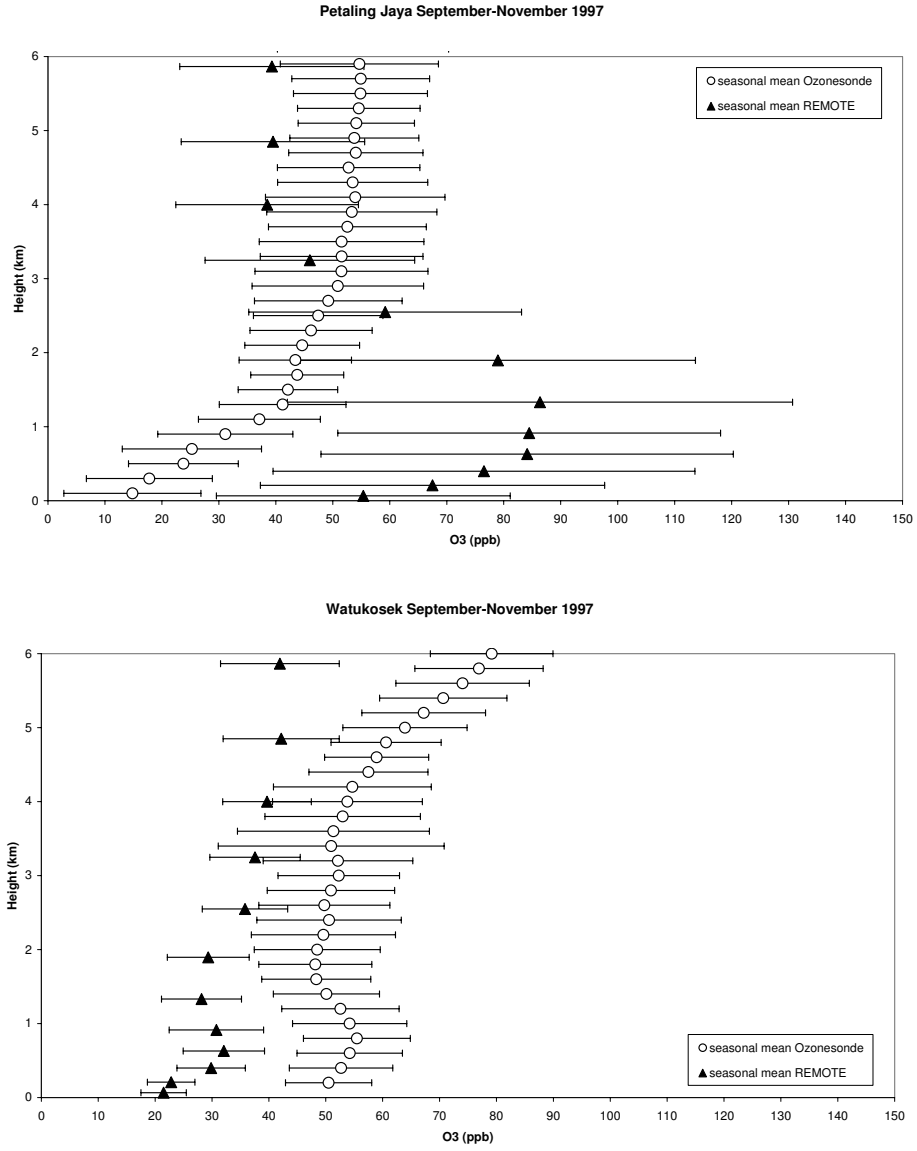

Figure 4.3 Vertical profiles of the average modeled (filled triangles) and measured (open circles) O_3 for September-November 1997 at Petaling Jaya, Malaysia (3.0° N, 101.5° E) and Watukosek, Indonesia (7.5° S, 112.6° E). Error bars indicate one standard deviation. Measurements at Petaling Jaya are from Yonemura et al. (2002a) and measurements at Watukosek are from Fujiwara et al. (2000). Measurements at Petaling Jaya were made on 6 dates: September 15 and 25, October 6 and 15, and November 3 and 17 and at Watukosek on 10 dates: September 17, October 1, 9, 15, 22, and 29, and November 6, 12, 19, and 26.

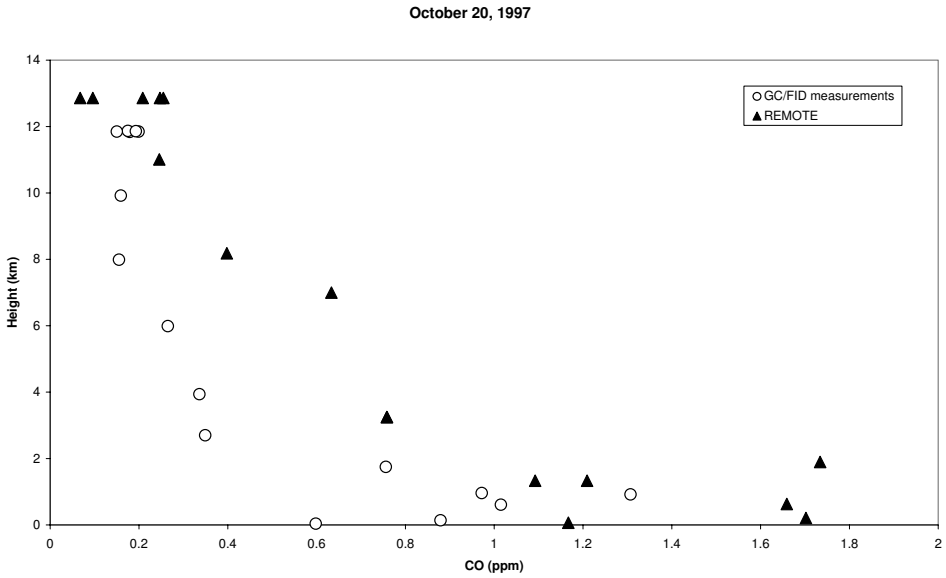

Figure 4.4 Vertical profiles of the modeled (filled triangles) and measured (open circles) CO for October 20, 1997 between 1 - 7° N and 103 - 109° E. The model results shown are for the horizontal gridbox and model level containing the latitude/longitude and elevation where a sample was collected. Heights of the measurements and model results are not equal because the model results are presented at the mean height of the model layer. Measurements were made using a gas chromatograph equipped with a flame ionization detector (GC/FID) from Matsueda and Inoue (1999).

4.3.2 Influence of anthropogenic and volcanic emissions

The influence of the anthropogenic emissions has been depicted by subtracting the surface concentration of the four species of interest calculated in the experiment without anthropogenic emissions (Volc-Fire) from the results of the reference experiment (Anth-Volc-Fire) (Figure 4.5). Correspondingly, the influence of the volcanic emissions is found by subtracting the results of the experiment without volcanic emissions (Anth-Fire) from Anth-Volc-Fire (not shown). The differences of atmospheric concentrations in Figure 4.5 are about one order of magnitude less than the concentrations of Figure 4.2. All four species have only positive values: the anthropogenic emissions produce an increase in the atmospheric concentrations of these pollutants. The greatest increase of SO_2 and NO_2 is found above Singapore, with an increase of 91 % for SO_2 and 99 % for NO_2 when the anthropogenic emissions are included in the experiments. The greatest effect for CO is above Kuala Lumpur, where the anthropogenic emissions increase the atmospheric CO by 58 % and for O_3 above Jakarta by 67 %. O_3 is not enhanced by the anthropogenic pollution over most of Kalimantan and southeastern Sumatra, where the fire emissions were the strongest. The influence of the volcanic emissions on these four species is not shown because when plotted using the same scale as used for Figure 4.5, a difference in atmospheric concentrations can only be seen for SO_2, with the volcanic emissions contributing SO_2 primarily over Java.

4.4 Discussion

The modeled and measured O_3 and CO differ by about a factor of two (Figures 4.3 and 4.4). The ozonesonde measurements are available on discrete days with very high vertical resolution and an uncertain horizontal range of the balloon, while the model results are recorded once every 6 hours for each of 20 vertical levels with one grid box representing approximately 55 km horizontally. The emission data is monthly, and for several anthropogenic species yearly, and will not reflect the specific conditions present on the days measurements are performed. We have shown the modeled and measured O_3 averaged

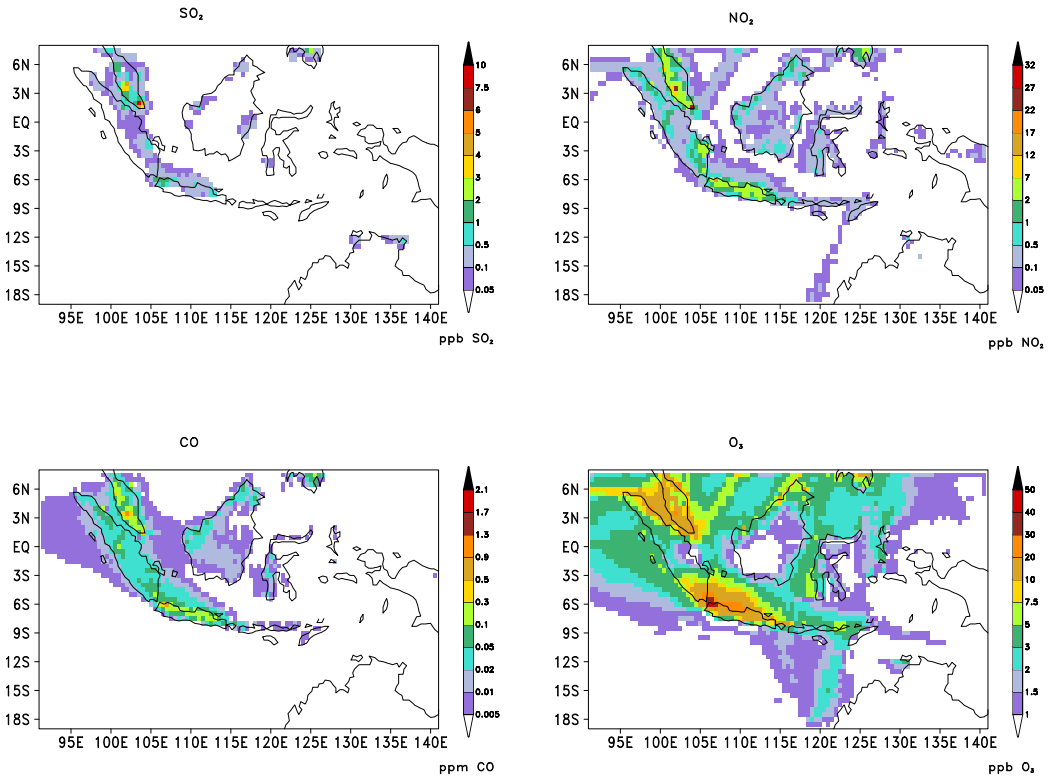

Figure 4.5 Difference in surface concentration of SO_2, NO_2, CO, and O_3 averaged over September-November 1997 for experiment Anth-Volc-Fire - Volc-Fire.

over three months to try and remove some of the temporal uncertainty in the comparison. Comparing the modeled O_3 at Watukosek with the global modeling results seen in Figure 8 of Duncan et al. (2003), we find that our near-surface O_3 is slightly less than that of Duncan et al. (2003). A possible explanation for our underestimation of the O_3 near to the surface is that we used a global MOZART simulation (Granier et al., 2003) for the year 1990 to provide the concentrations of O_3 at the boundaries of the model domain. In Figure 3 of Hauglustaine et al. (1999), MOZART simulations both including and excluding the fire emissions indicate approximately 24 ppb O_3 at the surface off of the southern coast of Kalimantan. This location is closer to the fires, but still upwind, compared with Watukosek, where we compare our modeling results with ozonesonde measurements. Measurements of CO within our modeling domain are only available for one date in a region slightly beyond where CO released by the fires is modeled to have been transported, where the measured values are very low. The modeled CO follows the vertical pattern of the measurements quite well, but is approximately double the measured. Very tentatively, the fire emissions included in this study may be overestimated, as

two locations downwind from the fires have approximately double the concentration of O_3 and CO than was measured. Another source of uncertainty is that the fire emission data is provided as monthly means, and as such cannot account for daily variations in the fire intensity. If may be that fire emissions were stronger on the days when sampling occurred than the monthly average, and as such the model simulation underestimates the concentrations on these specific days. As in the study of Duncan et al. (2003), we find that the fires decreased the atmospheric concentration of OH. A comparison between the modeled tropospheric column of NO_2 with GOME V2.0 observations (Global Ozone Monitoring Experiment, 2007; Richter et al., 2005, not shown) reveals that the maximum values for NO_2 in the region are at a greater distance downwind from the fires in the GOME observations than our simulation calculates. This disparity is not due to too weak winds, as in the upper panel of Figure 6 in Langmann and Heil (2004) it is shown that the REMOTE model slightly overestimates the winds at Petaling Jaya during September-November 1997. It is rather more likely that the model is removing NO_2 from the atmosphere too quickly.

The highest surface concentrations of SO_2, NO_2, CO, and O_3 in September-November 1997 were modeled to be directly above southeastern Sumatra and southern Kalimantan– the locations of the strongest fires, with winds transporting the pollution from the southeast to the northwest. The active Indonesian volcanoes are not downwind from the fires. They contributed only slightly to the surface concentration of SO_2 during the fires and did not discernibly influence the concentration of the secondary pollutant O_3. The anthropogenic pollution was greatest above the major cities in the region: Jakarta, Singapore, and Kuala Lumpur. Singapore and Kuala Lumpur are in the downwind path of the fire pollution, while Jakarta is upwind. The modeled concentrations of SO_2, NO_2, and CO were all highest at 7 AM (local time) as the pollutants are trapped in the nocturnal boundary layer. Summing together all of the model gridboxes that exceeded the Indonesian 1-hour air quality standards (Table 4.4) for these species at 7 AM from September through November indicates 133, 268, and 881 exceedances, respectively. The modeled concentration of O_3 was highest at 1 PM due to photochemical reactions, with 9802 exceedances of the 1-hour air quality standard at 1 PM during these three months. All exceedances of the one-hour air quality standards occur directly above the main fires. For SO_2, NO_2, and CO the exclusion of the anthropogenic pollution (experiment Anth-Volc-Fire - Volc-Fire)

produces a minor reduction in the number of exceedances at 7 AM. For O_3, however, the exclusion of the anthropogenic pollution reduces the total sum of exceedances for these three months by 4% (Figure 4.6). In the bottom right panel of Figure 4.5, it can be seen that some of the changes in surface O_3 due to anthropogenic emissions are due to NO_x pollution along the lines of international shipping (middle row Figure 4.1).

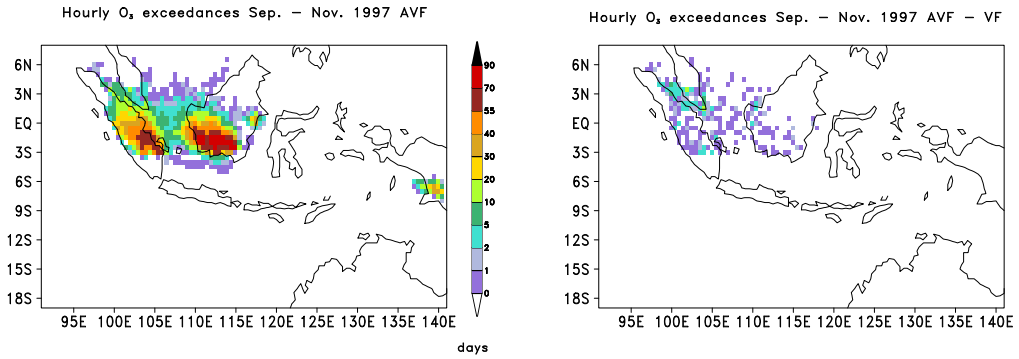

Figure 4.6 The number of days during September-November 1997 when the Indonesian hourly air quality standard for O_3 was exceeded at 13:00 for experiment Anth-Volc-Fire and the difference of Anth-Volc-Fire - Volc-Fire.

As the modeling results indicate that the anthropogenic pollution increased the severity and extent of the O_3 pollution during the 1997 wildfires, the question arises: by what means did the anthropogenic pollution produce this effect? Did the anthropogenic emissions simply add to the emissions of the fires, ”bumping” the atmospheric concentrations up above the air quality standard thresholds, or did the anthropogenic and fire emissions react in the atmosphere? We have addressed this question from two directions, examining if the anthropogenic emissions modified the fire emissions and if the fire emissions modified the anthropogenic emissions. In order to test if the anthropogenic emissions changed the fire emissions, we have looked at SO_2 *F* (the marked SO_2 specifically released by the fires).

It is shown by subtracting the SO_2 *F* in experiment Volc-Fire from Anth-Volc-Fire (top row Figure 4.7) that the difference of SO_2 *F* is negative over peninsular Malaysia and Java, near the large cities where the anthropogenic emissions are strongest, and positive above the southeastern Sumatra fires. The difference of SO_4^{2-} *F* is the reverse pattern: where the SO_2 *F* is negative, the SO_4^{2-} *F* is positive. The anthropogenic emissions enhance the conversion of the SO_2 released by the fires to SO_4^{2-}. This decrease in SO_2 *F* is in contrast

to the upper left panel in Figure 4.5 which shows an increase in the total SO_2. While the anthropogenic emissions decrease specifically SO_2 *F*, the total SO_2 is increased. The decrease in SO_2 *F* occurs in the same areas as where the anthropogenic emission have increased the surface concentration of O_3 (bottom right panel of Figure 4.5). The increase of O_3 by the anthropogenic emissions leads to the enhancement of the conversion of SO_2 to SO_4^{2-}. The evidence that the secondarily produced compound O_3 influences another secondarily produced compound, SO_4^{2-}, shows that the anthropogenic emissions are not simply adding to the fire emissions but are changing the atmospheric lifetime of the fire pollution.

As we looked at SO_2 *F* to see how the anthropogenic pollution affected the fire emissions, we have looked at SO_2 *A* (the SO_2 marked as specifically anthropogenic) to examine the influence of the fire emissions on the anthropogenic. The subtraction of SO_2 *A* in experiment Anth-Volc from Anth-Volc-Fire (bottom row Figure 4.7) shows that the difference of SO_2 *A* is negative. The difference of SO_4^{2-} *A* is positive above the main fires and negative above peninsular Malaysia. The fire emissions are leading to the more rapid oxidation of SO_2 *A* to SO_4^{2-} *A*. Above peninsular Malaysia, the SO_4^{2-} *A* is then being formed in a region with more precipitation (not shown), leading to a more rapid wash out of the SO_4^{2-} *A*, producing the negative difference of SO_4^{2-} *A*.

The significance of the finding of this study that the anthropogenic emissions played a role in the atmospheric concentration of the examined pollutants, particularly near to major cities, lies in the transboundary pollution issue. In Quah (2002), many different approaches are discussed for involving both Indonesia (the state where the fires occur) and ”victim states” including Singapore and Malaysia in fire prevention and fire reduction. All of the suggested mechanisms for reducing the fire-related haze events involve actively reducing the fires within Indonesia. This is very important, and a clear, logical approach to prevent future environmental disasters such as occurred during the 1997 fire. The results of this study suggest an additional approach for neighboring countries that are adversely affected by the fire-related haze: reducing urban air pollution during high-risk times. This may have the effect of keeping the atmospheric concentrations of dangerous pollutants in densely populated areas below the air-quality thresholds, reducing the health and economic consequences of the fires in major cities at a distance from the fires.

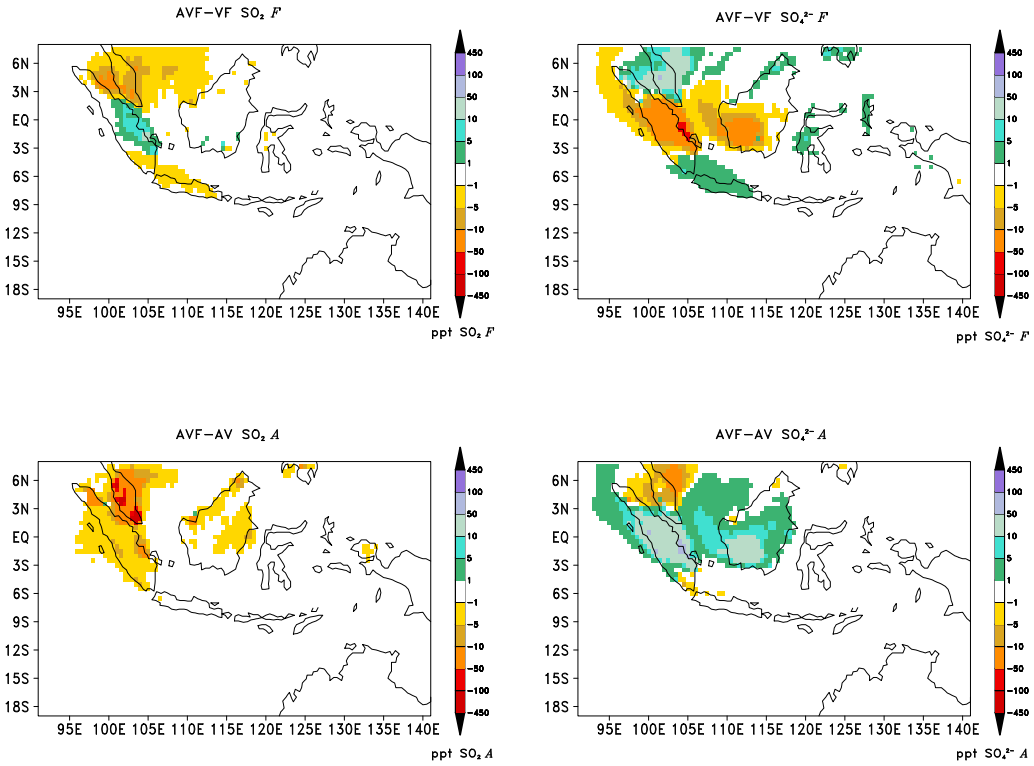

Figure 4.7 Difference of the average surface concentration for September 1997 of SO_2 *F* and SO_4^{2-} *F* for experiments Anth-Volc-Fire - Volc-Fire (top row) and of SO_2 *A* and SO_4^{2-} *A* for experiments Anth-Volc-Fire - Anth-Volc (bottom row).

4.5 Conclusions

Background levels of anthropogenic emissions in southeast Asia in the northern hemisphere autumn of 1997 contributed to the severity and extent of pollution from the Indonesian wildfires. The intensification of the pollution by the anthropogenic emissions is most significant for O_3. The increase of the atmospheric concentration of O_3 enhanced the rate of conversion of SO_2 released by the fires to SO_4^{2-}. The results of this study suggest that reducing the levels of anthropogenic pollution in large cities including Jakarta, Singapore, and Kuala Lumpur during high-risk times for fire-related pollution may help to prevent health and economic disturbances. Transboundary air pollution due to extreme events is a complicated political issue. Distinguishing the roles of different emission sources can help in creating solutions to reduce the harmful effects of fire pollution. The minor role of the volcanoes in this time period is indicative of the surface conditions present during this extreme event.

Acknowledgements

We thank Philipp Weis, Elina Marmer, and Sebastian Rast for their help and discussion. We thank the German Climate Computing Center (DKRZ) and Johann Feichter for computer time to run these experiments and Ulrike Niemeier for providing the MOZART results that were used as boundary conditions. O_3 measurements over Watukosek were made possible by the Indonesian National Institute of Aeronautics and Space and by the National Space Development Agency of Japan. O_3 measurements over Petaling Jaya were made available by Seiichiro Yonemura. CO measurements were made available by Hidekazu Matsueda. Andreas Richter and Mark Weber provided access to the GOME NO_2 observations. Martin Schultz provided access to the RETRO emissions. MAP was funded by the Ebelin and Gerd Bucerius ZEIT Foundation and by the American Association of University Women.

Chapter 5

The relative effects of volcanic and anthropogenic emissions on acid deposition and direct shortwave radiative forcing over Indonesia

Abstract

The transport and deposition of air pollution in Indonesia in 1999 has been studied with the regional atmospheric chemistry and climate model REMOTE. The acid deposition of volcanic sulfur (S) has been shown to not exceed a critical load value of 0.4 g(S)/m^2-yr. Anthropogenic S is deposited above this threshold in Java, northeastern Sumatra, and peninsular Malaysia. The modeled distribution of sulfate (SO_4^{2-}), organic carbon (OC), and black carbon (BC) have been used to calculate their direct shortwave radiative forcing using an offline radiation transfer model. The forcing efficiency of anthropogenic SO_4^{2-} is found to be greater than for volcanic when averaged over ocean + land, with annual mean values of -328 W/g(SO_4^{2-}) and -293 W/g(SO_4^{2-}) respectively. The total anthropogenic aerosol as calculated assuming an external aerosol mixture of SO_4^{2-} + OC + BC is found to have an annual mean forcing of -0.13 W/m^2 averaged over the model domain. The total anthropogenic forcing is dominated by OC released by biomass burning especially during the dry season of June-October when land-clearing fires are burning. The inclusion of biomass burning as an anthropogenic emission source changes the results for the calculated direct radiative forcing dramatically.

5.1 Introduction

Air pollution is a significant environmental problem in Indonesia, with increasing anthropogenic emissions due to its rapidly growing population and industrial sector (Resosudarmo, 2002). Large-scale wildfires set by people for land-conversion can also contribute greatly during the dry season (Heil and Goldammer, 2001). Additional sources of air pollution in Indonesia are volcanoes, as this is the region of the world with the largest number of historically active volcanoes (Simkin and Siebert, 1994). Air pollution can be harmful near to the emission sources and can be transported to affect ecosystems and people downwind. Problems on the surface include health hazards, reducing visibility, and acid deposition. Aerosol particles can also affect the climate by changing the way radiation is transmitted through the atmosphere. It is important to separate the environmental effects of air pollution based on if it is anthropogenic or natural in origin. Pollution from different sources can interact, changing their atmospheric lifetime and behavior (Pfeffer et al., 2007, Chapter 4). Distinguishing between natural and anthropogenic sources can give us information about the Earth during pre-industrial times and can provide suggestions for targeted reductions of pollution or for where it is least damaging to have major sources of pollution.

The environmental problem of acid deposition is primarily associated with the wet and dry deposition of sulfur and nitrogen (Kuylenstierna et al., 2001). Both sulfur (emitted as SO_2) and nitrogen (emitted as NO_x and NH_3) can produce acidification. ”Wet deposition” refers to deposition in acid rain, fog, snow, and other forms of precipitation and ”dry deposition” refers to deposition in the form of acidic gases and particles. Ecosystems are sensitive to acid deposition depending on if they are terrestrial or aquatic, the buffering ability of their soils and parent material, and the sensitivity of organisms living within the ecosystem to changes (Kuylenstierna et al., 2001). The ”critical load” of an ecosystem is an estimate of its sensitivity that describes the maximum amount of pollutants that an ecosystem can tolerate without being damaged. This critical load can be compared with modeled sulfur and nitrogen deposition rates, and the deposition above the critical load value can be assumed to harm the ecosystem.

Most studies of critical loads have focused on Europe and North America, however it is

in developing countries where emissions (particularly of S) are growing (Kuylenstierna et al., 2001). Kuylenstierna et al. (2001) developed a global map of critical loads in order to study acidification in developing countries. Their model results indicate that in the next 50 years, southern Asia, including Indonesia, is expected to have an increasing risk of acidification. Hettelingh et al. (1995) developed a critical load map for southeast Asia, including Indonesia, which has a low critical load, meaning it is sensitive to acid deposition. Engardt and Leong (2001) stress the importance of improved emission inventories, performing simulations at higher resolutions, and including biomass burning and natural emissions in order to more realistically model atmospheric S. Engardt et al. (2005) found that anthropogenic sulfur is deposited nearer to source with less long-range transport in Southeast Asia compared with Europe.

In addition to acid rain, the radiative forcing of aerosol pollution is an environmental concern in Indonesia. The direct radiative effect of aerosol particles is that they scatter and absorb solar radiation. The aerosol particles usually studied are sulfate, black carbon (BC), organic carbon (OC), dust, and sea salt. BC is an absorbing aerosol while OC and sulfate are dominantly scattering. These three aerosol types are mainly sub-micron in size and have their greatest influence on radiation in the shortwave part of the solar spectrum. In a region with multiple types of aerosol particles, the bulk aerosol properties can be estimated assuming an external or internal aerosol mixture. An assumption of an external mixture means that the components in a mixed aerosol are chemically pure and distinct while an assumption of an internal mixture means the mixed aerosol is a homogeneous combination of the chemical and physical properties of the contributing components. In reality, a mixed aerosol is generally between these two extremes. Most models, however, are not capable of resolving the mixing state of an aerosol and so these two extremes are used in order to estimate the aerosol's properties. The direct forcing of an externally mixed aerosol is calculated by summing together the forcing of each component. Calculating the forcing of an internally mixed aerosol requires many more assumptions and produces a significantly different forcing estimate. Boucher and Anderson (1995) introduced the concept of "forcing efficiency" which is the ratio of the direct radiative forcing of a given type of aerosol to its column burden. Forcing efficiency can vary between different emission sources, seasonally, and due to changing meteorological conditions

(Marmer, 2006). Previous modeling studies of the direct radiative forcing over specifically Indonesia have focused on the year 1997 (Duncan et al., 2003; Davison et al., 2004) when tremendous wildfires dominated the air pollution emissions in the region and the resulting radiative forcing.

In this paper, we have studied the relative effects of anthropogenic and volcanic emissions on acid deposition and direct radiative forcing in Indonesia using a regional atmospheric chemistry and climate model. The advantages of this work compared to previous research include that the most up-to-date emission estimates for anthropogenic and volcanic emissions have been used in the simulations. Our model utilizes full, on-line tropospheric chemistry compared with the schemes considering only sulfur chemistry used in most other studies and we use the relatively high resolution of 1/2 °. We have also chosen to simulate a normal year without any extraordinary meteorological conditions or pollution events in order to understand what is happening typically in the region.

5.2 Experimental Setup

Regional atmospheric chemistry and climate model simulations have been performed for the year 1999, a meteorologically “normal” year , i.e. neither “El Niño” nor “La Niña”.

5.2.1 Model

The model REMOTE (REgional MOdel with Tracer Extension; Langmann, 2000) has been used for this study. REMOTE combines the physics of the regional climate model REMO 5.0 with tropospheric chemical equations for 63 chemical species. The physical and dynamical equations in the model (Jacob, 2001) are based on the regional weather model EM/DM of the German Weather Service (Majewski, 1991) and include parameterizations from the global ECHAM 4 and ECHAM 5 models (Roeckner et al., 1996). The chemical tracer transport mechanisms include horizontal and vertical advection (Smolarkiewitz, 1983), convective up- and down-draft (Tiedtke, 1989), and vertical diffusion (Mellor and Yamada, 1974). Trace species can undergo chemical reactions in the atmosphere or can be removed from the atmosphere by wet and dry deposition or transport out

of the model boundaries. Dry deposition is dependent on friction velocities and ground level atmospheric stability (Wesley, 1989). Wet deposition is dependent on precipitation rate and mean cloud water concentration (Walcek and Taylor, 1986). 158 gasphase reactions from the RADM II photochemical mechanism (Stockwell et al., 1990) are included. 43 longer-lived chemical species are transported between gridboxes and 20 are calculated but too short-lived to be transported.

The model was applied with 20 vertical layers of increasing thickness between the Earth's surface and the 10 hPa pressure level (approximately 23 km). The model domain covers Indonesia and Northern Australia (91° E - 141° E; 19° S - 8° N) with a horizontal resolution of 0.5° (approximately 55 km). Analysis data of weather observations from the European Centre for Medium-Range Weather Forecasts (ECMWF) were used as meteorological boundary conditions every 6 hours. Results from a global chemical transport model (MOZART; Horowitz et al., 2003) simulation for the year 1990 (Granier et al., 2003) were used as chemical concentration boundary conditions every 6 hours for 14 chemical species including O_3, CH_2O, and H_2O_2. Background concentrations for 25 other species (Chang et al., 1987) including SO_2 and SO_4^{2-} were specified at the lateral model boundaries. The physical and chemical state of the atmosphere was calculated every 5 minutes.

5.2.2 Emissions

Volcanic and anthropogenic emissions are released as two separate categories (Table 5.1). The volcanic emissions are the same as in Pfeffer et al. (2007) (Chapter 4; as in Chapter 2): a "realistic" emission estimate averaged over the past century. These emissions are temporally constant and include only SO_2 and SO_4^{2-}. The anthropogenic emissions are from urban and biomass burning sources for 20 species including SO_2, CO, and NO_2. These emissions have been assembled from four sources: RETRO V1.2 anthropogenic (Schultz et al., in prep.), RETRO V1.2 vegetation fires (Schultz et al., submitted), AEROCOM B-2000 (Dentener et al., 2006), and Edgar V2.0 (Bouwman et al., 1997). The RETRO emissions are available as monthly data for 1999, the AEROCOM emissions are for the benchmark year 2000, and the Edgar emissions are for the benchmark year 1990. The

volcanic SO_x emissions are approximately 11 % of the total SO_x emissions; the anthropogenic approximately 88 %. The volcanic emissions were released into the model layer at the height of each volcano, which lie within the bottom 12 model levels (up to about 4 km). The anthropogenic emissions were released into the lowest model level.

Table 5.1 Annual mean emissions of selected species for 1999

Species	Anthropogenic Emissions	Volcanic Emissions
SO_x[1]	3769[a;b]	484[c]
NO_x[2]	3394[b;d]	—
NH_3[3]	1750[e]	—
Black Carbon (BC)[3]	308[a;b]	—
Organic Carbon (OC)[3]	998[b]	—

[1] SO_x: SO_2 + SO_4^{2-}; Gg (SO_2)/yr
[2] NO_x: NO_2 + NO; Gg (NO_2)/yr
[3] Gg (species)/yr
[a] AEROCOM; benchmark year 2000; Dentener et al. (2006)
[b] RETRO vegetation fires; Schultz et al. (submitted)
[c] Pfeffer et al. (2007); Chapter 2
[d] RETRO anthropogenic; Schultz et al. (in prep.)
[e] Edgar V2.0; benchmark year 1990; Bouwman et al. (1997)

5.2.3 Experiments

In order to determine the influence of the volcanic and anthropogenic emission sources on the acid deposition and aerosol loading in the region, two different techniques have been applied. The first technique relies on subtracting a sensitivity experiment where an emission source was excluded from a reference experiment where all emission sources were included. To this end, two experiments have been conducted: 1) Reference– emissions from the anthropogenic and volcanic sources were included in the model experiment; and 2) Volc – only volcanic emissions were included while anthropogenic sources were excluded. In order to determine the influence of the anthropogenic emissions on the deposition of a given species, for example HNO_3, the deposition of HNO_3 calculated by

experiment Volc $[HNO_3]_V$ has been subtracted from the reference experiment $[HNO_3]_R$. Anthropogenic HNO_3 calculated in this way will be referred to as $[HNO_3]_A$ and this notation will be used for all species calculated in this fashion. BC and OC are only emitted by anthropogenic sources and do not have defined background concentrations, so the values for the $[BC]_R$ and $[OC]_R$ calculated in the reference experiment will be used to examine these species. The second technique applies only to the sulfur species, SO_2 and SO_4^{2-}. These species have been individually "marked" into three categories: *A, V,* and *B* for anthropogenic, volcanic, and background sources. This marking allows sulfur from each source to be followed individually throughout the experiments from its emission as primarily SO_2 to its oxidation to SO_4^{2-} and/or deposition. In order to determine the influence of the volcanic and anthropogenic emissions on the deposition of SO_4^{2-}, the $[SO_4^{2-}\ V]$ and $[SO_4^{2-}\ A]$ calculated by the reference experiment will be examined.

5.2.4 Radiative forcing

The direct radiative short wave forcing at the top of the atmosphere (TOA) of sulfate, black carbon, and organic carbon aerosols was calculated using an Off-line Radiation Transfer Model (ORTM) described by Langmann et al. (1998) and Marmer (2006). The direct forcing is calculated based on the aerosol mass distribution and meteorological conditions provided by the REMOTE model simulations. The shortwave part of the solar spectrum, 0.2-5 μm subdivided into 18 wavelength intervals, is considered. Optical properties of the dry aerosols are determined from Mie theory calculations. The modification of aerosol specific extinction due to relative humidity of the ambient air is considered using an approximation adapted from the data given by Nemesure et al. (1995). "All sky" conditions were applied, meaning that the presence of clouds was considered. The direct radiative forcing of the total anthropogenic aerosol was calculated assuming that the $[SO_4^{2-}\ A]$, $[BC]_R$, and $[OC]_R$ were externally mixed and will be referred to as "externally mixed *A*".

5.3 Results

The comparison of the modeling results with measurements is presented first. Second, results relating to acid deposition in the modeled region are shown, followed by the modeled aerosol concentrations and calculated direct shortwave radiative forcing.

5.3.1 Comparison between model results and measurements

The results of the reference simulation have been compared with measurements from the Tropical Rainfall Measuring Mission (TRMM), Acid Deposition Monitoring Network in East Asia (EANET), World Data Centre for Greenhouse Gases (WDCGG), and Malaysian Meteorological Department (MMD) (Figure 5.1). With the exception of the TRMM satellite precipitation data which is available over the entire model domain, the measurements are station measurements which are being compared with the ground-level model gridbox containing the latitude/longitude of each sampling site. The modeled precipitation is significantly overestimated, particularly over the ocean, compared with the TRMM satellite observations (Figure 5.2). Over the entire modeling domain, the modeled precipitation is approximately double that observed by satellite. The simulated rainfall is much more consistent with the satellite observations over land (Figure 5.3). The modeled monthly accumulated precipitation compares reasonably well with that measured at three land-based sites, with a relatively consistent bias towards too much modeled precipitation (top row Figure 5.4). The annual pattern of precipitation is followed very well for Tanah Rata and Petaling Jaya, where the modeled precipitation is approximately 100 mm/month greater than the measured. The annual pattern for Serpong is not simulated well, and the modeled precipitation is much higher than the measured during the southern hemisphere summer.

The comparison of the wet deposition of $[HNO_3]_R$ and $[H_2SO_4]_R$ in the middle and bottom panel of Figure 5.4 shows little variation between the modeled deposition at these three sites while the measurements demonstrate greater variation. The modeled deposition generally lies within the envelope described by the deposition measured at the three sites. The greatest inconsistency lies at Petaling Jaya, a heavily polluted site. The measured wet deposition of both species is much higher for most of the year than the other

Source	Location	Location type	Measurement
TRMM	Model domain	-----	Monthly accumulated rainfall
EANET	Serpong, Indonesia (6 S, 106.5 E)	Industrial suburb	Monthly accumulated rainfall and wet deposition of HNO_3 and H_2SO_4
	Petaling Jaya, Malaysia (3 N, 101.5 E)	Urban	Monthly accumulated rainfall and wet deposition of HNO_3 and H_2SO_4
	Tanah Rata, Malaysia (4 N, 101 E)	Remote	Monthly accumulated rainfall and wet deposition of HNO_3 and H_2SO_4
WDCGG	Jakarta, Indonesia (6 S, 107 E)	Urban	Surface concentration of SO_2 and NO_2
	Bukit Koto Tabang, Indonesia (0 S, 100 E)	Remote	Surface concentration of SO_2 and NO_2
MMD	Petaling Jaya, Malaysia (3 N, 101.5 E)	Urban	Surface concentration of SO_2 and NO_2
	Tanah Rata, Malaysia (4 N, 101 E)	Remote	Surface concentration of SO_2, NO_2, NH_3, and H_2SO_4

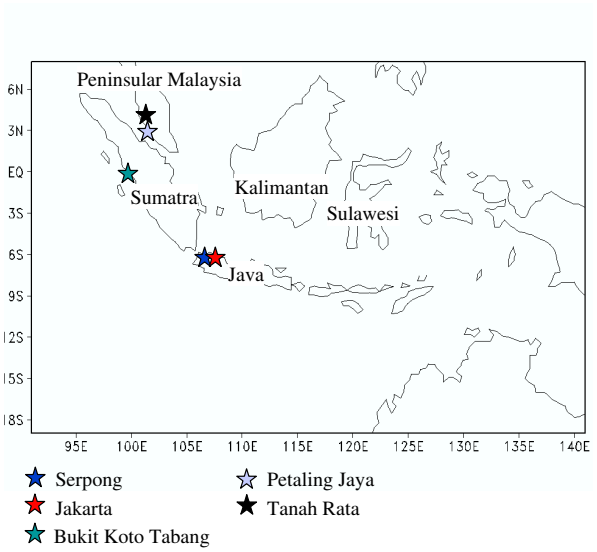

Figure 5.1 Summary of the measurement data used for comparison with the reference model simulation.

sampling sites, while the model does not reproduce this. This can be the result of releasing the emissions of a city into a grid box of approximately 50 km in size, diluting the urban emissions and dampening the difference between urban areas and their less polluted surroundings. The scatter-plot of the wet deposition of $[HNO_3]_R$ shows a random difference between the model and the measurements, while the model tends to wet deposit too much $[H_2SO_4]_R$ when the concentrations are low and too little when the concentrations are higher. This is another way of looking at how the model has less variation in the wet deposition of the H_2SO_4 than the measurements.

The measured surface concentrations of $[SO_2]_R$ and $[NO_2]_R$ are much higher at the urban

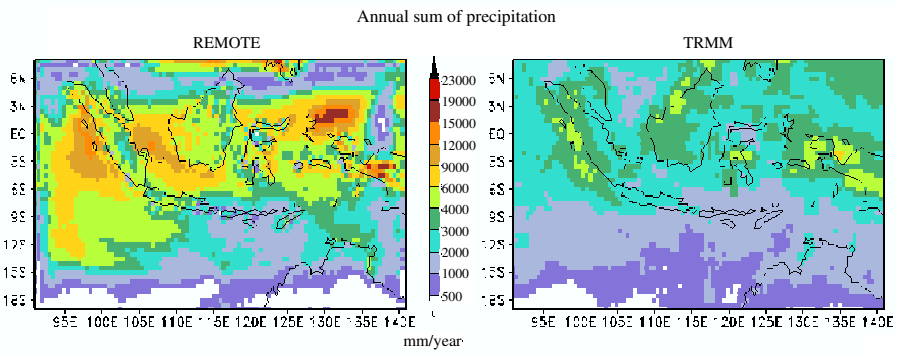

Figure 5.2 Annual sum of precipitation for 1999 for REMOTE (left panel) and Tropical Rainfall Measuring Mission (2007) satellite observations (right panel).

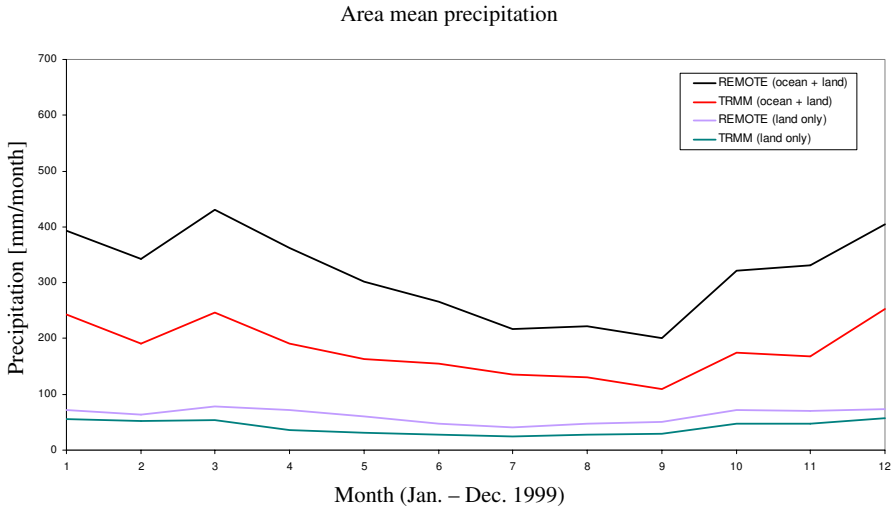

Figure 5.3 Area mean monthly total precipitation over the modeling domain (91 ° E - 141 ° E; 19 ° S - 8 ° N) for 1999. REMOTE and TRMM satellite observations over 'ocean + land' and 'land only'.

sites Jakarta and Petaling Jaya than at the remote sites Tanah Rata and Bukit Koto Tabang (top and middle rows of Figure 5.5). The modeled $[SO_2]_R$ is much higher than the measurements at Jakarta, much lower at Petaling Jaya, and reasonable for the remote sites. The modeled $[NO_2]_R$ is much lower for the polluted sites and reasonable for the remote sites. At Tanah Rata (bottom left panel of Figure 5.5), the simulated $[HNO_3]_R$ agrees very well with the measurements while $[NH_3]_R$ is generally too low except in August.

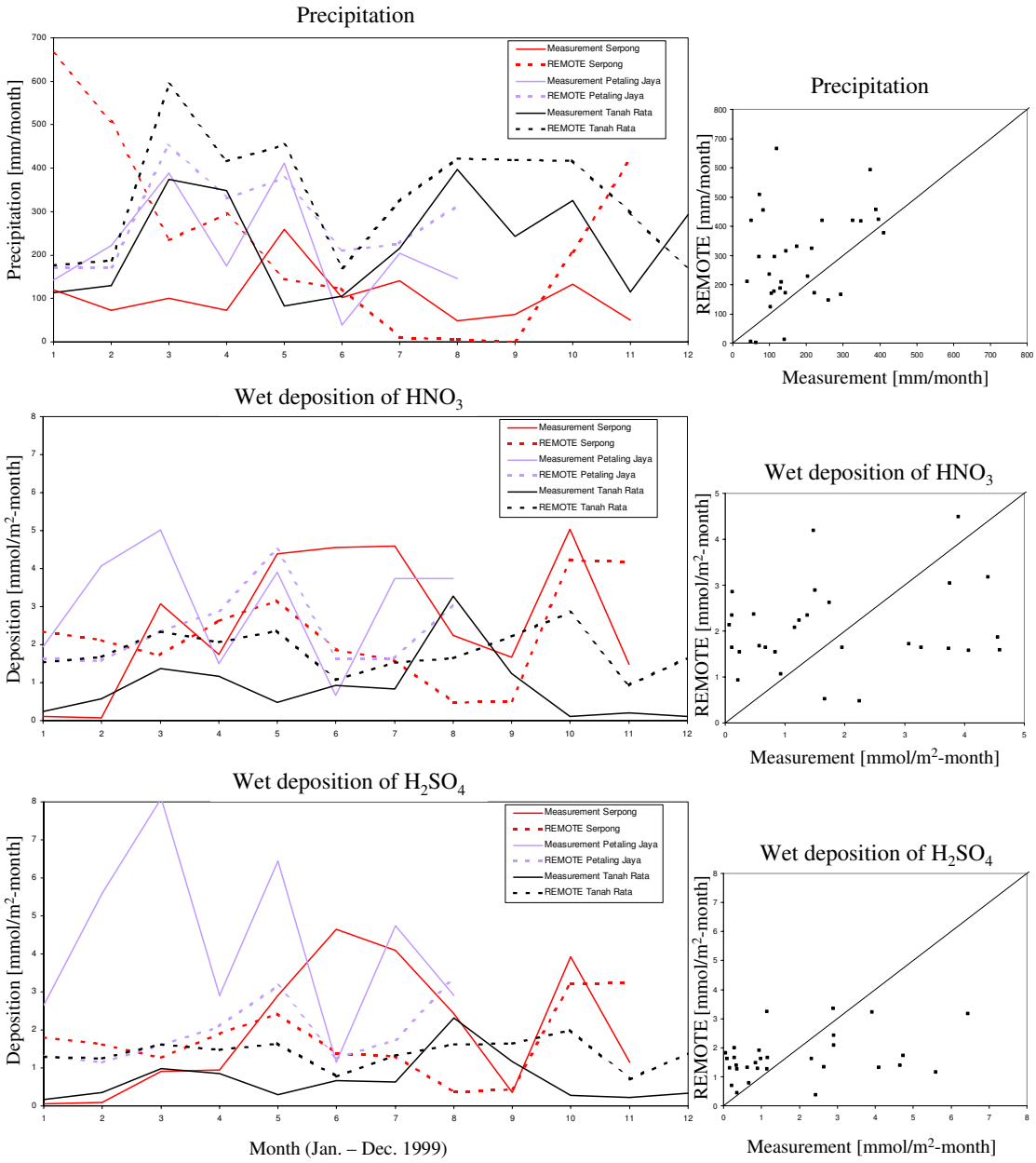

Figure 5.4 Monthly precipitation, wet deposition of HNO_3, and wet deposition of H_2SO_4 at Serpong, Indonesia (red), Petaling Jaya, Malaysia (purple), and Tanah Rata, Malaysia (black). Measurements are presented with solid lines and come from the Acid Deposition Monitoring Network in East Asia (EANET). Model results are presented with dashed lines for the ground-level horizontal gridbox containing the latitude/longitude of each sampling site. Scatter-plots of the compared data are shown in the right column.

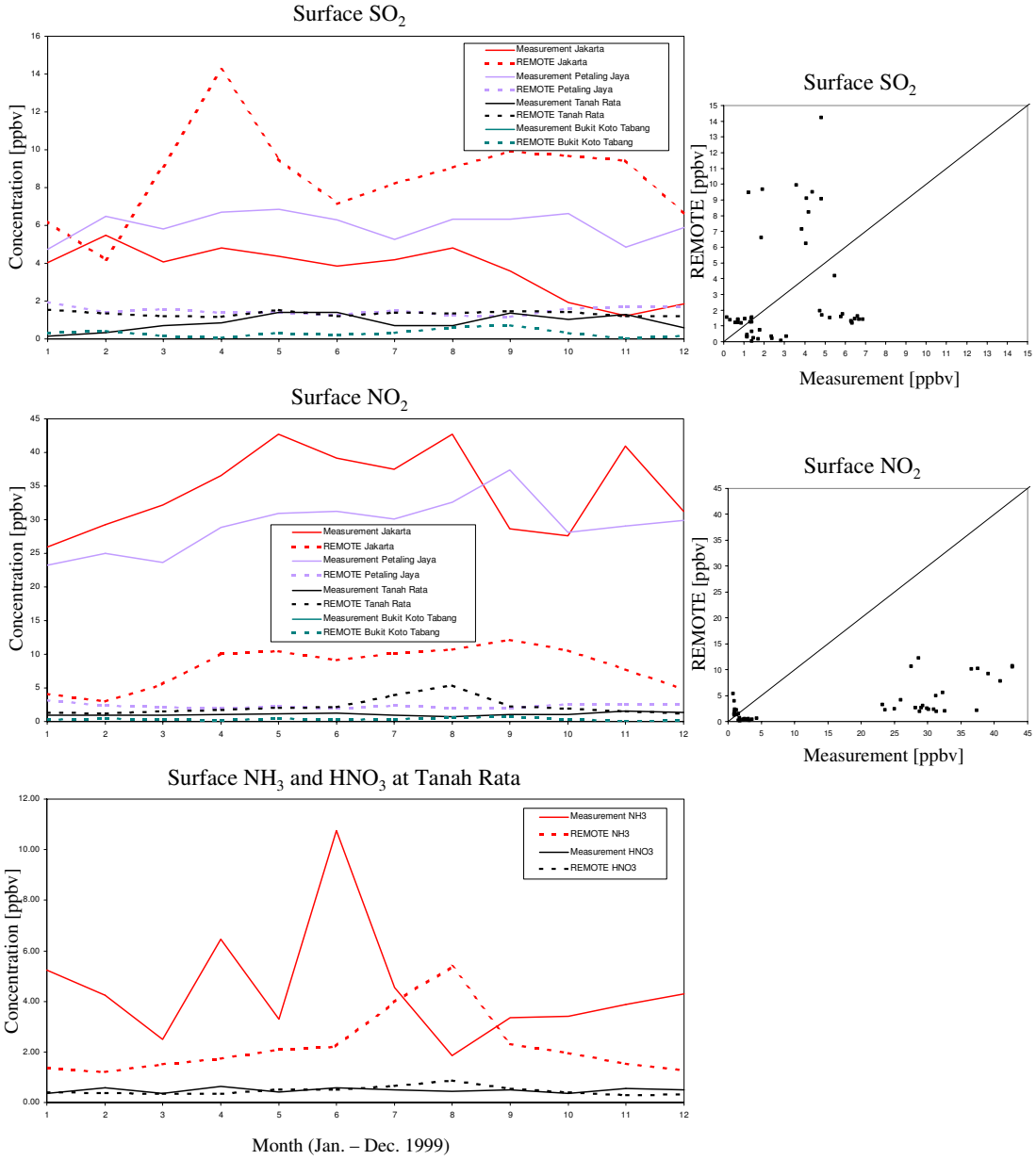

Figure 5.5 Monthly surface concentration of SO_2 and NO_2 at Jakarta, Indonesia (red), Petaling Jaya, Malaysia (purple), Tanah Rata, Malaysia (black), and Bukit Koto Tabang, Indonesia (green) and monthly surface concentration of NH_3 and HNO_3 at Tanah Rata (left column). Measurements are presented with solid lines and come from the World Data Centre for Greenhouse Gases (WDCGG) for Jakarta and Bukit Koto Tabang (the Indonesian sites) and from the Malaysian Meteorological Department (MMD) for Petaling Jaya and Tanah Rata (the Malaysian sites). Model results are presented with dashed lines for the ground-level horizontal gridbox containing the latitude/longitude of each sampling site. On average, the samples at the Indonesian sites were collected between 9:00 - 10:00, so the model results shown are an average of the hourly values recorded at 7:00 and 13:00. The samples at the Malaysian sites were collected on average at 20:00, so the model results shown are the hourly values recorded at 19:00. Scatter-plots of the compared multi-city data are shown in the right column.

5.3.2 Acid deposition

The model results show that the volcanic [SO_x V] deposition is strongest over Java, southern Sumatra, and northeastern Sulawesi (Figure 5.6). The anthropogenic acid deposition of [SO_x A] and $[HNO_3]_A$ covers most of Indonesia and is strongest over Java and the region of northeastern Sumatra and peninsular Malaysia. Adding together the annual sum of the acid deposition over the modeling domain produces the values for deposition given in Table 5.2. Approximately 11 % of S deposited is volcanic (Table 5.2), the same percentage as the SO_x released in the region that is volcanic (Table 5.1). For the volcanic sulfur, almost 87 % is wet deposited as [SO_4^{2-} V], with most of the remainder dry deposited as [SO_2 V]. The anthropogenic sulfur is deposited in a different manner, with a much higher percentage, approximately 34 %, dry deposited, mostly as [SO_2 A]. The other 66 % is mostly wet deposited as [SO_4^{2-} A]. In neither case is the dry deposition of SO_4^{2-} significant. Anthropogenic $[HNO_3]_A$ is almost 76 % wet deposited and lies intermediary between the volcanic and anthropogenic S for how much is dry deposited.

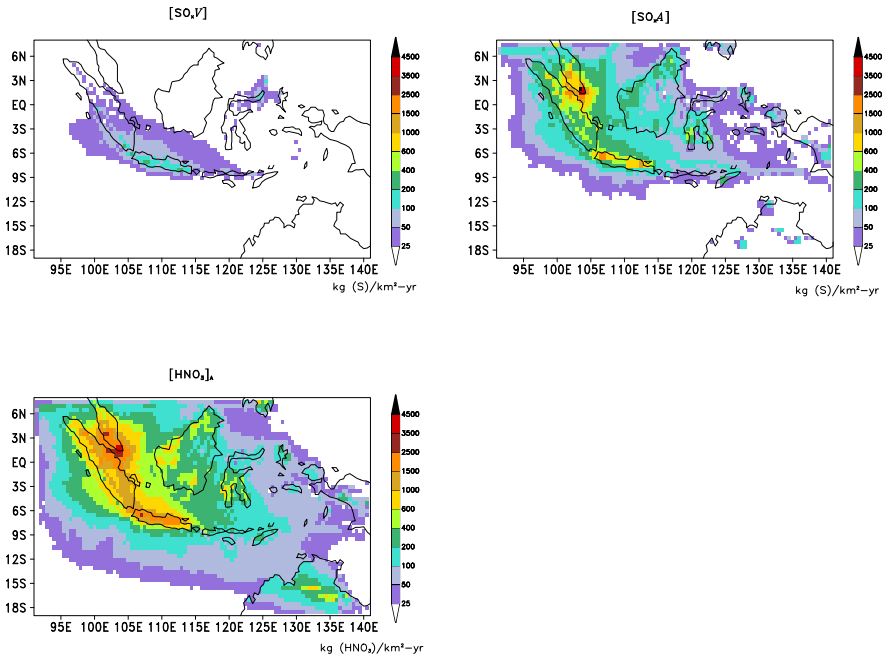

Figure 5.6 Annual sum of acid deposition for 1999 of [SO_x V], [SO_x A], and $[HNO_3]_A$.

Table 5.2 Acid deposition over Indonesia

Source and Species	Deposition	% of Total Deposition	% of Contributors	
Volcanic S [S *V*]	56.78[1]	11.6	wd [SO_4^{2-} *V*]	86.5
			dd [SO_4^{2-} *V*]	1.6
			dd [SO_2 *V*]	11.9
Anthropogenic S [S *A*]	431.01[1]	88.4	wd [SO_4^{2-} *A*]	65.8
			dd [SO_4^{2-} *A*]	1.7
			dd [SO_2 *A*]	32.5
Anthropogenic HNO_3 $[HNO_3]_A$	1066.17[2]	—	wd $[HNO_3]_A$	75.5
			dd $[HNO_3]_A$	24.5

wd: wet deposition
dd: dry deposition
[1]Mg [S] / km^2
[2]Mg [HNO_3] / km^2

5.3.3 Direct radiative forcing of tropospheric aerosols

The modeled distribution of aerosol concentrations, shown here as the column concentrations of $[BC]_R$, $[OC]_R$, $[SO_4^{2-}\ A]$, and $[SO_4^{2-}\ V]$ (left column Figure 5.7) is reflected in the calculated direct radiative forcing for each aerosol type (right column Figure 5.7). The forcing of the externally mixed anthropogenic aerosol [externally mixed *A*] is calculated by adding together the forcings of the $[BC]_R$, $[OC]_R$, and $[SO_4^{2-}\ A]$. BC is predominantly absorbing and so its direct radiative forcing is positive. OC and SO_4^{2-} are predominantly scattering, so their forcing is negative. Comparing the $[SO_4^{2-}\ A]$ and the $[SO_4^{2-}\ V]$ reveals that they are of the same order of magnitude, but that the $[SO_4^{2-}\ A]$ exerts its influence over a greater area due to its greater atmospheric concentration. The annual mean forcing of the $[SO_4^{2-}\ A]$ averaged over the modeling domain is -0.063 W/m^2, with a maximum of -0.83 W/m^2, and of the $[SO_4^{2-}\ V]$ -0.012 W/m^2, with a maximum of -0.25 W/m^2 (Table 5.3).

The [externally mixed *A*] is dominated by $[OC]_R$, and hence negative over most of the model domain, with an annual area mean value of -0.13 W/m^2 (Table 5.3). Java emerges as the most interesting region of the modeled domain (treated as the rectangular region marked in the bottom right panel of Figure 5.7 with the dimensions of 8.5° S - 6° S, 105.5° E - 114.5° E). This is where $[BC]_R$ has its greatest influence on the [externally mixed *A*], moving it to positive forcing in the land part of the rectangular region. An annual area mean value of -0.15 W/m^2 is found for this region. Java is also where the $[SO_4^{2-}\ V]$ has its greatest influence with an average over the island of -0.09 W/m^2. Averaged over the model domain, the greatest temporal variation of forcing occurs from June-October (Figure 5.8), the dry South-Monsoon season in Indonesia (Pfeffer et al., 2006a, Chapter 3). The strongest positive forcing of $[BC]_R$ and the strongest negative forcing of $[OC]_R$ and [externally mixed *A*] is in September. There is much more temporal variation seen in the forcing averaged over Java, where peaks can be seen as well in March and May. In this region, the $[SO_4^{2-}\ A]$, $[SO_4^{2-}\ V]$, and $[BC]_R$ are important for driving the [externally mixed *A*] except in the South-Monsoon season when the $[OC]_R$ dominates.

Table 5.3 Annual mean column concentration, forcing, and forcing efficiency of aerosols

Aerosol type	Area mean	Column Concentration (mg/m^2)	Forcing (W/m^2)	Forcing Efficiency (W/g (aerosol))
	model domain (ocean + land)	0.041	-0.012	-293
	model domain (land only)	0.048	-0.011	-229
Volcanic SO_4^{2-}	Java (ocean + land)	0.295	-0.093	-315
$[SO_4^{2-}\ V]$	Java (land only)	0.377	-0.120	-318
	model domain (ocean + land)	0.192	-0.063	-328
	model domain (land only)	0.306	-0.075	-245
Anthropogenic SO_4^{2-}	Java (ocean + land)	0.681	-0.221	-325
$[SO_4^{2-}\ A]$	Java (land only)	0.757	-0.231	-305
$[OC]_R$	model domain (ocean + land)	0.148	-0.104	-703
$[BC]_R$	model domain (ocean + land)	0.036	+0.040	1111
[externally mixed A]	model domain (ocean + land)	0.376	-0.127	-338

Java: 8.5° S - 6° S, 105.5° E - 114.5° E.

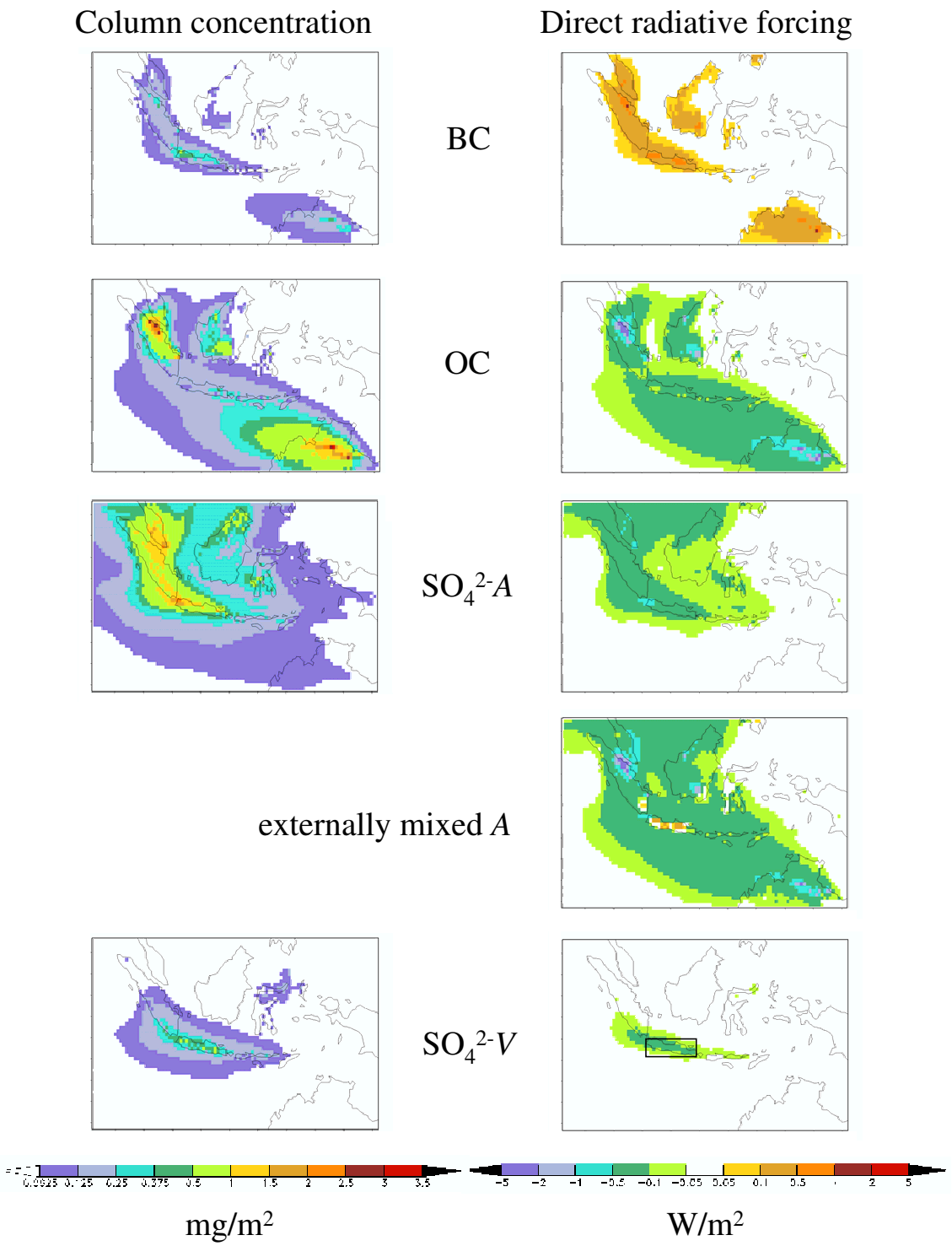

Figure 5.7 Annual mean column concentration of $[BC]_R$, $[OC]_R$, $[SO_4^{2-}\ A]$, and $[SO_4^{2-}\ V]$ (left column) and direct radiative forcing of $[BC]_R$, $[OC]_R$, $[SO_4^{2-}\ A]$, [externally mixed A], and $[SO_4^{2-}\ V]$ (right column). The rectangle in the forcing of $[SO_4^{2-}\ V]$ delineates the region treated as Java.

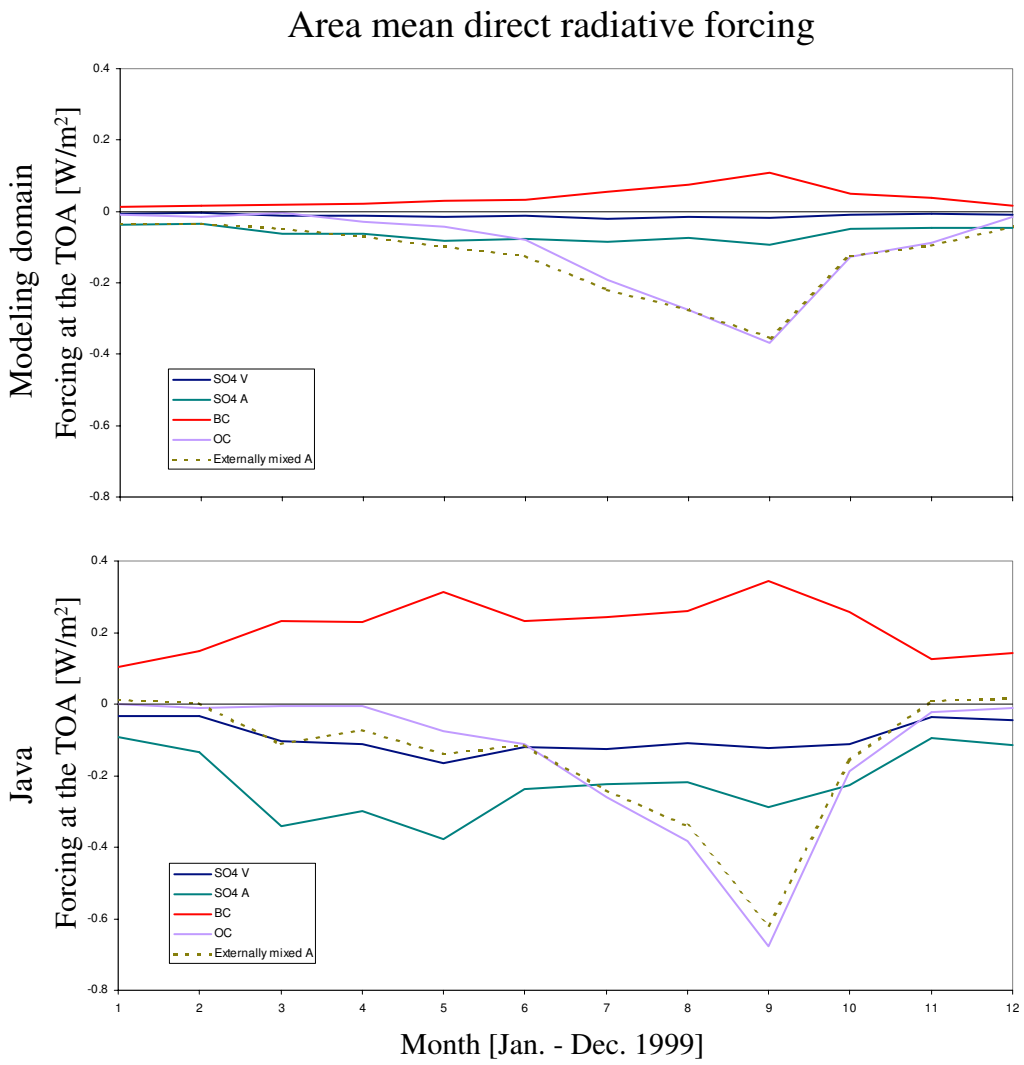

Figure 5.8 Area mean monthly direct radiative forcing of $[BC]_R$, $[OC]_R$, $[SO_4^{2-}\ A]$, [externally mixed A], and $[SO_4^{2-}\ V]$ over the modeling domain (upper panel) and over Java (lower panel; 8.5° S - 6° S, 105.5° E - 114.5° E.)

5.4 Discussion

Pfeffer et al. (2006a) (Chapter 3) have shown that wet deposition is the most important removal mechanism for volcanic sulfur in Indonesia, and Siniarovina and Engardt (2005) describe how earlier modeling studies have shown this to be true for sulfur in general throughout Southeast Asia. It is therefore very important to correctly simulate rainfall. The REMOTE and REMO models have been shown to overestimate rainfall in Indonesia (Langmann and Heil, 2004; Graf and Yang, 2007). The overprediction of rainfall means that the modeled concentrations of aerosol load in the atmosphere will be underestimated, as will the modeled transport of the aerosols away from their source regions. Because the overestimation of precipitation is less over land than over the ocean, these effects will be less pronounced on land where acid deposition is a concern. The TRMM observations have been found to represent the annual rainfall cycle over Indonesia very well (Chang et al., 2005). Compared with station rainfall data from years prior to the TRMM data availability, Chang et al. (2005) find no consistent bias of the TRMM observations towards too much or too little rainfall. In Siniarovina and Engardt (2005), the negative effects on the terrestrial ecosystem by acid deposition is assessed using the critical load limit of 0.4 g (S)/m^2-yr (25 mEq/m^2-yr) as recommended for southeast Asia by Cinderby et al. (1998). We find that the volcanic [SO_x V] does not exceed this value while the anthropogenic [SO_x A] exceeds it in the regions shown in red in Figure 5.9. In order to see if the modeled values for the sulfur deposition are reasonable or overestimated due to too much modeled precipitation, we have calculated the percentage difference in the annual sum of precipitation between the model results and the TRMM observations (right panel Figure 5.9). The rainfall is overestimated at the locations where the critical load value is modeled to be exceeded, mostly with less than a 75 % difference, or less than an approximate doubling.

In a study combining measured nitrate and sulfate concentrations in rain and SO_2 and NO gas mixing ratios with estimated dry deposition velocities, Gillett et al. (2000) found that total acidic S and N deposition was greater than 250 mEq/m^2-yr at Jakarta and about 23 mEq/m^2-yr at Bukit Koto Tabang in 1996. Adding together the $[S]_R$ and $[N]_R$ (from

$[HNO_3]_R$ and $[NO_x]_R$) deposited in our reference simulation gives a modeled acid deposition of 158.4 mEq/m^2-yr at Jakarta and 37.5 mEq/m^2-yr at Bukit Koto Tabang. Our results indicate less acid deposition than Gillett et al. (2000) at the heavily polluted site and slightly more at the remote site. Despite the overestimation of our modeled precipitation in the region affected by strong acid deposition, we conclude that our simulated acid deposition is not strongly overpredicted, and the model results point us towards a reliable estimation of the regions that may be threatened by the critical load exceedance. The region modeled to be in excess of the critical value is very large and our model results demonstrate that acid deposition is not just a problem for the future, but is already a danger to this region.

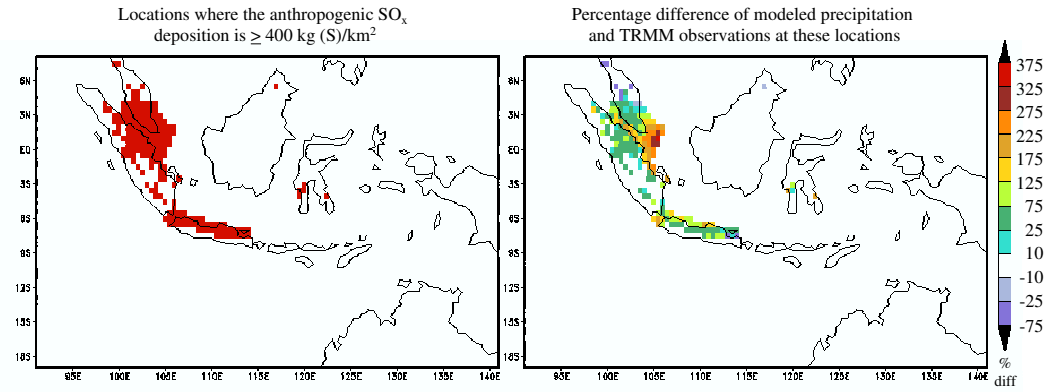

Figure 5.9 Locations where the anthropogenic SO_x deposition is $\geq$ the critical load value of 400 kg(S)/km^2-yr (left panel) and the percentage difference in precipitation between the model results and TRMM observations at these locations (right panel).

Arndt et al. (1997) participated in RAINS-ASIA, a project designed to study the effects of sulfur deposition in Asia. They describe a modeling study of anthropogenic and non-eruptive volcanic SO_2 emissions on a 1 $^\circ$ grid for 1987-1988. The atmospheric chemistry model they employed uses only sulfur chemistry. They found that volcanic emissions accounted for about 50 % of the total S deposition in Indonesia, as compared with our calculated 11 %. Their modeling results indicated that in the year 1990, southeastern Sumatra had S deposition above the 20 % critical load level, and in a projection to 2020, much of eastern Sumatra, peninsular Malaysia, and parts of Java will exceed this level. The 20 % critical load level indicates a sulfur deposition amount that protects 80 % of the ecosystem from harm. Our model simulation found that these are the very regions that

exceed the critical load values in the year 1999, earlier than indicated by their results. The anthropogenic SO_x emissions released in our study are from a newer inventory, for a later year, both of which make the anthropogenic emissions greater than those released in this earlier study. Our volcanic SO_x emissions are also less than those in this earlier study, leading to the results of the anthropogenic emissions strongly dominating acid deposition in Indonesia.

Duncan et al. (2003) found that at the top of atmosphere (TOA) the net direct radiative forcing of O_3, BC, and OC was approximately zero over most of the tropics except directly above the disastrous fires from September-November 1997. Studying the same time period, Davison et al. (2004) used many different assumptions than Duncan et al. (2003), including a lower estimate for the amount of BC released by the fires and that the aerosol was internally mixed, and found a much stronger negative forcing at the TOA. A recent global study of direct radiative forcing utilizing satellite data, ground-based measurements, and atmospheric chemistry modeling by Chung et al. (2005) found the annual mean anthropogenic aerosol forcing at the TOA to be -1 – -2 W/m^2 over Indonesia. The simulations presented here, representing a normal year while focusing on Indonesia, indicate that the direct radiative forcing of the anthropogenic aerosol over most of the region is between -0.1 – -0.5, with a range of -3.8 (northeastern Sumatra) to +0.25 (vicinity of Jakarta). Over the heavily polluted region around Jakarta, the direct radiative forcing of the volcanic sulfate aerosol is working in an opposite direction to the total anthropogenic aerosol. The total anthropogenic aerosol forcing as calculated by our simulations during typical conditions is not significantly different compared with the results of Duncan et al. (2003) during the extreme fires. Utilizing our high-resolution regional model, we are able to see more details than in the global study of Chung et al. (2005), particularly the positive forcing region around Jakarta. The direct radiative forcing of OC dominates the forcing over most of the model domain (Figure 5.7), which is emitted by vegetation fires and not included within most inventories of anthropogenic emissions. Our decision to include the biomass burning emissions as an anthropogenic source significantly influences our results for the direct radiative forcing of anthropogenic aerosol. The inclusion of fire emissions may be important not only in Indonesia, but also in Europe (Marmer, 2006). A comparison of our calculated direct radiative forcing with the values calculated by Graf et al.

(1997) shows that the influence of volcanoes relative to anthropogenic emissions is less than the global average of their study. We attribute our reduced relative importance of the volcanic emissions to the higher anthropogenic emissions and lower volcanic emissions included in our experiment, as in the discussion of acid deposition above.

The annual mean forcing efficiency (FE) of the anthropogenic sulfate is calculated to be -328 W/g (sulfate) averaged over the modeling domain (Table 5.3). The FE of the volcanic sulfate is found to be lower, with a value of -293 W/g (sulfate). Because the precursor to sulfate, SO_2, is released higher in the atmosphere for the volcanic emissions than for the anthropogenic, we had expected the volcanic FE to be higher. We examined why the anthropogenic FE is higher by focusing on the region of Java where both the volcanic and anthropogenic emissions of SO_x are strongest. Averaged over this domain, we find the anthropogenic FE to be -325 W/g (sulfate), while the volcanic is still lower, at -315 W/g (sulfate). Over surfaces with low albedo, such as the ocean, the negative forcing efficiency is stronger than over land (Boucher and Anderson, 1995). In our simulation, the anthropogenic [SO_4^{2-} *A*] spreads over the ocean while the volcanic [SO_4^{2-} *V*] tends to remain on land (Figure 5.7). In order to test if the greater FE for the [SO_4^{2-} *A*] is due to this enhancement over the ocean, we have calculated the FE for land only over both the modeling domain and over Java. Averaged over the model domain, both the volcanic and anthropogenic SO_4^{2-} have reduced FEs over land only. Over Java, the volcanic FE is essentially equivalent for ocean + land and land only, and it is only over Java land only where the volcanic FE is greater than the anthropogenic. Over Java ocean + land, the anthropogenic sulfate has an enhancement in its FE due to its being transported over the ocean compared with the volcanic sulfate which is more limited to land.

5.5 Conclusions

The role of volcanic emissions in Indonesia are found to be less significant relative to anthropogenic emissions for acid deposition and direct radiative forcing compared with earlier studies. This is a result of increased anthropogenic emissions in the year 1999 and reduced volcanic emissions based on a realistic emission scenario. Anthropogenic emissions have been shown to produce significant levels of acid deposition over much

of Indonesia and peninsular Malaysia. The direct radiative forcing of the anthropogenic aerosol is dominated by emissions of OC from biomass burning. This source of pollution is significant in Indonesia even under normal, non-drought conditions. Including biomass burning emissions changes the calculated direct radiative forcing of the anthropogenic emissions dramatically.

Acknowledgements

We thank Philipp Weis, Bärbel Langmann, and Hans Graf for their help and discussion. We thank the German Climate Computing Center (DKRZ) and Johann Feichter for computer time to run these experiments and Ulrike Niemeier for providing the MOZART results that were used as boundary conditions. Martin Schultz provided access to the RETRO emissions. The TRMM rainfall data used in this study were acquired as part of the Tropical Rainfall Measuring Mission (TRMM). The algorithms were developed by the TRMM Science Team. The data were processed by the TRMM Science Data and Information System (TSDIS) and the TRMM Office; they are archived and distributed by the Goddard Distributed Active Archive Center. TRMM is an international project jointly sponsored by the Japan National Space Development Agency (NASDA) and the U.S. National Aeronautics and Space Administration (NASA) Office of Earth Sciences. The EANET Data on the Acid Deposition in the East Asian Region was provided by Shinji Nakayama on CD and at http://www.eanet.cc/. Measurements of surface gas mixing ratios in Indonesia are available from the archive of the World Data Centre for Greenhouse Gases (WDCGG) at http://gaw.kishou.go.jp/wdcgg. Measurements of surface gas mixing ratios in Malaysia were kindly provided by Siniarovina of the Environmental Studies Division in the Malaysian Meteorological Department (MMD). MAP was funded by the Ebelin and Gerd Bucerius ZEIT Foundation and by the American Association of University Women.

Chapter 6

Conclusions and Outlook

The objective of this dissertation was to to study air pollution in Indonesia, with an emphasis on the role of volcanoes, by applying a regional atmospheric chemistry and climate model. The REMOTE model has been used to simulate the meteorological conditions and pollution transport and deposition in Indonesia. The major improvement of this work over earlier studies is the inclusion of updated, improved emission inventories for anthropogenic, biomass burning, and volcanic emissions. The volcanic emission inventories included in the three studies of this dissertation were developed within the framework of my doctoral work (Chapter 2). Additional advantages of the modeling approach utilized here are the relatively high resolution utilized and the use of full on-line tropospheric chemistry.

6.1 Conclusions

The first study of this dissertation focused on the relative transport and deposition patterns of two volcanic compounds: SO_2 and $PbCl_2$ (Chapter 3). The annual mean SO_2 loss rate for the Indonesian volcanoes was calculated to have an e-folding rate of approximately 1 day. The SO_2 loss rate was found to vary seasonally, be poorly correlated with wind speed, and to be uncorrelated with temperature or relative humidity. It was found that it is much more difficult to establish a "typical" SO_2 loss rate for volcanoes that are exposed to changeable, rather than consistent, winds. The solubility of volcanic emissions in water was shown to influence their atmospheric transport and deposition. High concentrations of $PbCl_2$ (treated within the study as a representative of highly-soluble volcanic compounds) were predicted to be deposited near to the volcanoes while volcanic S travels further away until removal from the atmosphere primarily via the wet deposition of SO_4^{2-}. The results of this study indicate that the common practice of assuming that the

ratio between the concentrations of highly soluble volcanic compounds and SO_2 within a plume is constant with that observed in fumarolic gases is reasonable at small distances from the volcanic vent. This assumption will, however, result in an underestimation of the emission flux of highly soluble species.

The second study focused on gaseous air pollution during the catastrophic Indonesian wildfire of 1997 (Chapter 4). It was found that during the extremely polluted conditions present during the wildfire, the Indonesian volcanoes contributed little to the surface pollution. Anthropogenic emissions from major cities in the region, however, were found to increase the atmospheric concentration of O_3, CO, NO_2, and SO_2 above the levels generated by the fires alone. This urban air pollution increased the number of days and the distance from the fires where O_3 exceeded the Indonesian hourly air quality standards. The increased concentration of O_3 due to the anthropogenic emissions was found to enhance the conversion of SO_2 released by the fires to SO_4^{2-}. This demonstrates that the urban pollution actively altered the atmospheric behavior and lifetime of the fire emissions. The results of this study suggest that reducing urban emissions during high-risk times for fire-related pollution may keep harmful pollutants below the air-quality thresholds in densely populated areas.

The third study examined the relative influences of volcanic and anthropogenic air pollution on acid deposition and direct radiative forcing in Indonesia in the meteorologically normal year of 1999 (Chapter 5). In this study, biomass burning emissions were grouped together with the other anthropogenic emissions and not treated separately as in Chapter 4. Approximately 11 % of the sulfur acid deposition in Indonesia is found to be volcanic in origin. The acid deposition of volcanic S is modeled to not exceed a critical load value of 0.4 g(S)/m^2-yr. Anthropogenic S is deposited above this threshold in Java, northeastern Sumatra, and peninsular Malaysia. The modeled distribution of SO_4^{2-}, organic carbon (OC), and black carbon (BC) were used as input to an off-line radiation transfer model to calculate their direct shortwave radiative forcing. The forcing of the anthropogenic and volcanic SO_4^{2-} aerosol are of the same order of magnitude, with the anthropogenic exerting its influence over a greater area due to its greater atmospheric burden. Averaged over the model domain, anthropogenic sulfate has an annual mean forcing of -0.063 W/m^2, with a

maximum of -0.83 W/m^2, and volcanic sulfate has a value of -0.012 W/m^2, with a maximum of -0.25 W/m^2. The forcing efficiency of the anthropogenic SO_4^{2-} is calculated to be greater than for volcanic, with annual mean values of -328 W/g(SO_4^{2-}) and -292 W/g(SO_4^{2-}) respectively. Over Java, this is found to be due to the enhancement of negative forcing efficiency over the ocean, as the anthropogenic sulfate is transported over the ocean while the volcanic tends to remain on land. The total forcing of the anthropogenic aerosol was calculated assuming an external mixture of SO_4^{2-}, BC, and OC. The externally mixed anthropogenic aerosol is dominated by OC released by biomass burning, particularly during the dry season of June-October. The forcing of the total anthropogenic aerosol is negative over most of the model domain, with an annual area mean value of -0.13 W/m^2. The inclusion of biomass burning as an anthropogenic emission source in our study changes the results for the calculated direct radiative forcing dramatically. Over Java, BC dominates the mixed anthropogenic aerosol, moving the radiative forcing to positive over land, where the volcanic forcing is the strongest. This means that the volcanic and anthropogenic forcing are pushing in opposite directions in this heavily polluted region. The influence of volcanic emissions relative to anthropogenic emissions on acid deposition and on direct radiative forcing is found to be lower in this study than in previous studies. This is attributed to an increase in anthropogenic emissions due to updated inventories and the inclusion of biomass burning as an anthropogenic source and to a reduction in volcanic emissions due to the realistic volcanic inventory.

6.2 Outlook

The largest uncertainty in assessing the role of volcanic emissions in the environment is accurately estimating emission flux rates and release heights. The realistic emission inventory established for this dissertation represents the best estimate possible with the currently available measurements. Indonesia has an immense number of active volcanoes that are constantly changing the Indonesian landscape, air, and water with very few observations of the volcanoes' emissions. Because a single measurement is only a snapshot of the conditions at one time, a series of measurements should be made in order to establish an envelope of the maximum and minimum emission flux rates and to provide an indication of the variability of the fumarolic gas compositions. In order to address the paucity

of volcanic emission data globally, the Network for Observation of Volcanic and Atmospheric Change (NOVAC) project began in 2005. This project will establish a network for measurements of the emissions of gases, in particular SO_2 and BrO, and aerosols by volcanoes, and will use the data from this network for risk assessment and volcanological research. As satellites are able to observe ever weaker emission plumes, and retrieval algorithms more consistently calculate the amount of a given compound present in the atmosphere, these observations can be used to develop a more reasonable volcanic emission inventory than any created until now. For model simulations of modern years, these emission scenarios could be established on yearly, or even monthly, timescales.

The emissions and effects of human activity and biomass burning are also largely uncertain. The lifetime of aerosols is very short, leading to huge temporal and spatial heterogeneities. The uncertainties of the role of aerosols can be studied with climate models which are limited by knowledge of the aerosol amount, aerosol properties, and aerosol interactions (Dentener et al., 2006). Treating aerosols within models as an interaction of species of differing mixing states, sizes, and compositions can provide a more realistic picture of the interactions between, and effects of, aerosols in the environment (Stier et al., 2005). Advances in the study of atmospheric aerosols can benefit from higher temporal resolution of emissions and consistent emission databases that also include trace gases that are involved in atmospheric chemistry (Dentener et al., 2006). Uncertainties in biomass burning emission inventories derive from establishing available fuel load, area burned, and burning efficiency data (Hoelzemann, 2006). Interpreting satellite data in conjunction with field observations in order to establish reliable estimates of area burned is an ongoing focus of research.

The transport and deposition of volcanic emissions differs from anthropogenic pollution, and this is largely because of the altitude in the atmosphere where the emissions are released. In the studies included within this dissertation, the volcanic emissions were released at the height of the volcano: a proxy for passive degassing, and the urban and biomass burning anthropogenic emissions were released at ground level. Eruptive volcanic emissions would have behaved even more differently from the anthropogenic emissions had they been injected higher into the atmosphere. The height at which urban and biomass burning emissions are released is also a source of uncertainty. In Indonesia, a

large proportion of the fire emissions come from the burning of peat areas (Heil et al., 2006), so releasing the biomass burning emissions at ground level is justified. In other regions of the world where the fires burn at a higher, flaming temperature, this may be less reasonable and the fire emissions should be injected at a higher elevation (Hoelzemann, 2006). In this study the urban pollution was also released at ground level, whereas in studies of Europe the anthropogenic emissions are often distributed vertically between several bottom model levels (e.g. Marmer and Langmann, 2005). This decision was made because in Indonesia there are comparatively few industrial stacks to raise the pollution above ground level. As Indonesia continues to grow economically and industrially, we can expect this situation to change and a different vertical distribution of anthropogenic emissions may be necessary for future studies.

With a modeling study, there are always limitations to what can be learned dependent on the limits of the model. I think REMOTE was an appropriate tool for the studies I conducted. The improvements that are currently being developed with the REMOTE model, namely coupling the tracer extension to an updated version of the REMO model and enabling it to run on parallel processors rather than serial (the PhD work of Claas Teichmann at the Max Planck Institute for Meteorology, in prep. 2007), integrating the size-resolving aerosol model M7 (Langmann, 2006), and integrating a convective cloud field model (CCFM; Graf and Yang, 2007), are all advances that will improve future studies conducted with the model. My studies focused on volcanic SO_2 and SO_4^{2-} with some treatment of the minor compound $PbCl_2$. Other volcanic compounds, including HCl and HF are potentially important for acid deposition and other metals are ecologically important. An expanded chemistry scheme that could consider more of the diversity of volcanic emissions would be beneficial.

This dissertation focuses on Indonesia, a fascinating region with air pollution from industrial and transportation sectors, seasonally set wildfires, and numerous volcanoes. Other regions of the world also have a complex interaction between natural and anthropogenic emissions that may be very different than this region with its rough topography, high humidity, and strong rains. Other locations with potentially strong interactions between urban and volcanic pollution include Mexico City, Mexico; Quito, Ecuador; and Naples, Italy. Simulating the air pollution in these places would lead to more knowledge about

the role of volcanoes in our modern world.

An interesting next step to the work presented here would be to use the nonhydrostatic, nonsteady-state plume model ATHAM (Active Tracer High Resolution Atmospheric Model) to simulate volcanic eruptions of varying strengths under different atmospheric regimes. The height reached in the atmosphere by weak and strong volcanic eruptions vary tremendously dependent on the latitude and season of the eruption (Halmer and Schmincke, 2003). The ATHAM model could explore this systematically in order to establish recommendations for injection heights for use in atmospheric chemistry and climate modeling studies. The vertical profile of emission plumes as described by the ATHAM model could be used as input for simulations with an advanced version of REMOTE that includes both M7 and the CCFM. One intriguing field of research that could be studied with this combination is the effect of volcanic aerosol particles on clouds, which is until now unquantified.

In conclusion, the work here represents a step forward in our understanding of the interactions between, and relative importance of, volcanic and anthropogenic air pollution in Indonesia. I have demonstrated that realistic modeling of volcanic emissions can lead to an improved understanding of the atmospheric processes occurring in the vicinity of active volcanoes. My results suggest that reducing the levels of urban pollution during high-risk times for fire-related pollution may help to prevent health and economic disturbances in areas with high populations. My research also indicates that the role of volcanic emissions in Indonesia is less significant relative to anthropogenic emissions for acid deposition and direct radiative forcing than was suggested by earlier studies. Improvements of emission scenarios and in model capabilities will enable us to continue making advances in our knowledge about the important topic of air pollution.

Bibliography

Acid Deposition Monitoring Network in East Asia (EANET): Report on the Acid Deposition Monitoring of EANET during the Preparatory Phase- Its Results, Major Constraints, and Ways to Overcome Them, EANET Data on the Acid Deposition in the East Asian Region, 2000.

Aiken, S. R.: Runaway fires, smoke-haze pollution, and unnatural disasters in Indonesia, Geograph. Rev., 94, 55–79, 2004.

Allard, P.: The origin of hydrogen, carbon, sulphur, nitrogen, and rare gases in volcanic exhalations: Evidence from isotope geochemistry, in Forecasting Volcanic Events, edited by H. Tazieff and J.-C. Sabroux, chap. 25, Elsevier, 1983.

Andres, R. J. and Kasgnoc, A. D.: A time-averaged inventory of subaerial volcanic sulfur emissions, J. Geophys. Res., 103, 25 251–25 261, 1998.

Arndt, R., Carmichael, G., Streets, D., and Bhatti, N.: Sulfur dioxide emissions and sectorial contributions to sulfur deposition in Asia, Atmos. Environ., 31, 1553–1572, 1997.

Bardintzeff, J.-M. and McBirney, A. R.: Volcanology, Jones and Bartlett, 2nd edn., 2000.

Benkovitz, C., Scholtz, M., Pacyna, J., Tarrason, L., Dignon, J., Voldner, E., Spiro, P., Logan, J., and Graedel, T.: Global gridded inventories of anthropogenic emissions of sulfur and nitrogen, J. Geophys. Res., 101, 29 239–29 253, 1996.

Berresheim, H. and Jaeschke, W.: The contribution of volcanoes to the global atmospheric sulfur budget, J. Geophys. Res., 88, 3732–3740, 1983.

Bluth, G., Rose, W., Sprod, I., and Krueger, A.: Stratospheric loading of sulfur from explosive volcanic eruptions, J. Geol., 105, 71–683, 1997.

Bluth, G. J. S., Casadevall, T. J., Schnetzler, C. C., Doiron, S. D., Walter, L. S., Krueger, A. J., and Badruddin, M.: Evaluation of sulfur dioxide emissions from explosive volcanism: the 1982–1983 eruptions of Galunggung, Java, Indonesia, J. Volcan. Geotherm. Res., 63, 243–256, 1994.

Boucher, O. and Anderson, T. L.: General circulation model assessment of the sensitivity of direct climate forcing by anthropogenic sulfate aerosols to aerosol size and chemistry, J. Geophys. Res., 100, 26,117–26,134, 1995.

Bouwman, A., Lee, D., Asman, W., Dentener, F., Van Der Hoek, K., and Olivier, J.: A global high-resolution emission inventory for ammonia, Gl. Biogeochem. Cycles, 11, 561–587, 1997.

Burrows, J., Weber, M., Buchwitz, M., Rozanov, V., Ladstätter-Weissenmayer, A., Richter, A., DeBeek, R., Hoogen, R., Bramstedt, K., Eichmann, K.-U., Eisinger, M., and Perner, D.: The global ozone monitoring experiment (GOME): Mission concept and first scientific results, J. Atmos. Sci., 56, 151–175, 1999.

Carn, S. and Bluth, G.: Prodigious sulfur dioxide emission from Nyamuragira volcano, D.R. Congo, Geophys. Res. Lett., 30, 2211, doi:10.1029/2003GL018465, 2003.

Chandra, S., Ziemke, J., Min, W., and Read, W.: Effects of 1997-1998 El Niño on tropospheric ozone and water vapor, Geophys. Res. Lett., 25, 3867–3870, 1998.

Chandra, S., Ziemke, J., Bhartia, P., and Martin, R.: Tropical tropospheric ozone: Implications for dynamics and biomass burning, J. Geophys. Res., 107, 4188, doi:10.1029/2001JD000447, 2002.

Chang, C.-P., Wang, Z., McBride, J., and Liu, C.-H.: Annual cycle of Southeast Asia–Maritime continent rainfall and the asymmetric monsoon transition, J. Clim., 18, 287–301, 2005.

Chang, J. S., Brost, R. A., Isaksen, S. A., Madronich, S., Middleton, O., Stockwell, W. R., and Walcek, C. J.: A three dimensional Eulerian acid deposition model: physical concepts and formulations, J. Geophys. Res., 92, 14 681–14 700, 1987.

Chung, C., Ramanthan, V., Kim, D., and Podgorny, I.: Global anthropogenic aerosol direct forcing derived from satellite and ground-based observations, J. Geophys. Res., 110, doi:10.1029/2005JD006356, 2005.

Cinderby, S., Cambridge, H., Herrera, R., Hicks, W., Kuylenstierna, J., Murray, F., and Olbrich, K.: Global assessment of ecosystem sensitivity to acidic deposition, Tech. rep., Stockholm Environmental Institute, iSBN 91 88714 58 6, 1998.

Clor, L., Fischer, T., Hilton, D., Sharp, Z., and Hartono, U.: Volatile and N isotope chemistry of the Molucca Sea collision zone: Tracing source components along the Sangihe Arc, Indonesia, Geochem. Geophys. Geosyst., 6, doi:10.1029/2004GC000825, 2005.

Davies, S. and Unam, L.: Smoke-haze from the 1997 Indonesian forest fires: effects on pollution levels, local climate, atmospheric CO_2 concentrations, and tree photosynthesis, For. Ecol. Manage., 124, 137–144, 1999.

Davison, P., Roberts, D., Arnold, R., and Colvile, R.: Estimating the direct radiative forcing due to haze from the 1997 forest fires in Indonesia, J. Geophys. Res., 109, doi:10.1029/2003JD004264, 2004.

de Hoog, J., Koetsier, G., Bronto, S., Sriwana, T., and van Bergen, M.: Sulfur and chlorine degassing from primitive arc magmas: temporal changes during the 1982-1983 eruptions of Galunggung (West Java, Indonesia), J. Volcan. Geotherm. Res., 108, 55–83, 2001.

Delmelle, P.: Environmental impacts of tropospheric volcanic gas plumes, in Volcanic Degassing, edited by C. Oppenheimer, D. M. Pyle, and J. Barclay, vol. 213 of *Special Publications*, pp. 381–399, Geol. Soc. Lon., London, 2003.

Delmelle, P., Bernard, A., Kusakabe, M., Fischer, T., and Takano, B.: Geochemistry of the magmatic-hydrothermal system of Kawah Ijen volcano, East Java, Indonesia, J. Volcan. Geotherm. Res., 97, 31–53, 2000.

Delmelle, P., Stix, J., Bourque, C.-A., Baxter, P., Garcia-Alvarez, J., and Barquero, J.: Dry deposition and heavy acid loading in the vicinity of Masaya Volcano, a major sulfur and chlorine source in Nicaragua, Environ. Sci. Technol., 35, 1289–1293, 2001.

Dentener, F., Kinne, S., Bond, T., Boucher, O., Cofala, J., Generoso, S., Ginoux, P., Gong, S., Hoelzemann, J. J., Ito, A., Marelli, L., Penner, J. E., Putaud, J.-P., Textor, C., Schulz, M., van der Werf, G. R., and Wilson, J.: Emissions of primary aerosol and precursor gases in the years 2000 and 1750, prescribed data-sets for AeroCom, Atmos. Chem. Phys., 6, 4321–4344, 2006.

Dignon, J., Eddleman, H., and Penner, J.: A black carbon emission data base for atmospheric chemistry and climate studies, Tech. rep., Lawrence Livermore National Lab., 1994.

Directorate of Volcanology and Geological Hazard Mitigation of Indonesia: http://www.vsi.esdm.go.id/mvo/mvomonitoring.html, 2005.

Duncan, B., Bey, I., Chin, M., Mickley, L., Fairlie, T., Martin, R., and Matsueda, H.: Indonesian wildfires of 1997: Impact on tropospheric chemistry, J. Geophys. Res., 108, 4458, doi:10.1029/2002JD003195, 2003.

Energy Information Administration: Indonesia: environmental issues, http://www.eia.doe.gov/emeu/cabs/indoe.html, 2004.

Engardt, M. and Leong, C.: Regional modelling of anthropogenic sulphur in Southeast Asia, Atmos. Environ., 5935–5947, 2001.

Engardt, M., Siniarovina, U., Khairul, N., and Leong, C.: Country to country transport of anthropogenic sulphur in Southeat Asia, Atmos. Environ., 39, 5137–5148, 2005.

Esterle, J. S. and Ferm, J. C.: Spatial variability in modern tropical peat deposits from Sarawak, Malaysia and Sumatra, Indonesia: analogues for coal, Int. J. Coal Geol., 26, 1–41, 1994.

Fang, M. and Huang, W.: Tracking the Indonesian forest fire using NOAA/AVHRR images, Int. J. Remote Sensing, 19, 387–390, 1998.

Frankenberg, E., McKee, D., and Thomas, D.: Health consequences of forest fires in Indonesia, California Center for Population Research On-Line Working Papers Series, CCPR-030-04, 2004.

Fujita, S.-i., Sakuri, T., and Matsuda, K.: Wet and dry deposition of sulfur associated with the eruption of Miyakejima volcano, Japan, J. Geophys. Res., 108, 4444, doi: 10.1029/2002JD003064, 2003.

Fujiwara, M., Kita, K., Kawakami, S., Ogawa, T., Komala, N., Saraspriya, S., and Suripto, A.: Tropospheric ozone enhancements during the Indonesian forest fire events in 1994 and 1997 as revealed by ground-based observations, Geophys. Res. Lett., 23, 2417–2420, 1999.

Fujiwara, M., Kita, K., Ogawa, T., Kawakami, S., Sano, T., Komala, N., Saraspriya, S., and Suripto, A.: Seasonal variation of tropospheric ozone in Indonesia revealed by 5-year ground-based observations, J. Geophys. Res., 105, 1879–1888, 2000.

Galle, B., Oppenheimer, C., Geyer, A., McGonigle, A., Edmonds, M., and Horrocks, L.: A miniaturised ultraviolet spectrometer for remote sensing of SO_2 fluxes: a new tool for volcano surveillance, J. Volcan. Geotherm. Res., 119, 241–254, 2002.

GEIA: http://www.geiacenter.org, 2006.

Giggenbach, W., Tedesco, D., Sulistiyo, Y., Caprai, A., Cioni, R., Favara, R., Fischer, T., Hirabayashi, J.-I., Korzhinsky, M., Martini, M., Menyailov, I., and Shinohara, H.: Evaluation of results from the fourth and fifth IAVCEI field workshops on volcanic gases, Vulcano island, Italy and Java, Indonesia, J. Volcan. Geotherm. Res., 108, 157–172, 2001.

Gillett, R., Ayers, G., Selleck, P., Tuti, M., and Harianto, H.: Concentrations of Nitrogen and Sulfur species in gas and rainwater from six sites in Indonesia, Water Air Soil Poll., 120, 205–215, 2000.

Global Ozone Monitoring Experiment (GOME), http://www.iup.uni-bremen.de/doas/gome.htm, 2007.

Graf, H.-F. and Yang, J.: Evaluation of a new convective cloud field model: Precipitation over the Maritime Continent, Atmos. Chem. Phys., 7, 409–421, 2007.

Graf, H.-F., Feichter, J., and Langmann, B.: Volcanic sulfur emissions: Estimates of source strength and its contribution to the global sulfate distribution, J. Geophys. Res., 102, 10 727–10 738, 1997.

Granier, C., Niemeier, U., Müller, J.-F., Olivier, J., Peters, J., Richter, A., Nües, H., and Burrows, J.: Variation of the atmospheric composition over the 1990-2000 period, Tech. Rep. 6, POET, EU project EVK2-1999-00011, 2003.

Grattan, J., Rabartin, R., Self, S., and Thordarson, T.: Volcanic air pollution and mortality in France 1783–1784, C.R. Geosci., 337, 641–651, 2005.

Halmer, M. and Schmincke, H.-U.: The impact of moderate-scale explosive eruptions on stratospheric gas injections, Bull. Volcanol., 65, 433–440, 2003.

Halmer, M. M., Schmincke, D. J., and Graf, H.-F.: The annual volcanic gas input into the atmosphere, in particular into the stratosphere: A global data set for the past 100 years, J. Volcan. Geotherm. Res., 115, 511–528, 2002.

Hauglustaine, D., Brasseur, G., and Levine, J.: A sensitivity simulation of tropospheric ozone changes due to the 1997 Indonesian fire emissions, Geophys. Res. Lett., 26, 3305–3308, 1999.

Heikens, A., Sumarti, S., van Bergen, M., Widianarko, B., Fokkert, L., van Leeuwen, K., and Seinen, W.: The impact of the hyperacid Ijen Crater Lake: risks of excess flouride to human health, Sci. Tot. Environ., 346, 56–69, 2005.

Heil, A. and Goldammer, J.: Smoke-haze pollution: a review of the 1997 episode in Southeast Asia, Reg. Environ. Change, 2, 24–37, 2001.

Heil, A., Langmann, B., and Aldrian, E.: Indonesian peat and vegetation fire emissions: Study on factors influencing large-scale smoke haze pollution using a regional atmospheric chemistry model, Mitig. and Adapt. Strat. for Glob. Change, doi:10.1007/s11027-006-9045-6, 2006.

Hettelingh, J.-P., Sverdrup, H., and Zhao, D.: Deriving critical loads for Asia, Water Air Soil Poll., 85, 2565–2570, 1995.

Hilton, D., Fischer, T. P., and Marty, B.: Noble gases and volatile recycling at subduction zones, in Reviews in Mineralogy & Geochemistry – Noble Gases in Geochemistry and Cosmochemistry, edited by D. Porcelli, C. J. Ballentine, and R. Weiler, vol. 47, pp. 319–370, Min. Soc. Am., Washington D.C., 2002.

Hinkley, T. K., Lamothe, P. J., Wilson, S. A., Finnegan, D. L., and Gerlach, T. M.: Metal emissions from Kilauea, and suggested revision of the estimatedworldwide metal output by quiescent degassing of volcanoes, Earth Plan. Lett., 170, 315–325, 1999.

Hoelzemann, J.: Global wildland fire emission modeling for atmospheric chemistry studies, Ph.D. thesis, Max-Planck-Institute for Meteorology, 2006.

Horowitz, L. W., Walters, S., Mauzerall, D. L., Emmons, L. K., Rasch, P. J., Granier, C., Tie, X., Lamarque, J.-F., Schultz, M., Tyndall, G., Orlando, J., and Brasseur, G. P.: A global simulation of tropospheric ozone and related tracers: Description and evaluation of MOZART, version 2, J. Geophys. Res., 108, 4784, doi:10.1029/2002JD002853, 2003.

Indonesia Environment Monitor, 2003- Special Focus: Reducing Pollution, Tech. rep., World Bank, http://www-wds.worldbank.org/, 2003.

Jacob, D.: A note to the simulation of the annual and inter-annual variability of the water budget over the Baltic Sea drainage basin, Met. Atmos. Phys., 77, 61–73, 2001.

Khandekar, M., Murty, T., Scott, D., and Baird, W.: The 1997 El Niño, Indonesian forest fires and the Malaysian smoke problem: a deadly combination of natural and man-made hazard, Nat. Hazards, 21, 131–144, 2000.

Kita, K., Fujiwara, M., and Kawakami, S.: Total ozone increase associated with forest fires over the Indonesian region and its relation to the El Niño-Southern Oscillation, Atmos. Environ., 34, 2681–2690, 2000.

Koe, L., Arellano Jr., A., and McGregor, J.: Investigating the haze transport from 1997 biomass burning in Southeast Asia: its impact upon Singapore, Atmos. Environ., 35, 2723–2734, 2001.

Kuylenstierna, J., Rodhe, H., Cinderby, S., and Hicks, K.: Acidification in developing countries: Ecosystem sensitivity and the critical load approach on a global scale, Ambio, 30, 20–28, 2001.

Kylander, M. E., Weiss, D. J., Martínez Cortízas, A., Spiro, B., Garcia-Sanchez, R., and Coles, B. J.: Refining the pre-industrial atmospheric Pb isotope evolution curve in Europe using an 8000 year old peat core from NW Spain, Earth Plan. Sci. Lett., 240, 467–485, 2005.

Langmann, B.: Numerical modelling of regional scale transport and photochemistry directly together with meteorological processes, Atmos. Environ., 34, 3585–3598, 2000.

Langmann, B.: Implementation of M7 in REMO, in Aerosol-, Cloud- and Chemistry Modeling in ECHAM5 Workshop Summary, 2006.

Langmann, B. and Graf, H. F.: Indonesian smoke aerosols from peat fires and the contribution from volcanic sulfur emissions, Geophys. Res. Lett., 30, 1547, doi:10.1029/2002GL016646, 2003.

Langmann, B. and Heil, A.: Release and dispersion of vegetation and peat fire emissions in the atmosphere over Indonesia 1997/1998, Atmos. Chem. Phys., 4, 2145–2160, www.atmos-chem-phys.org/acp/4/2145/, 2004.

Langmann, B., Herzog, M., and Graf, H. F.: Radiative forcing of climate by sulfate aerosols as determined by a regional circulation chemistry transport model, Atmos. Environ., 32, 2757–2768, 1998.

Le Guern, F.: Les débits de CO_2 et de SO_2 volcaniques dans l'atmosphère, Bull. Volcanol., 45, 197–202, 1982.

Le Guern, F., Gerlach, T., and Nohl, A.: Field gas chromatograph analyses of gases from a glowing dome at Merapi Volcano, Java, Indonesia, 1977, 1978, 1979, J. Volcan. Geotherm. Res., 14, 223–245, 1982.

Lee, T.-Y. and Lawver, L.: Cenozoic plate reconstruction of Southeast Asia, Tectonophysics, 251, 85–138, 1995.

Levine, J.: The 1997 fires in Kalimantan and Sumatra, Indonesia: Gaseous and particulate emissions, Geophys. Res. Lett., 26, 815–818, 1999.

Lide, D. R. and Frederikse, H. P. R., eds.: CRC Handbook of Chemistry and Physics, CRC Press, 1993.

Majewski, D.: The Europa Modell of the Deutscher Wetterdienst, vol. 2 of *Sem. Proc. ECMWF*, pp. 147–191, 1991.

Malaysian Meteorological Department (MMD): http://www.met.gov.my/english/pub lication/aaqr.html, 2007.

Mandeville, C., Carey, S., and Sigurdsson, H.: Magma mixing, fractional crystallization and volatile degassing during the 1883 eruption of Krakatau volcano, Indonesia, J. Volcan. Geotherm. Res., 74, 243–274, 1996.

Mandeville, C., Sasaki, A., Saito, G., Faure, K., King, R., and Hauri, E.: Open-system degassing of sulfur from Krakatau 1883 magma, Earth Plan. Space Lett., 160, 709–722, 1998.

Marmer, E.: Regional Modeling of Inorganic and Organic Aerosol Distribution and Climate Impact over Europe, Ph.D. thesis, Max Planck Institute for Meteorology, 2006.

Marmer, E. and Langmann, B.: Impact of ship emissions on Mediterranean summertime pollution and climate: A regional model study, Atmos. Environ., 39, 4659–4669, 2005.

Mather, T., Pyle, D., and Oppenheimer, C.: Tropospheric volcanic aerosol, in Volcanism and the Earth's atmosphere, edited by A. Robock and C. Oppenheimer, vol. 139 of *Geophysical Monograph*, AGU, Washington D.C., 2003.

Matsueda, H. and Inoue, H.: Aircraft measurements of trace gases between Japan and Singapore in October of 1993, 1996, and 1997, Geophys. Res. Lett., 26, 2413–2416, 1999.

Matsueda, H., Inoue, H., and Ishii, M.: Large injection of carbon monoxide into the upper troposphere due to intense biomass burning in 1997, J. Geophys. Res., 104, 26 867–26 879, 1999.

McGee, K. and Gerlach, T.: Volcano Hazards Fact Sheet, Tech. rep., U.S. Geological Survey, open-File Report 95-85, 1995.

McGonigle, A., Delmelle, P., Oppenheimer, C., Tsanev, V., Delfosse, T., Williams-Jones, G., Horton, K., and Mather, T.: SO_2 depletion in tropospheric volcanic plumes, Geophys. Res. Lett., 31, doi:10.1029/2004GL019990, 2004.

McGonigle, A. J. S. and Oppenheimer, C.: Optical sensing of volcanic gas and aerosol emissions, in Volcanic Degassing, edited by C. Oppenheimer, D. M. Pyle, and J. Barclay, vol. 213 of *Special Publications*, pp. 149–168, Geol. Soc. Lon., London, 2003.

Mellor, B. and Yamada, T.: A hierarchy of turbulence closure models for planetary boundary layers, J. Atmos. Sci., 31, 1791–1806, 1974.

Michaud, J.-P., Krupitsky, D., Grove, J., and Anderson, B.: Volcano related atmospheric toxicants in Hilo and Hawaii Volcanoes National Park: Implications for human health, Neurotoxicology, 26, 555–563, 2005.

Monna, F., Aiuppa, A., Varrica, D., and Dongarra, G.: Pb isotope composition in lichens and aerosols from eastern Sicily: Insights into the regional impact of volcanoes on the environment, Environ. Sci. Technol., 33, 2517–2523, 1999.

Moore, T., Blodau, C., Turunen, J., Roulet, N., and Richard, P.: Patterns of nitrogen and sulfur accumulation and retention in ombrotrophic bogs, eastern Canada, Gl. Ch. Biol., 11, 356–367, doi: 10.1111/j.1365-2486.2004.00882.x, 2004.

Nakajima, T., Higurashi, A., Takeuchi, N., and Herman, J.: Satellite and ground-based study of optical properties of 1997 Indonesian forest fire aerosols, Geophys. Res. Lett., 26, 2421–2424, 1999.

Nemesure, S., Wagner, R., and Schwartz, S. E.: Direct shortwave forcing of climate by the anthropogenic sulfate aerosol: Sensitivity to particle size, composition, and relative humidity, J. Geophys. Res., 100, 26,105–26,116, 1995.

Newhall, C. G. and Self, S.: The volcanic explosivity index (VEI): An estimate of explosive magnitude for historical volcanism, J. Geophys. Res., 87, 1231–1238, 1982.

Nho, E.-Y., Le Cloarec, M.-F., Ardouin, B., and Tjetjep, W. S.: Source strength assessment of volcanic trace elements emitted from the Indonesian arc, J. Volcan. Geotherm. Res., 74, 121–129, 1996.

Novák, M., Adomová, M., Wieder, R., and Bottrell, S.: Sulfur mobility in peat, Appl. Geochem., 20, 673–681, 2005.

Nriagu, J.: A global assessment of natural sources of atmospheric trace metals, Nature, 338, 47–49, 1989.

Olivier, J. G. J., Bouwman, A. F., van der Maas, C. W. M., Berdowski, J. J. M., Veldt, C., Bloos, J. P. J., Visschedijk, A. J. H., Zandveld, P. Y. J., and Haverlag, J. L.: Description of EDGAR Version 2.0: A set of global emission inventories of greenhouse gases and ozone-depleting substances for all anthropogenic and most natural sources on a per country basis and on 1x1 grid, Tech. Rep. Report no. 771060 002/ TNO-MEP report no. R96/119, National Institute of Public Health and the Environment (RIVM), 1996.

Oppenheimer, C., Francis, P., and Stix, J.: Depletion rates of sulfur dioxide in tropospheric volcanic plumes, Geophys. Res. Lett., 25, 2671–2674, 1998.

Page, S. E., Rieley, J. O., Shotyk, O. W., and Weiss, D.: Interdependence of peat and vegetation in a tropical peat swamp forest, Phil. Trans. R. Soc. Lond., B, 1885–1897, 1999.

Penner, J., Eddleman, H., and Novakov, T.: Towards the development of a global inventory of black carbon emissions, Atmos. Environ., 27A, 1277–1295, 1993.

Pfeffer, M., Langmann, B., and Graf, H.-F.: Atmospheric transport and deposition of Indonesian volcanic emissions, Atmos. Chem. Phys., 6, 2525–2537, 2006a.

Pfeffer, M., Rietmeijer, F., Brearley, A., and Fischer, T.: Electron microbeam analyses of aerosol particles from the plume of Poás Volcano, Costa Rica and comparison with equilibrium plume chemistry modeling, J. Volcan. Geotherm. Res., 152, 174–188, 2006b.

Pfeffer, M., Langmann, B., Heil, A., and Graf, H.-F.: The role of anthropogenic and volcanic emissions during the 1997 Indonesian wildfire pollution event, J. Geophys. Res., submitted, 2007.

Podgorny, I., Li, F., and Ramanthan, V.: Large aerosol radiative forcing due to the 1997 Indonesian forest fire, Geophys. Res. Lett., 30, 1028, doi:10.1029/2002GL015979, 2003.

Poorter, R., Varekamp, J., Poreda, R., van Bergen, M., and Kreulen, R.: Chemical and isotopic compositions of volcanic gases from the east Sunda and Banda arcs, Indonesia, Geochim. Cosmochim. Acta, 55, 3795–3807, 1991.

Pyle, D. M. and Mather, T. A.: The importance of volcanic emissions for the global atmospheric mercury cycle, Atmos. Environ., 37, 5115–5124, 2003.

Quah, E.: Transboundary pollution in Southeast Asia: The Indonesian fires, World Develop., 30, 429–441, 2002.

Resosudarmo, B.: Indonesia's Clean Air Program, Bull. Indonesian Econ. Stud., 38, 343–365, 2002.

Richter, A., Burrows, J., Nüß, H., Granier, C., and Niemeier, U.: Increase in tropospheric nitrogen dioxide over China observed from space, Nature, 437, 129–132, doi: 10.1038/nature04092, 2005.

Robock, A.: Mount Pinatubo as a Test of Climate Feedback Mechanisms, in Volcanism and the Earth's atmosphere, edited by A. Robock and C. Oppenheimer, vol. 139 of *Geophysical Monograph*, AGU, Washington D.C., 2003.

Roeckner, E., Arpe, K., Bengtsson, L., Christoph, M., Claussen, M., Duemenis, L., Esch, M., Giorgetta, M., Schlese, M., and Schulzweida, U.: The atmospheric general circulation model ECHAM-4: Model description and simulation of present-day climate, Tech. Rep. 218, MPI, Hamburg, Germany, 1996.

Roos-Barraclough, F., Martinez-Cortizas, A., García-Rodeja, E., and Shotyk, W.: A 14,500 year record of the accumulation of atmospheric mercury in peat: Volcanic signals, anthropogenic influences and a correlation to bromine accumulation, Earth Plan. Sci. Lett., 202, 435–451, 2002.

Sastry, N.: Forest fires, air pollution, and mortality in Southeast Asia, Demography, 39, 1–23, 2002.

Scaillet, B., Luhr, J., and Carroll, M.: Petrological and Volcanological Constraints on Volcanic Sulfur Emissions to the Atmosphere, in Volcanism and the Earth's atmosphere, edited by A. Robock and C. Oppenheimer, vol. 139 of *Geophysical Monograph*, AGU, Washington D.C., 2003.

Schnetzler, C. C., Bluth, G. J. S., Krueger, A. J., and Walter, L. S.: A proposed volcanic sulfur dioxide index (VSI), J. Geophys. Res., 102, 20 087–20 092, 1997.

Schultz, M., Pulles, T., Brand, R., van het Bolscher, M., and Dalsoren, S.: A global data set of anthropogenic CO, NOx, and NMVOC emissions for 1960-2000, in prep.

Schultz, M., Heil, A., Hoelzemann, J., Spessa, A., Thonicke, K., Goldammer, J., Held, A., and Pereira, J.: Global Emissions from Vegetation Fires from 1960 to 2000, Global Biogeochem. Cycles, submitted.

Self, S. and King, A.: Petrology and sulfur and chlorine emissions of the 1963 eruption of Gunung Agung, Bali, Indonesia, Bull. Volcan., 58, 263–285, 1996.

Self, S., Gertisser, R., Thordarson, T., Rampino, M., and Wolff, J.: Magma volume, volatile emissions, and stratospheric aerosols from the 1815 eruption of Tambora, Geophys. Res. Lett., 31, art. No.: L20608, 2004.

Shah, J., Nagpal, T., Johnson, T., Amann, M., Carmichael, G., Foell, W., Green, C., Hettelingh, J.-P., Hordijk, L., Li, J., Peng, C., Pu, Y., Ramankutty, R., and Streets, D.: Integrated analysis for acid rain in Asia: Policy implications and results of RAINS-Asia model, Annu. Rev. Energy Environ., 25, 339–375, 2000.

Shimada, S., Takahashi, H., Haraguchi, A., and Kaneko, M.: The carbon content characteristics of tropical peats in Central Kalimantan, Indonesia: Estimating their spatial variability in density, Biogeochem., 53, 249–267, 2001.

Simkin, T.: Terrestrial volcanism in space and time, Annu. Rev. Earth Plan. Sci., 21, 427–452, 1993.

Simkin, T. and Siebert, L.: Volcanoes of the World, Geoscience Press in association with the Smithsonian Institution Global Volcanism Program, 2nd edn., 1994.

Siniarovina, U. and Engardt, M.: High-resolution model simulations of anthropogenic sulphate and sulphur dioxide in Southeast Asia, Atmos. Environ., 39, 2021–2034, 2005.

Smolarkiewitz, P. K.: A simple positive definite advection scheme with small implicit diffusion, Month. Weath. Rev., 111, 476–479, 1983.

Spiro, P. A., Jacob, D. J., and Logan, D. J.: Global inventory of sulfur emissions with $1^\circ \times 1^\circ$ resolution, J. Geophys. Res., 97, 6023–6036, 1992.

Sriwana, T., van Bergen, M., Sumarti, S., de Hoog, J., van Os, B., Wahyuningsih, R., and Dam, M.: Volcanogenic pollution by acid water discharges along Ciwidey River, West Java (Indonesia), J. Geochem. Expl., 62, 161–182, 1998.

Sriwana, T., van Bergen, M., Varekamp, J., Sumarti, S., Takano, B., van Os, B., and Leng, M.: Geochemistry of the acid Kawah Putih lake, Patuha Volcano, West Java, Indonesia, J. Volcan. Geotherm. Res., 97, 77–104, 2000.

Stier, P., Feichter, J., Kinne, S., Kloster, S., Vignati, E., Wilson, J., Ganzeveld, L., Tegen, I., Werner, M., Balkanski, Y., Schultz, M., Boucher, O., Minikin, A., and Petzold, A.: The aerosol-climate model ECHAM5-HAM, Atmos. Chem. Phys., 5, 1125–1156, 2005.

Stockwell, W. R., Middleton, P., Chang, J. S., and Tang, X.: The second generation regional acid deposition model: Chemical mechanism for regional air quality modeling, J. Geophys. Res., 95, 16 343–16 367, 1990.

Stoiber, R. E., Malinconico Jr., L. L., and Williams, S. N.: Use of the correlation spectrometer at volcanoes, in Forecasting Volcanic Events, edited by H. Tazieff and J.-C. Sabroux, Elsevier, 1983.

Supardi, Subekty, A. D., and Neuzil, S. G.: General geology and peat resources of the Siak Kanan and Bengkalis Island peat deposits, Sumatra, Indonesia, in Modern and Ancient Coal-Forming, edited by J. C. Cobb and C. B. Cecil, vol. 286 of *Special Paper*, Geol. Soc. Am., Boulder, CO, 1993.

Syahril, S., Resosudarmo, B., and Tomo, H.: Study on Air Quality in Jakarta, Indonesia: Future Trends, Health Impacts, Economic Value and Policy Options, Tech. rep., Asian Development Bank, 2002.

Symonds, R. B., Rose, W. I., Reed, M. H., Lichte, F. E., and Finnegan, D. L.: Volatilization, transport and sublimation of metallic and non-metallic elements in high temperature gases at Merapi Volcano, Indonesia, Geochim. Cosmochim. Acta, 51, 2083–2101, 1987.

Textor, C., Graf, H.-F., Herzog, M., and Oberhuber, J. M.: Injection of gases into the stratosphere by explosive volcanic eruptions, J. Geophys. Res., 108, 4606, doi:10.1029/2002JD002987, 2003.

Thompson, A. and Bottrell, S.: Sulphur isotopic investigation of a polluted raised bog and the uptake of pollutant sulphur by *Sphagnum*, Env. Poll., 101, 201–207, 1998.

Tiedtke, M.: A comprehensive mass flux scheme for cumulus parameterization in large-scale models, Month. Weath. Rev., 117, 1778–1800, 1989.

Tropical Rainfall Measuring Mission: http://trmm.gsfc.nasa.gov/.

Tsutsumi, Y., Sawa, Y., Makino, Y., Jensen, J., Gras, J., Ryan, B., Diharto, S., and Harjanto, H.: Aircraft measurements of ozone, NO_x, CO, and aerosol concentrations in biomass burning smoke over Indonesia and Australia in October 1997: Depleted ozone layer at low altitude over Indonesia, Geophys. Res. Lett., 26, 595–598, 1999.

Walcek, C. J. and Taylor, G. R.: A theoretical method for computing vertical distributions of acidity and sulfate production within cumulus clouds, J. Atmos. Sci., 43, 339–355, 1986.

Watson, I., Realmuto, V., Rose, W., Prata, A., Bluth, G., Gu, Y., Bader, C., and Yu, T.: Thermal infrared remote sensing of volcanic emissions using the moderate resolution imaging spectroradiometer, J. Volcan. Geotherm. Res., 135, 75–89, 2004.

Weibring, P., Swartling, J., Ednre, H., Svanberg, S., Caltabiano, T., Condarelli, T., Cecchi, G., and Pantani, L.: Optical monitoring of volcanic sulphur dioxide emissions – comparison between four different remote-sensing spectroscopic techniques, Opt. Laser Eng., 37, 267–284, 2002.

Weiss, D., Shotyk, W., Cheburkin, A. K., Gloor, M., and Reese, S.: Atmospheric lead deposition from 12,400 to ca. 2,000 yrs BP in a peat bog profile, Jura Mountains, Switzerland, Water Air Soil Poll., 100, 311–324, 1997.

Weiss, D., Shotyk, W., Rieley, J., Page, S., Gloor, M., Reese, S., and Martinez-Cortizas, A.: The geochemistry of major and selected trace elements in a forested peat bog, Kalimantan, SE Asia, and its implications for past atmospheric dust deposition, Geochim. Cosmochim. Acta, 66, 2307–2323, 2002.

Wesley, M. L.: Parameterization of surface resistances to gaseous dry deposition in regional-scale numerical models, Atmos. Environ., 23, 1293–1304, 1989.

Wooster, M., Ceccato, P., and Flasse, S.: Indonesian fires observed using AVHRR, Int. J. Remote Sensing, 19, 383–386, 1998.

World Data Centre for Greenhouse Gases (WDCGG): http://gaw.kishou.go.jp/wdcgg.html, 2007.

Wüst, R. A. J. and Bustin, R. M.: Low ash peat deposits from a dendritic, intermontane basin in the tropics: A new model for good quality coals, J. Coal Geol., 46, 179–206, 2001.

Yonemura, S., Tsuruta, H., Kawashima, S., Sudo, S., Peng, L., Fook, L., Johar, Z., and Hayashi, M.: Tropospheric ozone climatology over Peninsular Malaysia from 1992 to 1999, J. Geophys. Res., 107, 4229, doi:10.1029/2001JD000993, 2002a.

Yonemura, S., Tsuruta, H., Maeda, T., Kawashima, S., Sudo, S., and Hayashi, M.: Tropospheric ozone variability over Singapore from August 1996 to December 1999, Atmos. Environ., 36, 2061–2070, 2002b.

Young, S. R., Voight, B., and Duffell, H. J.: Magma extrusion dynamics revealed by high-frequency gas monitoring at Soufrière Hills volcano, Montserrat, in Volcanic Degassing, edited by C. Oppenheimer, D. M. Pyle, and J. Barclay, vol. 213 of *Special Publications*, pp. 219–230, Geol. Soc. Lon., London, 2003.

Acknowledgements

I would like to thank my supervisors, Bärbel Langmann and Hans Graf, for their guidance, trust, and support of my work and Matthias Hort and Hartmut Grassl for their help and encouragement.

Philipp Weis has assisted at every stage in this work, shaping chaos into (hopefully!) meaning. My first friend in Hamburg, and my first in Zürich, thank you.

Elina Marmer is a patient teacher, an insightful colleague, and a loving friend. I'm glad we were able to share our office and these years together.

I thank Angelika Heil for the intensity and focus she brings to everything around her.

Thank you to the International Max Planck Research School on Earth System Modelling for enabling me to come to Germany and complete this work, and to Antje Weitz and Conni Kampmann for all of their help.

Thanks go to my parents, Mark and Susan Pfeffer, for their constant support, mailing of necessities (particularly chocolate chips), and instilling in me the strength to question.

The most important thank you goes to my love, Ole Poulsen, for everything he brings to my life.

I have been funded by the Ebelin and Gerd Bucerius ZEIT Foundation and by the American Association of University Women.

Publikationsreihe des MPI-M
„Berichte zur Erdsystemforschung“ , „*Reports on Earth System Science*“, ISSN 1614-1199
Sie enthält wissenschaftliche und technische Beiträge, inklusive Dissertationen.

Berichte zur Erdsystemforschung Nr.1 Juli 2004	**Simulation of Low-Frequency Climate Variability in the North Atlantic Ocean and the Arctic** Helmuth Haak
Berichte zur Erdsystemforschung Nr.2 Juli 2004	**Satellitenfernerkundung des Emissionsvermögens von Landoberflächen im Mikrowellenbereich** Claudia Wunram
Berichte zur Erdsystemforschung Nr.3 Juli 2004	**A Multi-Actor Dynamic Integrated Assessment Model (MADIAM)** Michael Weber
Berichte zur Erdsystemforschung Nr.4 November 2004	**The Impact of International Greenhouse Gas Emissions Reduction on Indonesia** Armi Susandi
Berichte zur Erdsystemforschung Nr.5 Januar 2005	**Proceedings of the first HyCARE meeting, Hamburg, 16-17 December 2004** Edited by Martin G. Schultz
Berichte zur Erdsystemforschung Nr.6 Januar 2005	**Mechanisms and Predictability of North Atlantic - European Climate** Holger Pohlmann
Berichte zur Erdsystemforschung Nr.7 November 2004	**Interannual and Decadal Variability in the Air-Sea Exchange of CO2 - a Model Study** Patrick Wetzel
Berichte zur Erdsystemforschung Nr.8 Dezember 2004	**Interannual Climate Variability in the Tropical Indian Ocean: A Study with a Hierarchy of Coupled General Circulation Models** Astrid Baquero Bernal
Berichte zur Erdsystemforschung Nr9 Februar 2005	**Towards the Assessment of the Aerosol Radiative Effects, A Global Modelling Approach** Philip Stier
Berichte zur Erdsystemforschung Nr.10 März 2005	**Validation of the hydrological cycle of ERA40** Stefan Hagemann, Klaus Arpe and Lennart Bengtsson
Berichte zur Erdsystemforschung Nr.11 Februar 2005	**Tropical Pacific/Atlantic Climate Variability and the Subtropical-Tropical Cells** Katja Lohmann
Berichte zur Erdsystemforschung Nr.12 Juli 2005	**Sea Ice Export through Fram Strait: Variability and Interactions with Climate**- Torben Königk
Berichte zur Erdsystemforschung Nr.13 August 2005	**Global oceanic heat and fresh water forcing datasets based on ERA-40 and ERA-15** Frank Röske
Berichte zur Erdsystemforschung Nr.14 August 2005	**The** HAM**burg** O**cean** C**arbon** C**ycle Model HAMOCC5.1 - Technical Description Release 1.1** Ernst Maier-Reimer, Iris Kriest, Joachim Segschneider, Patrick Wetzel
Berichte zur Erdsystemforschung Nr.15 Juli 2005	**Long-range Atmospheric Transport and Total Environmental Fate of Persistent Organic Pollutants - A Study using a General Circulation Model** Semeena Valiyaveetil Shamsudheen

Publikationsreihe des MPI-M
„Berichte zur Erdsystemforschung“ , „*Reports on Earth System Science*“, ISSN 1614-1199
Sie enthält wissenschaftliche und technische Beiträge, inklusive Dissertationen.

Publikationsreihe des MPI-M
„Berichte zur Erdsystemforschung“ , „*Reports on Earth System Science*“, ISSN 1614-1199
Sie enthält wissenschaftliche und technische Beiträge, inklusive Dissertationen.

Berichte zur Erdsystemforschung Nr.30 November 2006	**Long-term interactions between ice sheets and climate under anthropogenic greenhouse forcing Simulations with two complex Earth System Models** Miren Vizcaino
Berichte zur Erdsystemforschung Nr.31 November 2006	**Effect of Daily Surface Flux Anomalies on the Time-Mean Oceanic Circulation** Balan Sarojini Beena
Berichte zur Erdsystemforschung Nr.32 November 2006	**Managing the Transition to Hydrogen and Fuel Cell Vehicles – Insights from Agent-based and Evolutionary Models –** Malte Schwoon
Berichte zur Erdsystemforschung Nr.33 November 2006	**Modeling the economic impacts of changes in thermohaline circulation with an emphasis on the Barents Sea fisheries** Peter Michael Link
Berichte zur Erdsystemforschung Nr.34 November 2006	**Indirect Aerosol Effects Observed from Space** Olaf Krüger
Berichte zur Erdsystemforschung Nr.35 Dezember 2006	**Climatological analysis of planetary wave propagation in Northern Hemisphere winter** Qian Li
Berichte zur Erdsystemforschung Nr.36 Dezember 2006	**Ocean Tides and the Earth’s Rotation - Results of a High-Resolving Ocean Model forced by the Lunisolar Tidal Potential** Philipp Weis
Berichte zur Erdsystemforschung Nr.37 Dezember 2006	**Modelling the Global Dynamics of Rain-fed and Irrigated Croplands** Maik Heistermann
Berichte zur Erdsystemforschung Nr.38 Dezember 2006	**Monitoring and detecting changes in the meridional overturning circulation at 26°N in the Atlantic Ocean- The simulation of an observing array in numerical models** Johanna Baehr
Berichte zur Erdsystemforschung Nr.39 Februar 2007	**Low Frequency Variability of the Meridional Overturning Circulation** Xiuhua Zhu
Berichte zur Erdsystemforschung Nr.40 März 2007	**Aggregated Carbon Cycle, Atmospheric Chemistry, and Climate Model (ACC2) – Description of the forward and inverse modes –** Katsumasa Tanaka, Elmar Kriegler
Berichte zur Erdsystemforschung Nr.41 März 2007	**Climate Change and Global Land-Use Patterns — Quantifying the Human Impact on the Terrestrial Biosphere** Christoph Müller
Berichte zur Erdsystemforschung Nr.42 April 2007	**A Subgrid Glacier Parameterisation for Use in Regional Climate Modelling** Sven Kotlarski

Publikationsreihe des MPI-M
„Berichte zur Erdsystemforschung“ , „*Reports on Earth System Science*“, ISSN 1614-1199
Sie enthält wissenschaftliche und technische Beiträge, inklusive Dissertationen.



ISSN 1614-1199